Spring 3-9-2022

APPLICATIONS OF SIMULATION ANALYSIS TO GENERATE REFERENCE POINTS AND EVALUATE MANAGEMENT CONTROL RULES IN THREE EASTERN US FISHERIES

Laura Solinger

Recommended Citation

Solinger, Laura, "APPLICATIONS OF SIMULATION ANALYSIS TO GENERATE REFERENCE POINTS AND EVALUATE MANAGEMENT CONTROL RULES IN THREE EASTERN US FISHERIES" (2022). *Dissertations*. 2000.
https://aquila.usm.edu/dissertations/2000

APPLICATIONS OF SIMULATION ANALYSIS TO GENERATE REFERENCE POINTS AND EVALUATE MANAGEMENT CONTROL RULES IN THREE EASTERN US FISHERIES

by

Laura Katelyn Solinger

A Dissertation
Submitted to the Graduate School,
the College of Arts and Sciences
and the School of Ocean Science and Engineering
at The University of Southern Mississippi
in Partial Fulfillment of the Requirements
for the Degree of Doctor of Philosophy

Approved by:

Dr. Eric N. Powell, Committee Chair
Dr. Steven X. Cadrin
Dr. Daniel R. Hennen
Dr. Robert Leaf
Dr. Wei Wu

May 2022

Published by the Graduate School

ABSTRACT

Myriad sources of uncertainty are characteristic of or impact all commercial and recreational fisheries, contributing uncertainty to the determination of stock status. In the face of these uncertainties, fisheries managers tend to reserve fishery resources from the management targets to allow for variability. Simulation analysis is a useful tool to complement and extend formal stock assessment models to better inform managers of the risk that a management strategy results in an overfished stock or overfishing occurs over some period of time. Three examples of simulation analysis are presented to address risk-tolerance and development of management thresholds for three commercially important U.S. fisheries- Eastern oyster (*Crassostrea virginica*), Atlantic surfclam (*Spisula solidissima*) and summer flounder (*Paralichthys dentatus*). The assessment and management of each of these species has been affected by various uncertainties that affect fisheries throughout the US including difficulty in estimating (and differentiating) natural and disease mortality, parameterization of the stock-recruitment curve, and the cost-benefit analysis of including complex sex-specific dynamics into assessment models. The following analyses provide frameworks from which risk-based assessments can be adapted to other fishery resources with similar uncertainties and support efforts to conduct risk-based assessments of management decisions.

ACKNOWLEDGMENTS

This research was supported by the NOAA Saltonstall-Kennedy Grant Program #NA18NMF4270200 and the National Science Foundation Industry/University Cooperative Research Center SCeMFiS (Science Center for Marine Fisheries) through membership fees under the direction of the Industry Advisory Board (IAB). SCeMFiS administrative support is provided by NSF awards #1266057 and #1841112. This project was also supported by the National Science Foundation Non-Academic Research Internships for Graduate Students (INTERN) Supplemental Funding opportunity. We recognize the many individuals over many years that have contributed to the data collection, monitoring, and modelling of the Eastern oyster, Atlantic surfclam and summer flounder, without whom this work would not have been possible.

TABLE OF CONTENTS

LIST OF TABLES

LIST OF ILLUSTRATIONS

LIST OF ABBREVIATIONS

USM	The University of Southern Mississippi
M	Natural Mortality
F	Fishing Mortality
D	Disease Mortality
SSB	Spawning Stock Biomass
MSY	Maximum Sustainable Yield
F_{MSY}	Fishing Mortality at MSY
B_{MSY}	Biomass at MSY
SSB_{MSY}	Spawning Stock Biomass at MSY
OFL	Overfishing Limit
ABC	Acceptable Biological Catch
HM	High-mortality Oyster Bed Group
MM	Medium-mortality Oyster Bed Group
LM	Low-mortality Oyster Bed Group
SR	Shell Rock Oyster Bed
ESA	Effective Surface Area
RHL	Recreational Harvest Limit
SSC	Scientific and Statistical Committee

CHAPTER I - BACKROUND

1.1 Introduction

1.1.1 Sources of Error in Estimation of Fishery Stock Status

Myriad sources of uncertainty are characteristic of or impact all commercial and recreational fisheries, contributing uncertainty to the determination of stock status and subsequent development of management targets (Rosenberg & Restrepo, 1994; Roughgarden & Smith, 1996; Punt et al. 2014). Environmental stochasticity and harvest-implemented changes in spatial distribution or age-composition can lead to interannual variation in population dynamics. This variability is a type of process error and is generally described as noise in stock assessment models. Models account for this noise by applying a certain amount and distribution of uncertainty around parameter estimates (informed by fishery-dependent and -independent data), though this method is imperfect at capturing interannual variations in population dynamics and the eventual estimation of stock status (Hilborn, 1987). Observation error also contributes uncertainty to the estimation of stock status. Each data point, whether it be an observation of age-composition, length-composition, on an abundance index, is not a census of the stock, but instead a snapshot with associated sampling error (Maunder & Piner, 2015). Stock assessment models use the sampling error to define a sampling distribution and likelihood function for each index or composition, though how well these are characterized (or not) has consequences on estimation of stock status and eventual management decisions. A third major source of uncertainty in fisheries is implementation error, where the designated management strategy is imperfectly executed on the stock (Butterworth & Punt, 1999). Implementation error increases uncertainty in forecasted stock status, an important metric to evaluate future impacts of prospective management decisions. In the face of these uncertainties, fisheries managers tend to reserve fishery resources from the management targets to allow for variability (Hilborn, 1987).

1.1.2 Simulation Analysis

Simulation analysis is a useful tool to complement and extend formal stock assessment models to better inform managers of the risk that a management strategy results in an overfished stock or overfishing occurs over some period of time (Smith, 1994; Butterworth et al. 2010; Punt et al. 2016). At the core of simulation analyses are operating models, models conditioned on the presumed underlying population dynamics of the stock (Hilborn & Walters, 1992). Multiple operating models can be developed to capture various plausible realities that span a range of uncertainties for the stock, including spatial structure, sexual-dimorphism, and time-varying fishery selectivity (Szuwalski & Punt, 2012; Punt et al. 2014). Simulations of the stock are generated from the operating model using the observed data and associated error distribution, producing realizations of the stock coincident with population dynamics specified in the operating model structure. When a simulation is assessed by the operating model that generated the simulation, the resulting stock status reflects the “true” status of that simulation.

Depending on the goal of a simulation analysis, an estimation model can then evaluate stock status of each simulation for comparison with operating model results. Estimation models are generally less complex than the operating model, reflecting the complexity that an assessment model can support given the available data. Disparities in complexity between operating model and estimation model results can be evaluated to inform managers on what uncertainties are the most consequential for accurate estimation of stock status. A simulation can then be forecasted according to harvest control rules and associated implementation error relevant to the fishery. If a simulation is forecasted with an estimation model, the resulting estimated stock status is compared to the status determined by the operating model. This process allows for the evaluation of management strategy performance in supporting management targets and the ability of the estimation model to effectively estimate stock status of a simulation. Duration of the forecast may be relevant to management cycle timelines (during which harvest control rules are reevaluated) or generation time of the stock to inform on long-term effectiveness of management decisions. Ultimately, relative importance of population dynamics or data uncertainty can be evaluated to decide on management strategies that conform to the risk tolerance policies of management councils (Punt et al. 2014).

1.1.3 Dissertation Overview

In the face of uncertainties, fisheries managers tend to make conservative management decisions and reserve fishery resources in favor of sustainability (Hilborn, 1987), though how these decisions relate to the risk-tolerance policy of the management council is infrequently evaluated (though see Shertzer et al. 2008, Catalano & Jones, 2013, Wiedenmann et al. 2016). The following three chapters present applications of simulation analysis to address risk-tolerance and development of management thresholds for three commercially important U.S. fisheries- Eastern oyster (*Crassostrea virginica*), Atlantic surfclam (*Spisula solidissima*) and summer flounder (*Paralichthys dentatus*). Historically, the assessment and management of each of these species has been affected by uncertainties characteristic of most US fisheries including difficulty in estimating (and differentiating) natural and disease mortality, parameterization of the stock-recruitment curve, and the cost-benefit analysis of including complex sex-specific dynamics into assessment models. The following analyses provide frameworks from which risk-based assessments can be adapted to other fishery resources with similar uncertainties and support efforts to conduct risk-based assessments of management decisions.

CHAPTER II - OYSTERS BEGET SHELL AND VICE VERSA: GENERATING MANAGEMENT GOALS FOR LIVE OYSTERS AND THE ASSOCIATED REEF TO PROMOTE MAXIMUM SUSTAINABLE YIELD OF *Crassostrea virginica*

Note: this chapter has previously been accepted for publication in the Canadian Journal of Fisheries and Aquatic Sciences. Tables and citations are formatted in keeping with the conventions of this journal.

Solinger, L. K., Ashton-Alcox, K. A., Powell, E. N., Hemeon, K. M., Hennen, D. R., Soniat, T. M. (2021). Oysters beget shell (and vice versa): Generating management goals for live oysters and the associated reef to promote maximum sustainable yield of Crassostrea virginica. *Canadian Journal of Fisheries and Aquatic Sciences,* DOI:10.1139/cjfas-2021-0277.

2.1 Introduction

The use of biological reference points for sustainable management of commercial fisheries is well ensconced in the management of U.S. federal fisheries, wherein achieving maximum sustainable yield (MSY) is the primary objective and biomass and fishing mortality rate at MSY (B_{MSY} and F_{MSY}, respectively) are the critical metrics. An expansive library of literature has been developed relating to the evaluation of these metrics and their proxies (e.g., Haltuch et al. 2008; Cordue 2012; Punt & Szuwalski 2012; Zhou et al. 2012; Mangel et al. 2013; Rothschild & Jiao 2013) and the advantages and limitations of their implementation (e.g., Maunder 2003; Hartill et al. 2005; O'Leary et al. 2011; Finley & Oreskes 2013). Management strategy evaluations and related modeling approaches are exemplars for consideration of management options for the implementation of these metrics (e.g., Miller et al. 2010; Hilborn 2012; Stobart et al.

2013; Hennen 2015; Kjelland et al. 2015; Solinger et al. submitted). The evolution of reference-point based management for oysters has followed a different route than that for other stocks. This divergence is due to the relationship of the living oyster stock to the integrity of the reef (e.g., Harding et al. 2010; Southworth et al. 2010; Swannack et al. 2014; Beck & La Peyre 2015; Soniat et al. 2019) and a strong influence of the estuarine salinity gradient on population dynamics (e.g., Bergquist et al. 2006; Tolley et al. 2006; La Peyre et al. 2009, 2016; Pusack et al. 2019), which together have historically limited the application of whole-stock reference points. Unlike most management challenges for commercially fished stocks, oysters require simultaneous management of the population dynamics and the dynamics of the shell bed (Powell et al. 2012a), thus management must inherently be area-based to compensate for the salinity-dependent physiology (Powell et al. 1997; La Peyre et al. 2009; Ascenio et al. 2016; Leonhardt et al. 2017), predator distributional patterns (Stauber, 1958; Garton & Stickle 1980; Dekshenieks et al. 2000; Johnson & Smee 2014), disease-induced variations in adult mortality rate (Andrews 1988, Powell et al. 1996, Bushek et al. 2012, Powell et al. 2018), and the net downestuary flux of larvae (Narváez et al. 2012a,b, Soniat et al. 2012b). Only in the ecosystem context does the management of other fisheries approach such a complex amalgam (Link et al. 2002; Zabel et al. 2003; Worm et al. 2009).

Arguably, reference point-based management of an oyster fishery began with Haskin’s 40% rule (Fegley et al. 2003; Powell et al. 2018), which was historically applied to the Delaware Bay seed fishery in New Jersey and specified that fishing on a reef would cease when the volume of live oysters in a bushel of dredged material dropped to 40% of the total volume. Retrospective analysis of the period when this measure was used (approximately 1950s to 1990) showed that the fishing mortality rate rarely exceeded 5% of market abundance (Powell et al. 2008) and the annual survey time series demonstrated that this was a period of sustainable management. At the onset of Dermo disease in 1990 (Ford 1996; Bushek et al. 2012), this approach faltered and the consequent reduction in oyster abundance both voided application of the 40% rule and closed the seed fishery (Powell et al. 2008, 2009a). In the late 1990s, Klinck et al. (2001) developed the first reference point model, essentially a surplus production model that required the abundance of marketable oysters at the end of the year be no lower than the abundance present at the start of the year. The model permitted rebuilding by establishing the option of increased abundance at year's end, but defining *MSY* and a rebuilding goal remained elusive (Powell et al. 2009b). Nonetheless, the constant-abundance reference point brought back a period of sustainable harvest in the Delaware Bay after Dermo made the 40% rule impracticable (Powell et al. 2008). Powell et al. (2018) introduced a more sophisticated surplus production model based on that of Klinck et al. (2001) and suggested that the landings established therefrom were close to maximum sustainable yield under the enhanced natural mortality rate produced by Dermo disease.

The importance of shell-bed integrity to sustainable production of oysters has long been known, supported by a variety of shell addition and enhancement efforts over the last century (Woodward & Waller 1932; Smith et al. 2005; MacKenzie 2007; Harding et al. 2012). Whereas concerns over shell removal and reef degradation as a product of fishing have been well delineated (Lenihan & Peterson 1998; Powell et al. 2001; Woods et al. 2005; Beck et al. 2011), the importance of natural processes responsible for reef degradation and shell loss have only recently been acknowledged as a primary driver of shell-bed integrity. Studies suggest that rates of taphonomic degradation for oyster shell are much higher than those for most bivalve species (Powell et al. 2006; Powell et al. 2011a,b), and the transience of oyster shell is a persistent characteristic over a range of estuarine conditions (Powell & Klinck 2007; Mann et al. 2009a; Pace et al. 2020a). As a consequence of these findings, Soniat et al. (2012a, 2014) patterned a constant shell model after the constant abundance model of Klinck et al. (2001) in which surficial shell or cultch, not oyster abundance, was conserved yearly. This was the first effort to sustainably manage the oyster reef rather than solely the living oyster stock.

In a review of reference point-based management of oyster fisheries, Powell et al. (2018) underscored the discordance between management aimed at stock sustainability and management aimed at cultch (surficial shell) sustainability. The oyster stock begets shell and vice versa, thus the concept of sustainability applied to one does not necessarily result in management that will be sustainable to the other. The underlying challenge is the inability to explain a broodstock-recruitment relationship (Powell et al. 2008) in the classic terms of the relationship between recruitment and spawning stock biomass (Rothschild 2000; Brooks and Powers 2007; Zhou 2007; Martell et al. 2008). As recruitment has consistently been enhanced by the planting of clean shell during the appropriate time of the spawning cycle, recruitment cannot be a function solely of spawning stock biomass and larval availability. Furthermore, the enhanced attractiveness of planted shell is impermanent. Ashton-Alcox et al. (2021) recently estimated that the degree of enhancement declined exponentially with a half-life of somewhat less than one year. This clearly demonstrates that substrate quality is substantively responsible for recruitment dynamics. This understanding has been advanced by Pace et al. (2020b) who demonstrated larval preference for settlement on live oysters and the inner surface of boxes rather than loose shell, a predilection consistent with previous observations (e.g., Soniat et al. 2004; Tamburri et al. 2008; Powell et al. 2008, 2020b and references therein). Live oysters and box interiors are the newest naturally occurring surfaces and thus can be expected to provide settlement characteristics similar to planted shell.

The confluence of these observations led Hemeon et al. (2020) to propose a new interpretation of the broodstock-recruitment relationship of Powell et al. (2008), where recruitment of oysters is a function of surface area quality, rather than spawning stock abundance and fecundity. Hemeon et al. (2020) defined for the first time a distinct relationship between live oyster and shell abundance in establishing sustainability with potential for the development of reference point-based management goals for both the live oyster stock and shell bed. Herein is proposed a new model joining these two processes from which are derived reference points that establish *MSY* criteria for management of cultch quantity and stock abundance using effective surface area as the primary metric establishing sustainability.

2.2 Methods

2.2.1 Oyster Bed Groups

The data on which this study is based come from the annual stock assessment surveys for the New Jersey portion of the Delaware Bay. Survey details can be found in the stock assessment workshop reports housed at the Haskin Shellfish Research Laboratory in New Jersey (https://hsrl.rutgers.edu; see also Powell et al. 2008 and Hemeon et al. 2020). The oyster beds in the New Jersey waters of Delaware Bay have historically been divided into regional groups based on long-term trends in mortality and productivity. The groupings used here are those used by Hemeon et al. (2020): low-mortality (LM), medium-mortality (MM), Shell Rock (SR), and high-mortality (HM) (Figure 2.1).

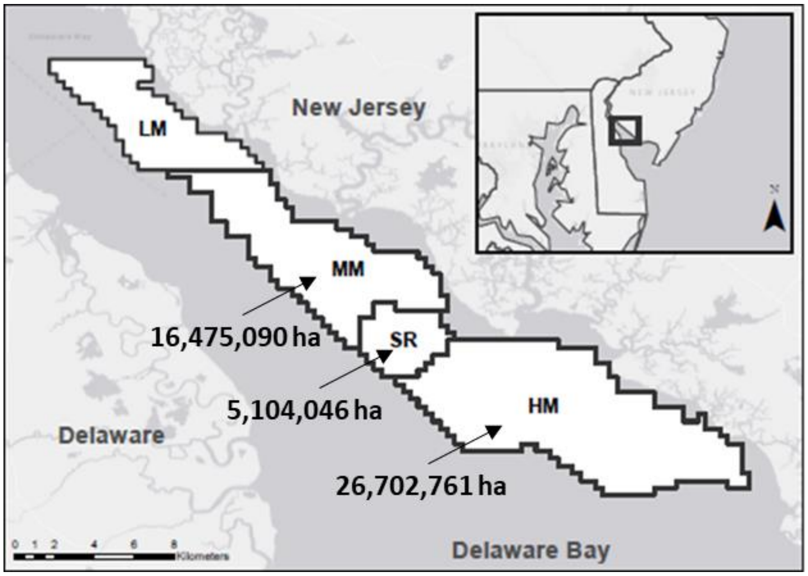

Figure 2.1 *Map of Delaware Bay oyster bed groups*

From Hemeon et al. (2020), map of low-mortality (LM), medium-mortality (MM), Shell Rock (SR) and high-mortality (HM) oyster bed groups in the Delaware Bay. Values to the left of bed group designation are bbed area in hectaries (ha).

These groups rest within the salinity gradient that drives mortality and productivity (Bushek et al. 2012). The low-mortality group was excluded from the following model simulations because recruitment in this region is limited to self-recruitment and minimal upestuary transport of larvae, rather than available substrate for settlement (Narváez et al. 2012a,b; Munroe et al. 2013, 2014; Hemeon et al. 2020). The singularity of Shell Rock, a one-bed group, originates from its high productivity. This bed sits between a region of higher predation and disease intensity (HM) and a region of slower growth and lower mortality (MM) (Kraeuter et al. 2007; Bushek et al. 2012). Bed areas for the three simulated groups are provided in Figure 2.1.

Models for the medium-mortality, high-mortality, and Shell Rock groups were developed using data collected between 1953 and 2017. To capture multiple generations of oysters, the simulated population was run for 800 months, nearly 70 years, and model output was reported at each monthly interval. In the first 200 months, only natural mortality (*M*) and fishing mortality (*F*) were causes of mortality on oyster beds. Adult mortality due to disease, henceforth termed Dermo mortality (*D*) was added in month 201. Fifteen thousand simulations were run for each bed group.

2.2.2 Summary of Population Dynamics

The model uses a simple approach to population dynamics for the living oyster population based on parameterization of growth, recruitment, and mortality. Mortality is split into three components: non-disease natural mortality, disease (Dermo) mortality, and fishing mortality, with size- and age-dependent selectivity for each type of mortality discussed later. “Dermo” mortality as it is defined here encompasses mortality sources that are associated with downestuary, higher salinity reaches of the estuary. Whereas Dermo is a primary source of mortality, other diseases such as MSX and predation on market-size oysters are subsumed under this designation. Unlike most surplus production models, the model does not invoke a standard broodstock-recruitment relationship. Rather, the “broodstock” is specified in terms of surface area suitable for larval settlement and this ‘effective surface area’ (Hemeon et al. 2020) is the sum of three contributing components, live oysters, boxes (dead oysters with articulated valves), and cultch (disarticulated surficial shell). This establishes a necessary relationship between the living population and the supporting reef structure required for the species' survival. In addition, the model includes a carbonate submodel that implements the dynamics of shell addition and loss, thereby completing the feedback loop between the living population, the reef structure, and the provision of new recruits to the population. The submodel specifies carbonate effective surface area for the three constituent types (live animal, box, and cultch) as well as the rates of addition and loss of carbonate for each of them. The model, then, is a fully integrated population dynamics-carbonate budget model.

2.2.3 Mortality

Mortality rates throughout the text and figures are specified as fractions or percentages per year, unless identified as specific rates in units of ($time^{-1}$). As simulations are modeled at monthly increments, annual mortality rates are adjusted to evenly distribute over 12 months. The non-disease natural mortality rate (M_a) was based on analyses of Powell et al. (2006, 2008) and Bushek et al. (2012). Parameterization of M was consistent between bed groups and varied in a stepwise fashion according to age and length. Mortality of oysters <35mm is elevated relative to larger individuals (Powell et al. 2008), thus a 90% mortality was enforced on individuals below this threshold size. Mortality then stabilized between eight and ten percent mortality for oysters >35mm until individuals reached 156 months of age (13 years). At 156 months of age, natural mortality was elevated to 50%, consistent with Powell et al. (2011c, 2012b) and Munroe et al. (2015). Maximum age was set to 240 months (20 years) following presumptions of Mann et al. (2009b). Hereafter, time is not included in the mathematical expressions involving mortality because mortality at age remained constant at each time step.

In each simulation, Dermo (D) and fishing (F) mortality were randomly selected from rates ranging from no fishing or disease mortality to mortalities that would lead to extinction. F was selected from a range of 0 to 55% mortality per year, which was applied evenly at monthly increments and remained constant throughout the simulation until the simulation either reached the terminal month or the simulated population became extinct. Fishery selectivity followed that of the commercial fishery in Delaware Bay, fully selecting for oysters >63mm, as only a small percentage of smaller animals were landed by the New Jersey fishery (Powell et al. 2005). Monthly fishing mortality at age was thus described by equation 1, where F is converted from annual to monthly mortality rate, a is age in months and FS is fishery selectivity.

$$1\,) \qquad F_a = \frac{F}{12} * FS_a$$

D was handled in much the same way as F, though the simulation was allowed to stabilize or crash under F over a period of 200 months before D induced additional mortality on the simulated population. For each simulation, D was randomly selected from a range of 0 to 55% annual mortality rate and was fully selected for oysters >40mm. D was constant from month 200 to 800 unless the simulated population became extinct before the terminal month. Annual Dermo mortality at age is described in the following equation, where DS is Dermo selectivity.

$$2\,) \qquad D_a = \frac{D}{12} * DS_a$$

Total monthly mortality at age (Z_a) in month 201 when natural, fishery, and Dermo mortality were all acting on the oyster population was then described by equation 3.

$$3)\qquad Z_a = M_a + F_a + D_a$$

A separate mortality metric was calculated to account for oyster mortality that would contribute to the shell stock, initially as a box, and eventually as cultch. Since the fishery removes oysters, fished oysters do not contribute shell to the reef to support future recruitment. Only natural (*M*) and Dermo (*D*) mortality contribute shell to the reef. Mortality at age contributing to available shell surface area is described by equation 4,

$$4)\qquad SM_a = M_a + D_a$$

where SM_a is mortality contributing to shell surface area of the bed.

2.2.4 Surface Area Calculations

The surface area of each individual oyster was calculated by first generating the length at age of each oyster using the Von Bertalanffy growth equation

$$5)\qquad L_a = L_{inf}(1 - e^{-K((a/12)-t_0)})$$

where L_a is length at age a in mm, L_{inf} is the asymptotic maximum length in mm, K is the growth rate per year (adjusted to a monthly growth rate) and t_0 is the theoretical age at length zero. Kraeuter et al. (2007) provide values for these parameters for Shell Rock and beds in the medium- and high-mortality groups (Table 2.1).

Table 2.1 *Von Bertalanffy Parameters*

Group	L_{inf}	t_0	K
Shell Rock	125mm	0.2 years	0.23 / year
High-mortality	125mm	0.2 years	0.2 / year
Medium-mortality	140mm	0.2 years	0.23 / year

Parameters determined in Kraeuter et al. (2007), used here in the von Bertalanffy growth equation to determine the length at age of oysters from each region.

Shell width was generated using the allometric equation

$$6\ )\ W_a = g * L_a^b$$

where W_a is shell width in mm at each respective age, g is the growth constant, L_a is shell length at age a, and b is the growth rate. Parameterization for g and b were derived from Powell et al. (2016) and remained constant across bed groups, at 2.71 and 0.71, respectively.

Length and width values at age were used to generate the total surface area of each individual oyster, using the following equation from Hemeon et al. (2020)

$$7\ )\qquad LSA_a = L_a * W_a * 2 * 0.8$$

where LSA_a is surface area of a live oyster at age a in mm^2. The equation includes two constants, (1) a multiplication factor of 2 to account for the the two oyster valves and (2) a shape correction factor of 0.8 to account for the ovoid shape (Kuykendall et al. 2015). LSA_a is multiplied by the numbers at age in each month ($N_{a,t}$) to generate the total effective live surface area at simulation time t ($LSA_{a,t}$) contributing to the surface area-recruitment relationship.

$$8\ )\qquad LSA_{a,t} = LSA_a * N_{a,t}$$

The number of oysters at each age is reported for each month of simulation. A portion of these experience natural or Dermo mortality and contribute to box and eventually cultch surface area. Fished oysters are removed from the population and do not contribute to the surface area-recruitment relationship. If an oyster dies due to either natural or Dermo mortality, the recently deceased oyster first becomes a box. As a box, both the interior of the shell and the exterior can be used for settlement, and the box effective surface area is calculated using equation 9.

$$9) \qquad BSA_{a,t} = LSA_{a,t-1} * (1 - e^{-SM_a}) * 2 * 0.8 * C_{b'}$$

$BSA_{a,t}$ is box surface area at age a (corresponding to the age of the oyster at death) in mm^2, calculated by accumulating the shell from $LSA_{a,t}$ that died from natural or Dermo mortality (SM_a), then multiplying by two to account for the interior and exterior surface area of the shell, and finally multiplying by a correction factor for boxes, $C_{b'}$. Because not all surface area is equally conducive to recruitment, Hemeon et al. (2020) developed correction factors for box and cultch surface area (C_b and C_c) scaled to *LSA*. Two box correction factors are specified to respectively represent the inside and outside of boxes, as the inside is generally cleaner and more attractive to larval settlement. These two values are summarized, averaging the C_b and C_c values to obtain the box correction factor used here, $C_{b'}$ (Table 2.2).

Table 2.2 *Correction Factors*

Group	**Box Correction ($C_{b'}$)**	**Cultch Correction (C_c)**
Shell Rock	0.73	0.40
High-mortality	0.72	0.21
Medium-mortality	0.675	0.53

Correction factors for box and cultch in the three modeled groups.

The accumulation of boxes is also traced through the simulation as oysters die, creating new boxes, while old boxes disarticulate. The total box surface area contributing to the surface area-recruitment relationship is then calculated for each month of simulation using the equation

$$10\,) \qquad BSA_t = \Sigma(BSA_{a,t}) + (BSA_{t-1} * e^{-\lambda_b})$$

where BSA_t is total box effective surface area in mm^2 at time t, calculated as the sum of new $BSA_{a,t}$ and the *BSA* from simulation time *t-1* that has not disarticulated by time t, the disarticulation rate being λ_b. The disarticulation rate was generated from Ford et al. (2006), which estimated the half-life of boxes in the Delaware Bay at four and a half months. Limited information is available on the influence of salinity and other environmental factors on disarticulation rates, thus the rate was set as constant across regions. This value is similar to that used by Pace et al. (2020a) and Damiano and Wilberg (2019), but faster than Christmas et al. (1997).

As boxes disarticulate, the disarticulated valves are added to the cultch effective surface area, calculated using the equation

$$11\ )\ CSA_t = (BSA_{t-1} * \left(1 - e^{-\lambda_b}\right) * C_c/C_{b*}) + (CSA_{t-1} * e^{-\lambda_c}) - ((LSA_t + BSA_t) * 0.18))$$

where cultch effective surface area in mm^2 at time t, CSA_t, comprises newly disarticulated boxes adjusted by the cultch correction factor (C_c), and cultch from simulation time t-1 that has not decayed, according to decay rate, λ_c. The decay rate of cultch (λ_c) across regions was set to a 2.5-year half-life, consistent with Powell et al. (2006), Mann et al. (2009a), and Pace et al. (2020a). Values in Powell et al. (2006) cover a relatively wide range of half-lives, and the value used herein is at the lower end of that range, but within reasonable estimates of an average condition.

Finally, cultch volume has historically been difficult to quantify from survey observations, as it is infrequently culled from live oyster and boxes that are collected in surveys. The Delaware Bay survey estimated that attached cultch accounted for 18% of the reported live oyster and box volume. Thus, cultch surface area was debited by 18% of the live oyster and box surface area in these simulations with expectation that this surface area was not accounted for in survey estimates of cultch weight. An important presumption is that this underestimate would routinely be found in survey datasets, as shell is rarely culled from live oysters or boxes when cultch weights are recorded.

The total effective surface area (*ESA*) at time *t* is generated by the following equation

$$12\ ) \qquad ESA_t(ha) = LSA_t + BSA_t + CSA_t * \ 10^{-10}(mm^2)$$

where LSA_t, BSA_t, and CSA_t are summed and converted from mm^2 to hectares (ha). This surface area is then available at time *t* to oyster recruits.

2.2.5 Surface Area-Recruitment

The number of recruits was determined in each month of simulation using a modified Beverton-Holt stock-recruitment curve, where instead of using spawning stock biomass to generate recruitment, the effective surface area available to newly recruiting oysters determined year-class success. This process is described in the following equation taken from Hemeon et al. (2020)

$$13\ ) \qquad R_t = \frac{a_R(ESA_t - X)}{1 + b_R(ESA_t - X)}$$

where R_t is the number of recruits at time *t*, ESA_t is total effective surface area at time *t*, and a_R, b_R, and *X* are model parameters (Table 2.3). To force the shell surface area-recruit relationship to go through or near zero, an X-axis shift (*X*) was developed by Hemeon et al. (2020) and is subtracted by ESA_t to determine the number of recruits, effectively inserting the analogue of an Allee effect.

Table 2.3 *Beverton-Holt Parameters*

Group	a_R	b_R	*X (axis shift)*
Shell Rock	0.73	0.40	211 ha
High-mortality	0.725	0.21	275 ha
Medium-mortality	0.675	0.53	876 ha

Hemeon et al. (2020) parameters of the adjusted BEverton-Holt shell surface area-recruitment curve for the three simulated oyster bed groups.

2.2.6 Model Spin-up

The initial number of live oysters at age (*LAA*) was generated using the natural mortality rate (M_a) to distribute the starting population number (N_{zero}) across the 240 age classes. Values of N_{zero} at each bed group were somewhat arbitrarily selected between two and six billion oysters, values meant to ensure the population came to a stabilization point within the first 1000 months of simulation. The eventual point of stabilization did not vary based on values of N_{zero}, and instead was determined by population dynamics of the bed group. Equilibrium surface area values for live oyster, box and cultch components in month 1000 then fed into the next phase of spin-up.

The number of oysters allocated from N_{zero} to age-class one represented the base number of recruits (R_0) for the first 1000 months of spin-up. The number of oysters from ages 2 to 240 were calculated following the equation

$$14\,)\qquad N_{a,t} = N_{a-1,t-1} * e^{-M_{a-1}}$$

where the number of live animals at age a at time t is equal to the number of live animals from age a-1 at time t-1 that survived natural mortality associated with age a-1. Mortality is also the only mechanism for death in the following 1000 months of spin-up from t = 1001 to t = 2000. LAA_{1000} informed on the population size and age distribution for the second spin-up, and LSA_{1000}, BSA_{1000}, and CSA_{1000} were used to calculate the effective surface area (*ESA*) contributing to oyster recruitment at time 1000. With this, from time 1001 to 1999, R_t was generated using the surface area-recruitment relationship described in equation 13.

2.2.7 Simulating Fishing and Dermo Mortality

For the following simulated time, the clock resets and results from spin-up t = 2000 are now the initial population for a simulation beginning at t = 1. For the first 200 months of simulation, the bed groups face only natural and fishing mortality, allowing the population to come to a new equilibrium with fishing mortality before Dermo mortality begins acting on the population. $ESA_{t=1}$ from the model spin-up generates the number of recruits (age = 1), and number of oysters at age 2 – 240 are generated from the following equation

$$15\ ) \qquad N_{a(2-240),t(1-200)} = N_{a-1,t-1} * e^{-Z_{a-1}}$$

where Z_a (See Equation 3) is the total mortality, with Dermo mortality (D_a) set to zero. Over the course of 200 months the amount and distribution of live, box, and cultch surface area either stabilizes and comes into equilibrium with the higher total mortality rate or the simulated population experiences extinction from fishing mortality.

At t = 201, D is added to total mortality, and the simulation is allowed to continue to t = 800, where again, the population has either experienced extinction from a combination of F and D, or is sustained to the terminal month, t = 800. Populations that survived to t = 800, or approximately 70 years, were described as maintaining sustainable levels of fishing and Dermo mortality. In addition to levels of F and D, other relevant statistics to describe the theoretically sustainable populations including type, amount, and ratio of surface area, as well as catch, were extracted from t = 800.

2.2.8 Threshold Metrics

Three metrics were assessed for each region to determine population thresholds that sustained fishing pressure through gradients of Dermo mortality. These metrics represent thresholds that oyster fishery managers can use to evaluate the current status of a region, and suggest fishery regulations, stock biomass, and F relative to F_{MSY} and B_{MSY}. They also provide the option for setting rebuilding targets and threshold control points for B and F leading to fishery closure. The first metric is number of live oysters m^{-2} larger than 63mm, the size of full fishery selectivity in Delaware Bay (Powell et al. 2005). The oyster fishery is managed primarily by the number of bushels landed, each bushel having a known range of market size individuals (Powell et al. 2005), regardless of biomass. At time t = 800, live oysters >63mm were tallied, and this value was divided by the total region area (Figure 1) to generate density as number of market size oysters m^{-2}.

Mass of cultch m^{-2} was the second threshold to describe sustainable population characteristics. In t = 800, cultch surface area, in hectares was converted to kg m^{-2} using the following equation

$$16\,)\qquad Cultch_{KG} = (CSA) * \frac{0.69kg}{0.111m^2}$$

where the constant 0.69 kg per 0.111 m^2 (Kuykendall et al. 2015, Hemeon et al. 2020) is used to convert effective CSA from area (m^2) to mass (kg). This is done largely to create a more realistic comparison with field data collected on oyster beds, as surface area is a metric rarely recorded in historical data. Finally, mass of cultch is divided by bed group area (m^2) and used to determine sustainability thresholds for cultch mass across the range of fishing and Dermo mortality levels.

Finally, the ratio of live surface area to total effective surface area at $t = 800$ was reported. This metric is analogous to the original 40% rule of Haskin that produced sustainable harvests for several decades prior to the onset of Dermo disease in Delaware Bay (Powell et al. 2008), in that it compares a volume-based ratio of box and cultch surface area to that available from live oysters. For scale, the total effective surface area is also reported.

2.2.9 Model Verification

Simulations for each bed group were verified against fall survey data for Delaware Bay oyster beds collected annually since 1953 (Fegley et al. 2003, Powell et al. 2008, Ashton-Alcox et al. 2018). Estimates for total number of live oysters, number of boxes, and volume of cultch are recorded in the survey and were subsequently converted to effective surface area in Hemeon et al. (2020). They are used for verification here. Box and cultch surface area were adjusted according to the correction factors in Table 2. The oyster population in Delaware Bay in the 1970s is considered to have been near carrying capacity (Powell et al. 2009a, 2012a) and fishing mortality was consistently ≤5% of the stock. The range of observed total effective surface area (*ESA*) from 1970–1979 in addition to the mean and standard deviation of *ESA* during this period, was compared to the terminal month of spin-up values from each regional model. During the 2000s, Delaware Bay oyster populations had declined due primarily to Dermo mortality, and the range, mean, and standard deviation of observed *ESA* from 2000–2009 were compared to the terminal month ($t = 800$) of each region model for simulations with $F = 10\%$ and $D =$

10%. These are reasonable estimates of Dermo and fishing mortality to represent this period in the Delaware Bay (Powell et al. 2012b, 2018).

2.3 Results

2.3.1 Model Verification

Across model regions, spin-up and terminal month *ESA* values were well-within empirical *ESA* observations (Table 2.4). Shell Rock (SR) is the smallest bed group, and predictably had the lowest standard deviation during both the 1970s and 2000s, though model estimates were still within the first standard deviation of the mean within both periods. High-mortality (HM) beds demonstrated a large range in *ESA* during the 1970s, and the *ESA* after spin-up was just below the mean, well-within the range of observed values. The range of *ESA* contracted substantially during the 2000s when fishing and Dermo mortality were in effect, and the model simulation for high-mortality beds with $F = 10\%$ and $D = 10\%$ captured this decrease well, generating a terminal *ESA* of 788ha, above the mean though within the range of observed values. Medium-mortality (MM) *ESA* also varied considerably during the 1970s, though spin-up values fell near the mean. Effective surface area at $t = 800$ was 1095ha, within the first standard deviation of the mean during the 2000s.

Table 2.4 *Model Verification*

Group	**ESA$_{1970s}$**			**ESA$_{Spin\text{-}Up}$**	**ESA$_{2000s}$**			**ESA$_{t = 800}$**
	Mean	*SD*	*Range*		*Mean*	*SD*	*Range*	
Shell Rock	1006	321	669 – 1773	1326	464	209	222 – 869	633
High-mortality	2893	2735	1044 – 8595	2365	531	180	355 – 826	788
Medium-mortality	3551	2120	1771 – 8144	3419	1682	673	886 – 2735	1095

Comparison of Delaware Bay survey observations of effective surface area (*ESA*; in hectares) at Shell Rock, high-mortality and medium-mortality oyster beds to effective surface area estimated during model spin-up at t = 800. Values at t = 800 represent *ESA* coincident with Dermo and fishing mortality at 10%.

2.3.2 Ratio of Live Shell to Total Shell

Simulations of SR were the most resilient to varying Dermo and fishing mortality, with simulated populations only becoming extinct when Dermo and fishing mortality were most elevated. The ratio of live surface area (*LSA*) to total effective surface area (*ESA*) at Shell Rock ranged from 25% at the highest mortality rates to 56% at the lowest imposed mortality (Figure 2.2). Whereas the decline in the ratio of live-to-total effective surface area was relatively linear with Dermo and fishing mortality at SR, the HM and MM regions demonstrated an increased rate of decline in this ratio with elevated fishing mortality. At HM, the live-to-total effective surface area ratio ranges from 53% to 74%, declining by approximately 1% with each 1% increase in Dermo mortality, though ratios remain stable through 10% fishing mortality. At D = 15%, an increase in F from 5% to 10% results in a reduction in live ratio of only 1%, while further increase in F from 10% to 15% reduces ratio of live-to-total effective surface area by 6%, demonstrating an accelerating decline in ratio with increased fishing mortality. Medium-mortality beds exhibit a similar trend, though the range of the ratio of live-to-total effective surface area is lower, from 19% to 50%. Again, medium-mortality beds experience a 1% decline in this ratio with each 1% increase in Dermo mortality, though the ratio is relatively stable with fishing mortality up to 10%, at which point declines in live ratio increase and eventually lead to extinction. Fishing much above 20%, even in the absence of Dermo, results in extinction of the medium-mortality bed.

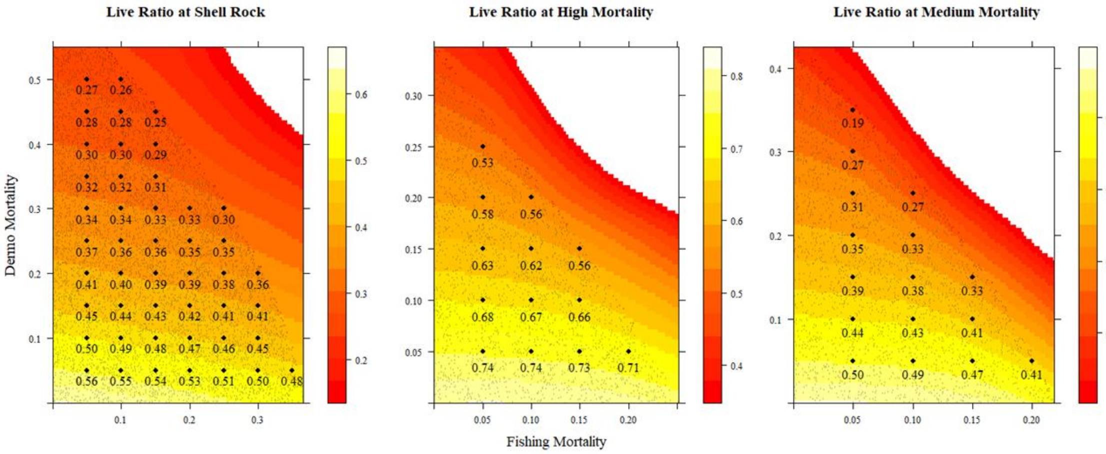

Figure 2.2 *Live Ratio*

Heat map showing contours of the ratio of live oyster surface area to total effective surface area at Shell Rock (left) the high-mortality beds (center) and the medium-mortality beds (right). All x-axes are fishing mortality (*F*) as fractions of the marketable stock and all y-axes are Dermo mortality (*D*) as fractions of the stock. Dots indicate individual simulations of *F* and *D* that reached *t* = 800. Color bars indicating values of the ratio contour are shown to the right of individual graphs.

2.3.3 Shell Rock

Shell Rock was able to sustain higher levels of fishing mortality across a range of Dermo mortality rates than either HM or MM. The threshold for extinction was *F* = 36% and *D* = 55% (Figure 2.3). Catch peaked at 3.8 million landed oysters per month at *F* = 25% when *D* = 5%. As Dermo increased, fishing at this level reduced overall catch by around half a million oysters with each 5% increase in Dermo mortality. At *D* up to 20%, fishing at *F* = 25% also generated the greatest catch for this level of disease, though the increase was minimal compared to if the population were fished more cautiously at F = 20%. Once Dermo reached 25%, fishing at F = 20% maintains or declines total landed catch and risks extinction if Dermo mortality is greater than expected or fishing at F = 20% is improperly implemented. Consistent with a total natural mortality rate of 18-20% (Powell et al. 2018), D = 10% was used to develop threshold metrics of cultch kg/m^2, number of market size oysters (>63mm) m^{-2} (hereafter referred to as oysters m^{-2}) and total effective surface area (*ESA*). At D = 10%, catch is maximized at F = 25% and Shell Rock would require 2.1 kg m^{-2} of cultch, 29 oysters m^{-2}, and 430ha of *ESA* to sustain this level of catch. Note that cultch mass has much greater sensitivity to F than D because fishing mortality removes shell from the stock while Dermo mortality continues to contribute shell. Oysters m^{-2} and *ESA* respond more evenly to both F and D because both sources of mortality result in death.

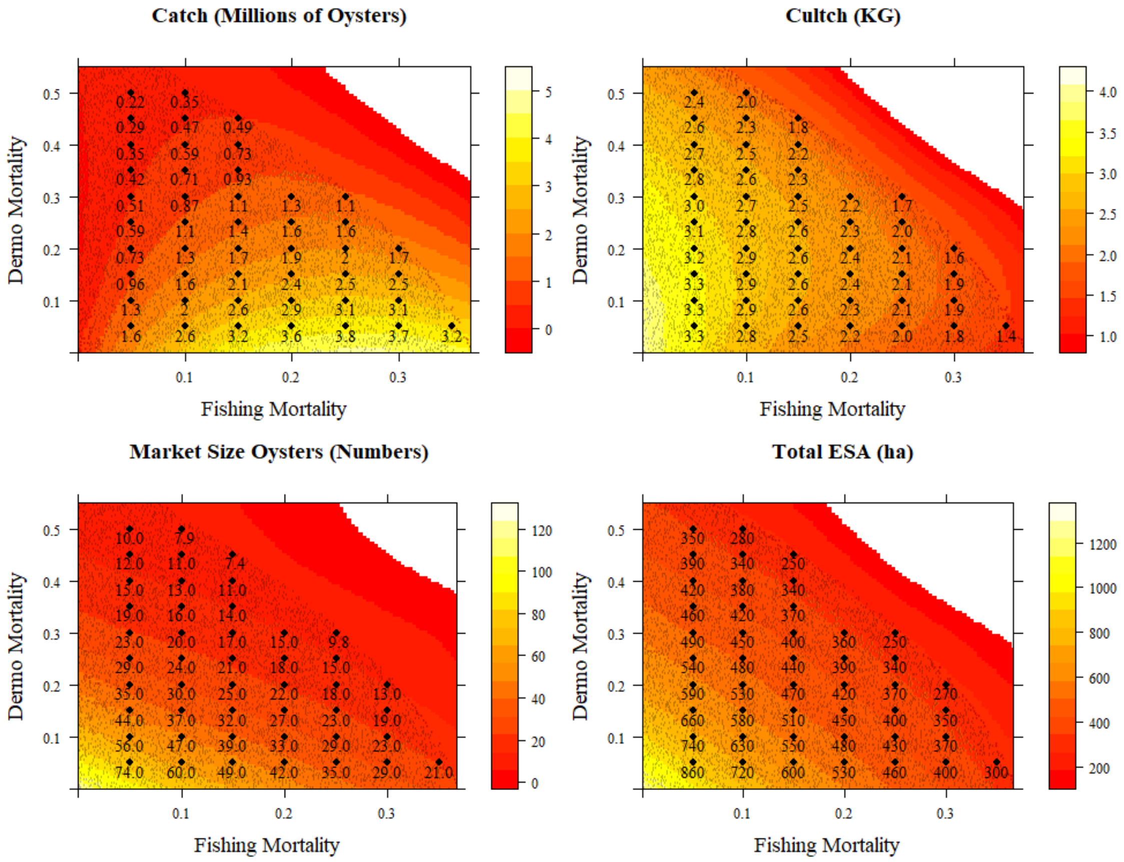

Figure 2.3 *Shell Rock Contours*

Heat map showing contours of catch in numbers (top-left), kg of cultch m^{-2} (top-right), number of market size oysters (>63mm) m^{-2} (bottom-left) and total effective surface area (bottom-right) for Shell Rock. Dots indicate individual simulations of *F* and *D* that reached *t* = 800. Color bars indicating values of the z-axis contour are shown to the right of individual graphs.

2.3.4 High-mortality

The threshold of extinction in the HM group was a total fishing and Dermo mortality of around 35%, though simulations were more sensitive to fishing than Dermo (Figure 2.4; note that x- and y- axis scales vary across heat maps in Figure 2.3 – Figure 2.5). Whereas simulated populations remained viable with Dermo as high as 35%, fishing mortality above 24%, independent of Dermo mortality, resulted in extinction. At *F* = 24%, catch declined substantially from the maximum of 5.1 million oysters at *F* = 15%. Following the analysis used for Shell Rock, *D* = 10% was used to develop threshold metrics. In this case, catch is maximized at F = 15%, landing 3.5 million oysters. At HM, however, population stability is far more precarious, and an increase of F from 15% to 20% at D = 10% results in extinction, whereas a reduction in fishing mortality from 15% to 10% results only in a modest decline in catch from 3.5 to 3.4 million oysters. At D = 10% and F = 15%, HM sustains 0.22 cultch kg/m^2, 9 oysters m^{-2}, and 560ha of *ESA.* The volatility of catch, cultch, and number of oysters over a wide range of D and F, relative to Shell Rock, emphasizes the sensitivity of the high-mortality bed group to variations in exploitation rate.

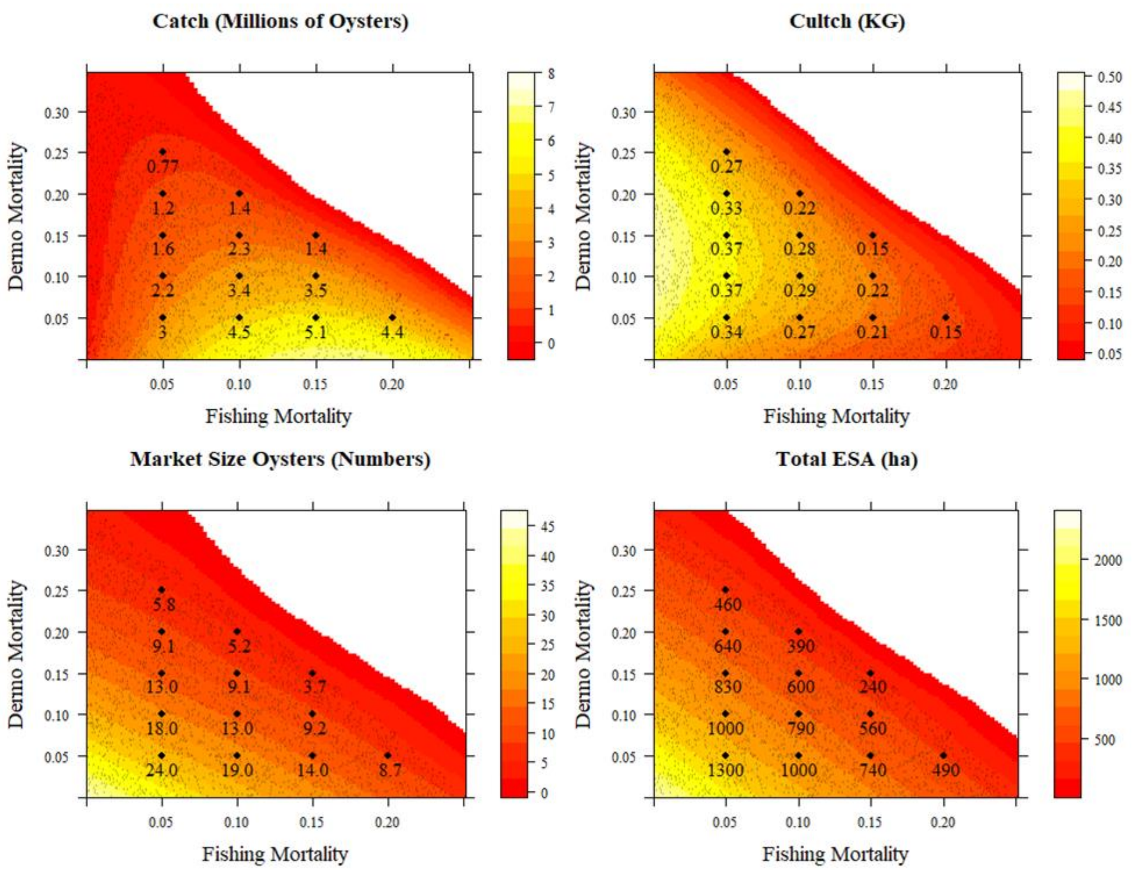

Figure 2.4 *High-mortality Contours*

Heat map showing contours of catch in numbers (top-left), kg of cultch m^{-2} (top-right), number of market size oysters (>63mm) m^{-2} (bottom-left) and total effective surface area (bottom-right) for High-mortality region. Dots indicate individual simulations of F and D that reached t = 800. Color bars indicating values of the z-axis contour are shown to the right of individual graphs.

2.3.5 Medium-mortality

The medium-mortality region was far more sensitive to fishing than Dermo mortality (Figure 2.5). When F = 0%, Dermo mortality as high as 42% maintained a population to t = 800, while independent of D, fishing mortality above 23% resulted in extinction. Maximum catch at MM occurred at lower fishing rates than both HM and SR, at 4.5 million oysters with F = 10% and D = 5%. Despite low D, catch declines above and below F = 10%. Following SR and HM, D = 0.10 was used to develop threshold metrics. Catch at *D* = 10% is maximized at *F* = 10%, landing three million oysters, with 1.9 cultch kg m^{-2}, 23 oysters m^{-2}, and 1100ha of *ESA*.

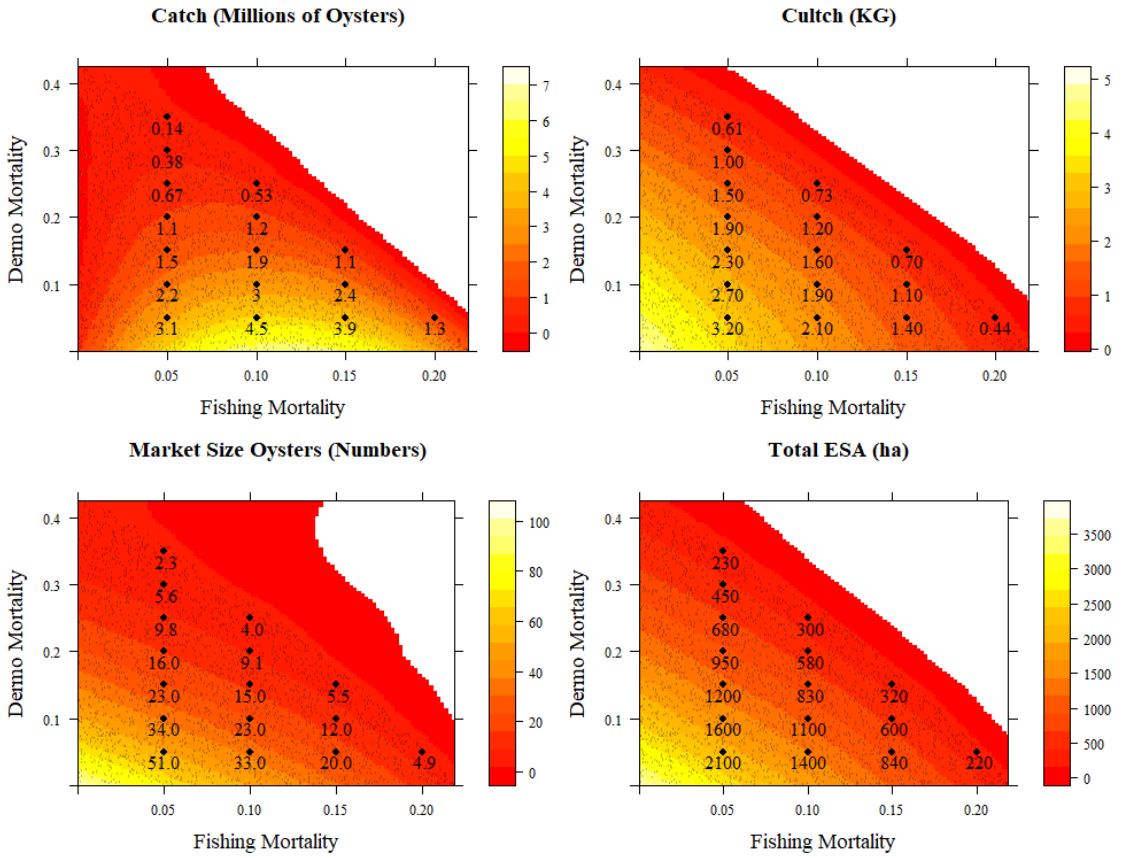
Catch (Millions of Oysters)

Cultch (KG)

Market Size Oysters (Numbers)

Total ESA (ha)

Figure 2.5 *Medium-mortality Contours*

Heat map showing contours of catch in numbers (top-left), kg of cultch m^{-2} (top-right), number of market size oysters (>63mm) m^{-2} (bottom-left) and total effective surface area (bottom-right) for Medium-mortality region. Dots indicate individual simulations of *F* and *D* that reached *t* = 800. Color bars indicating values of the z-axis contour are shown to the right of individual graphs.

2.4 Discussion

2.4.1 Perspective

The importance of the Eastern oyster and its reef in the ecology, biodiversity, nutrient cycling, and provision of other ecosystem services in estuaries is well described (Peterson et al. 2003; Coen et al. 2007; Boothe & Heck 2009; Grabowski et al. 2012; Gedan et al. 2014; Kritzer et al. 2016; McCay et al. 2017; McAfee & Bishop 2019), though sustainable management of this important resource has been rare (Hargis & Haven 1988; Jackson et al. 2001; Mann & Powell 2007; Camp et al. 2015). An exception was the 40% rule in the Delaware Bay, which successfully used supporting science to implement a simple reference point-based management strategy (Hargis & Haven 1988; Jackson et al. 2001; Mann & Powell 2007; Camp et al. 2015). Though successful for many decades, this management strategy proved inadequate upon the onset of Dermo in the 1990s. Declines in populations of Eastern oysters have been thoroughly characterized (Rothschild et al. 1994; Beck et al. 2009; zu Ermgassen et al. 2012; Powell et al. 2018), and some considerable portion of the decline over the last few decades is owed to Dermo disease which unduly impacts adult mortality rates with biased emphasis on adult oysters (Powell et al. 2013; Harding et al. 2013). Dermo increases the mortality rate, but the oyster cannot respond by increasing production of larvae (Powell et al. 2009a). Accordingly, population abundance must decline, even in unfished populations (Powell et al. 1996, 2018). The concomitant decline in surplus production imperils the stock if fishing is not carefully managed (Powell et al. 2009b; 2018).

The most substantive scientific failure in supporting management throughout periods of decline has been the failure to understand the impermanence of oyster shell. A primary factor influencing the observed historical degradation of reefs was likely an imbalance between carbonate addition and loss, inescapably leading to loss of reef acreage that amplified with the emergence of Dermo (Smith et al. 2005; Mann & Powell 2007; Mann et al. 2009a; Powell et al. 2012a). Mann and Powell (2007) and Powell and Klinck (2007) raised this issue as an urgent challenge to management and restoration and Soniat et al. (2012) proffered a focus on cultch management as a primary assessment tool to achieve sustainability. None of these offered a way to link the population dynamics of the oyster with the carbonate budget sustaining the reef, however, and subsequently, Powell et al. (2018) was unable to provide a solution.

A key to this problem came from a proposed link between recruitment and effective surface area (Hemeon et al. 2020), rather than the classic dependency of recruitment on spawning stock biomass or fecundity. This linkage stems from a wealth of previous observational, experimental, and practical evidence of the importance of "clean" shell for recruitment enhancement (Ashton-Alcox et al. 2021), including the preference by oyster larvae to settle on new shell, be it the living animal, new boxes, or planted shell (Pace et al. 2020a). Live oysters produce both recruits and the habitat necessary for them to settle, whether from inherent provision of new live shell or through death providing boxes and cultch. Effective surface area supports settlement of recruits that contribute both to the live population and to its habitat, first while alive, and ultimately by death as their shell continues to be part of the reef. This feedback loop between live oysters and effective surface area defines the integrated role of population dynamics and the carbonate budget to support surplus production and a sustainable fishery. Simulations presented herein define the ambit of sustainability for the oyster-reef system, including characteristics leading to maximum sustainable yield and conditions leading to population (and reef) extinction.

2.4.2 States of Sustainability

In these simulations, oyster bed groups consistently remained sustainable with Dermo mortality rates as high as 25% (total natural and disease mortality ~35%). These values are higher than sustainable fishing mortality rates, likely because the population and reef can withstand greater Dermo mortality than fishing mortality as Dermo mortality continues to contribute shell to the oyster bed, whereas fishing does not. Fishing mortality removes live shell surface area and ultimately box and cultch surface area, thereby preventing the contribution of shell to the effective surface area-recruitment relationship. Consequently, susceptibility to fishing mortality was more variable across bed groups.

The Shell Rock population was able to withstand the greatest fishing mortality without experiencing extinction before the terminal month. Shell Rock sits in an ideal region of the Delaware Bay that averages 15‰ salinity, a situation where salinity is not so high as to unduly increase adult mortality, nor too low to restrain growth rate or larval availability. Thus, growth and recruitment rates are high on Shell Rock and mortality rates tend to be lower than those on the more saline high-mortality beds (Powell et al. 2008). Moreover, the value of cultch as effective surface area is relatively high (Table 2.2), and the decline in live-to-total effective surface area ratio is not confounded by fishing mortality, instead remaining relatively linear with offsetting declines in Dermo mortality and increased fishing (Figure 2.2). These advantages foster resiliency not observed in either the high-mortality or medium-mortality regions. Sustainable fishing mortality was restricted to far lower values on the medium-mortality and high-mortality beds, with catch maximized between $F = 10\%$ to $F = 15\%$, above which catch declined. Interestingly, maximum catch associated with $D = 10\%$ was similar across bed groups, ranging between three and four million oysters per month, despite bed-group-specific fishing mortality associated with maximized catch at $D = 10\%$. This equivalency, however, disregards the vast acreage of the high mortality region in comparison to the smaller medium-mortality region and smaller-still Shell Rock. The productivity per unit area necessary to support a similar catch is very different between regions. The balance between productivity and bed acreage, with acreage highest in the high-mortality region balancing the lowest per-m^2 productivity, reiterates the importance in dynamics of larval supply, cultch quality, and adult mortality in determining spatial variability in reef productivity.

However, the model assumes constant adherence to the effective surface area-recruitment model without error which is likely to allow for greater sustained fishing mortality and catch than would be observed in true stock assessments. In reality, oyster recruitment is highly variable (Austin et al. 1996; Powell et al. 2008; Mann et al. 2009a), with increased variability at regions that are farther upestuary as events that transport larvae upestuary (thereby contributing recruits) are infrequent while upestuary beds contribute larvae downbay as part of the typical downbay larval drift. Model simulations did not invoke uncertainty in the recruitment-effective surface area relationship described in Hemeon et al. (2020). Given the narrow window of conditions leading to sustainability at *MSY* as shown in Figure 2.3 – Figure 2.5, precautionary management maintaining fishing mortality rate below F_{MSY} would appear prudent.

Furthermore, whereas each simulation was run for 800 months, or about 70 years, some simulations with Dermo and fishing mortality near extinction levels continued to decline slowly but did not reach extinction within the simulated time allotment. Though the time series could have been extended, 70 years captures 10+ generations of oysters (see Kraeuter et al. 2007, for typical age ranges), greater than the minimum 1-2 generations suggested by Punt et al. (2016). These marginal simulations serve to capture the boundaries of fishing mortality and Dermo mortality that can be sustained by an oyster population for a time, but these bounds are unlikely to sustain the population long-term given natural stochasticity in population dynamics.

2.4.3 Reference Points

These simulations confirm the urgency of maintaining a low F under conditions of a natural mortality rate above ~10%, arguably the historical pre-disease rate for at least some estuarine regions. Powell et al. (2018) proffered a FMSY ~6%, near the level that has proven sustainable in Delaware Bay (Powell et al. 2009a,b) and well below historical catch levels in most oyster fisheries (e.g., Jordan et al. 2002; Jordan & Coakley 2004; Wilberg et al. 2013; Pine et al. 2015). The present set of simulations, based for the first time on an integrated model that projects sustainability of both the stock and the shell bed, reinforces the requirement of maintaining a low F with natural mortality rates that are above 10% per year in order to limit the otherwise inexorable decline in the shell base that eventually results in reef demise. Simulations show, however, that at low natural mortality (D = 0%), sustainable F rises from lower rates into the range of 10 - 15% per year in the medium-mortality and high-mortality regions. Survey data from the initial years of the Delaware Bay time series, prior to the introduction of MSX, show that F at 20-25% resulted in population collapse (Powell et al. 2008), consistent with the results of these simulations.

The present model establishes a mechanism to identify analogues to the commonly used reference points of today, BMSY and FMSY. Given a rate of Dermo mortality, MSY is specified in terms of the stock size (numbers m-2) and fishing mortality (F). These effectively represent BMSY (actually NMSY, as biomass is a poor measure of oyster landings due to variable condition index [Soniat et al. 1989; Rheault & Rice 1996; Powell et al. 2016]) and FMSY at the point of highest catch yielding a sustainable stock. Finally, total effective surface area (live + box + cultch) represents a reference point for the sustainability of the reef, designated here as EMSY, which includes the requirement to sustainably manage the shell bed. Simulations show that EMSY represents a unique balance of available cultch, stock abundance, and the rate of box formation generated by natural mortality. Modern MSY-based reference points generally accept the Schaefer model of surplus production, wherein the biomass at MSY (where surplus production is maximized) is approximately one-half of carrying capacity (Maunder 2003; Mangel et al. 2013; Powell et al. 2018). The premise is primarily an outcome of the relationship of broodstock to recruitment (Brooks & Powers 2007; Brooks 2013; Punt et al. 2013). Removal of the classic broodstock-recruitment relationship in the present model might be expected to jeopardize the primary basis for MSY, the parabolic shape of the surplus production to spawning stock biomass relationship. Interestingly, the parabolic form remains, likely due to the large influence of live animals on ESA and the requirement of live animals to support cultch ESA. Thus, the original rationale for modern-day reference points is retained and the analogy with FMSY and BMSY uncompromised, while the third necessary reference point, EMSY, is incorporated.

The model also derives sustainability in terms of the ratio of live to total ESA. This augurs back to the first reference point used for oysters, the 40% rule implemented by Haskin for the New Jersey oyster beds of Delaware bay. This reference point is a volume-based reference point, and thus inherently ratio based. The opportunity is thus presented to use a simple ratio derived during surveys to evaluate both stock and reef status, advocated by Mann et al. (2009a) and Soniat et al. (2018). This ratio may provide an approach for setting stock status in cases where survey time series data are insufficient. The challenge of managing data poor stocks is well described (Cope 2013; Dowling et al. 2015; Newman et al. 2015) and often imperils evaluation of oyster fisheries wherein short survey time series or insufficient data are collected to represent the status of both the living stock and the reef.

2.5 Area Management

Area management is essential for oysters due to the strong influence of the salinity gradient on growth, recruitment, and mortality, though it is challenging to accomplish as all metrics used to evaluate stock status must be local. Growth rate and mortality are inherently local, but recruitment in its classic form (broodstock-recruitment) is evaluated for either the whole-stock or within a connected component of the stock, though the region of connectivity is often hard to judge (Narváez et al. 2012a,b; Munroe et al. 2013, 2014). The new formulation overcomes this impediment as ESA is inherently local. Accordingly, area-based reference points can now be routinely obtained as all necessary metrics are locally derived.

The formulations of Hemeon et al. (2020) show that ESA values for its components (live oysters, boxes, and cultch) vary along the salinity gradient. Generally, the value of cultch as a source of ESA increases upestuary, to the extent that cultch ESA is nearly as valuable as box or live ESA in low salinities but offers very poor substrate at high salinities. Given the estuarine influence, the question becomes the degree to which a location can be assigned to one of the regions defined by Hemeon et al. (2020). One possible option, given a data-poor condition, is to use natural mortality (D+M) as a key decision tool if data resources are not sufficient to generate a formal ESA-recruitment relationship.

2.5.1 Application to Shell Planting

This model provides information about sustainable cultch mass, numbers of oysters, and the sustainable ratio of live oyster-to-total effective surface area. Shell-planting, though not included here, could be incorporated into the model as well. The dynamics of shell-planting are important to understand, as this shell enters the population as new shell that is ideal for the enhancement of larval oyster settling (Ashton-Alcox et al. 2021). The enhancement factor of planted shell decreases with a half-life similar to the disarticulation rate of boxes, the inner valves of which are similarly attractive to larval settlement. Cultch quantity at MSY and the ratio of live oyster-to-total surface area are useful metrics to quantify the influence of shell-planting efforts that have had variable success throughout the continental U.S. (Abbe 1988; Mann & Powell 2007; Powers et al. 2009; Kennedy et al. 2011; Harding et al. 2012). Although mass of cultch matters, and cultch can be planted, how this mass relates to the ratio of live oyster-to-total surface area is infrequently assessed (though see Ashton-Alcox et al. 2021). Differences in the stability of the ratio of live oyster-to-total surface area between regions coincide with sensitivity to fishing mortality, emphasizing the need to carefully evaluate outcomes to provide best results from finite funds supporting recruitment enhancement programs.

Smothering an oyster bed with healthy cultch that overwhelms the relevance of live surface area would seem to be detrimental, especially as the value of new cultch decays over the initial years but remains as part of the shell bed for years beyond that. Complementary to shell planting, transplanting oysters from one region to another is another method of reef rehabilitation that has proven effective in the Delaware Bay (Ashton-Alcox et al. 2013) and has expanded to the use of hatchery seed in other areas (Carlsson et al. 2008; Kennedy et al. 2011). Transplanting not only provides increased oyster abundance but also encourages recruitment through the provision of the most effective ESA, live oyster shell. Incorporating both shell-planting and transplanting into simulation analyses may help determine optimal levels of both enhancement methods to support cultch mass, maintain the ratio of live oyster-to-total surface area, and subsequently sustain an increased fishing effort.

2.5.2 Precautionary Comments

The simulations considered here have used the relationships between *ESA* and recruitment obtained by Hemeon et al. (2020) for Delaware Bay. The degree to which these relationships vary beyond the Delaware Bay is unknown. For example, oysters in the Gulf of Mexico have a higher frequency of spawning (Ingle 1951; Hopkins et al. 1954; Hayes & Menzel 1981; Hofmann et al. 1992; Choi et al. 1994), and it is likely that recruitment rate per *ESA* may be higher. This represents a critical uncertainty in exporting this model to regions differing substantively in oyster recruitment dynamics.

The relationship between effective surface area and recruitment in each of the three regions simulated herein, contains what is basically an Allee effect, the magnitude of which is likely to vary given regionally-explicit recruitment dynamics (Kraeuter et al. 2005; Moore et al. 2018; Aalto et al. 2019). The Allee effect specifies that at a certain non-zero value of *ESA*, recruitment ceases, the population subsequently goes extinct, and over sufficient time, the cultch degrades and the reef itself dies. The low value of degraded cultch in providing *ESA* strongly suggests that a practical extinction point likely does exist. The Hemeon et al. (2020) dataset does not include low *ESA* values because Delaware Bay has been managed under successful reference points for more than half a century, so the *ESA*-recruitment relationship at low *ESA* remains obscure. These simulations focus attention on the incidence of mass mortality events in oyster populations (Munroe et al. 2013; Cheng et al. 2016; Grizzle et al. 2018; Gledhill et al. 2020; Pace et al. 2020a,b) and the implications for recovery when a primary source of *ESA*, live oysters, no longer contributes to the *ESA* on the reef.

Finally, this model rests on a well-established, multi-decadal time series from Delaware Bay that permits detailed estimates of *ESA*, ranges of natural and fishing mortality, and related metrics. Some of the model parameters are much less well constrained. That oyster shell has a relatively short half-life in comparison to other molluscan shells, save for mussels, is well established (Pace et al. 2020a); however, the range of values for the specific rate of shell loss is relatively large. Understanding the mechanisms that influence the rate of shell loss is a critical component in describing the carbonate budget of a reef and should receive focused research (Frérotte et al. 1983; Waldbusser et al. 2011; Subbas et al. 2018). The disarticulation rate for boxes is also uncertain, resting on a very small sample size that identifies a relatively wide range of box half-lives (Christmas et al. 1997; Pace et al. 2020a, as inferred from Ford et al. 2006), yet boxes provide an important source of *ESA*. As boxes are also used for the direct measurement of mortality rate (Ford et al. 2006; Powell et al. 2008; Vølstad et al. 2008; Summerhayes et al. 2009; Doering et al. 2021), well-constrained estimates of disarticulation rates are urgently needed. Parameterization of the box disarticulation rates used conforms with observations from direct measurements and time series data for

Delaware Bay. Alternate rates are likely to be required for application under other estuarine conditions. An additional poorly constrained parameter is the degree of survivorship from settlement to yearling age, with an important source of uncertainty being the tendency for the recruit index to be measured after substantive post-settlement mortality has occurred (e.g., Hopkins 1954; Newell et al. 2000).

2.6 Conclusions

Achieving sustainability has been elusive in managing the Eastern oyster fishery throughout much of its range. The world-wide demise of oyster reefs suggests that the Eastern oyster is not an unusual case. Underlying this management predicament is the assumed applicability of standard approaches to managing any commercial species. The oyster is unique in temperate estuaries, however, in requiring a supporting physical structure that it itself creates. Thus, sustainable management of the stock in the absence of proper management of the critical substrate upon which it depends and creates is inherently impossible over the long term. The tendency for the shell loss rate to be slower than the turnover rate of the oyster population generates an illusion of permanence that in fact, does not exist. The challenge has been to develop reference points that permit specification of rebuilding goals, optimal yield, and threshold control rules which include the necessary provision of a sustainable shell bed. The present model propounds a resolution to this dilemma in defining recruitment in terms of characteristics of the habitat as well as the stock. One of the singular revelations is the importance of the living populations not just to provide larvae for the coming generation but to provide habitat for settlement. Two corollaries are of immediate concern. The first is that maintaining the shell bed demands a population density and this coincident with a fishing mortality rate well below that typical of an animal with a 10-20-year lifespan. The fishing mortality rate must be maintained well below 15% per year. The second is the likely presence of an Allee-like effect, in which a condition can be achieved where the reef continues to exist for a time, but recovery of the population is no longer a feasible option without external intervention in the form of reef rehabilitation efforts. Thus, precautionary management is critical as the cost of restoration and the time required for rebuilding involve much more than the need for one good recruitment event or one round of shell planting. The left-skewed relationship between F, M, and surplus production, in which the decline in surplus production occurs much more rapidly at F>FMSY than at F< FMSY spotlights the need for routine and substantive precautionary management. What is argued here is that the science base for sustainable management is now present and can be implemented under strong reference-point criteria and that doing so can provide a cost-efficient option for restoring the Eastern oyster across its range.

CHAPTER III – ATLANTIC SURFCLAM BIOMASS AND DENSITY ARE RESISTANT TO CURRENT FISHING PRESSURE DESPITE UNCERTAINTIES IN MORTALITY AND RECRUITMENT

Note: this chapter has previously been submitted to the journal Fisheries Research. Tables and citations are formatted in keeping with the conventions of this journal.

Solinger, L. K., Hennen, D. R., Cadrin, S.X., Powell, E. N. (2021). Atlantic surfclam biomass and density are resistant to current fishing pressure despite uncertainties in mortality and recruitment. *Fisheries Research,* Submitted.

3.1 Introduction

Many sources of uncertainty impact determination of fishery management targets (e.g., acceptable biological catch) for all managed commercial and recreational fisheries (Rosenberg and Restrepo, 1994; Roughgarden and Smith, 1996; Punt et al., 2016). In the face of these uncertainties, fishery managers often make explicitly conservative management decisions and reserve fishery resources (Walters, 1984; Hilborn, 1987; Francis and Shotton, 1997), though how these decisions relate to the risk-tolerance policy of management councils is rarely evaluated (Shertzer et al., 2008; Wiedenmann et al., 2017; Prager and Shertzer, 2019). Simulation analysis based on alternative operating models allows managers to evaluate alternative control rules and the relative importance of various sources of uncertainty to make management decisions that conform to the designated Council's risk-tolerance policy.

Atlantic surfclam (*Spisula solidissima*) is a historically important resource for the north- and mid-Atlantic commercial fisheries (McCay et al., 2011; Hofmann et al., 2018), though uncertainties in population dynamics complicate determination of management targets (Munroe et al., 2016; Timbs et al., 2018; Hennen et al., 2018). The 2016 stock assessment determined that the surfclam stock was not overfished ($SSB > SSB_{Threshold}$) and overfishing was not occurring ($F > F_{MSY}$; NEFSC, 2017), though substantial uncertainty around the estimate of absolute spawning stock biomass (SSB) from the assessment model led the Mid-Atlantic Fishery Management Council (MAFMC) to decrease the acceptable biological catch (ABC) from 60,313 metric tons (mt) to 45,524 mt (MAFMC, 2017) (this decision was later reversed). The fishery quota has long been set at 26,218 mt, below the ABC, as a result of economic constraints within the fishery. Despite the absence of a precise SSB estimate, relative biomass of the surfclam stock was estimable from the assessment, and biological reference points relative to biomass were based on the ratio of terminal to unfished SSB. The fishing mortality (*F*) reference points were more difficult to define in the absence of precise biomass estimates, but were ultimately derived from F_{MSY} (fishing mortality at maximum sustainable yield) estimated outside the stock assessment model at 0.12 yr^{-1} (Hennen et al., 2018).

Uncertainty in the absolute SSB can be largely attributed to fishery-independent survey estimates of catch per unit effort (CPUE). Relatively low dredge efficiency early in the timeseries (Hennen et al., 2012; NEFSC, 2017), uncertainty in the methodology used to calibrate dredge efficiency (Hennen et al., 2012; Poussard et al., 2021), patchiness of surfclam spatial distribution (Timbs et al., 2019), and range shifts influencing survey design (Jacobson and Hennen, 2019) led to a relatively uninformative timeseries of CPUE from 1982 to 2011. In 2012 a new fishery-independent sampling system began on a vessel with higher dredge-efficiency (Hennen, 2018) and an improved survey design was implemented in 2016 (Jacobson and Hennen, 2019), though too few observations were yet available to the 2016 assessment to overcome historical sampling error for a more certain estimate of SSB.

In addition to an uninformative survey CPUE timeseries, commercial dredges rarely select clams <120 mm, approximately an age-5 surfclam (Munroe et al., 2013; Chute et al., 2016; Kuykendall et al., 2017), limiting the information available for young individuals. As the broodstock-recruitment relationship is also uninformed, estimates of recruitment success (or failure) in stock assessment models are lagged and only become estimable when clams reach minimum size for gear-selectivity. Further uncertainty in future stock status persists, as steepness of the broodstock-recruitment curve and natural mortality are likely to vary with warming of the northwest Atlantic (Pershing et al., 2015; Saba et al., 2016; Friedland et al., 2020). This warming has instigated large-scale and rapid changes in recruitment, mortality, and stock distribution (Hennen et al., 2018). These uncertainties have led the MAFMC to make conservative management decisions for the surfclam fishery, though adherence to the MAFMC risk-tolerance policy has not been evaluated.

We developed a simulation analysis for Atlantic surfclam to evaluate potential consequences of these uncertainties on management decisions and the efficacy relative to the risk-tolerance policy of the management council. Multiple operating models were created with alternative parameterizations of steepness of the broodstock-recruitment curve and natural mortality that reflected uncertainties in these population dynamics. Simulations were generated from the alternative model structures and forecasted with a series of harvest control rules. Forecasted status of simulated stocks was compared to performance indicators that captured objectives of the management council (e.g., risk that a stock becomes overfished or overfishing occurs) and the commercial fishery (e.g., future availability of fishable surfclam patches). To the latter point, the assessment model estimates spawning stock biomass and fishing mortality compared to thresholds of overfished and overfishing, but regional density of the biomass for the patchy stock is not informed by the assessment. The commercial fishery relies on a minimum clam density to permit landings of >1 cage hr^{-1} to remain profitable (1 cage = 32 surfclam bushels; Powell et al., 2015). Thus, while the stock may remain within management thresholds, the dispersion of the stock at lower biomass or higher fishing may beget an unprofitable fishery. Accordingly, a secondary objective for this work was to generate estimates of future availability of fishable surfclam patches from assessment model outputs. This estimation uses previously reported metrics of patchiness in surfclams throughout their range (Timbs et al., 2019) to evaluate the risk of stock reduction to unfishable levels, albeit still meeting stock sustainability thresholds for biomass and fishing mortality.

3.2 Methods

3.2.1 Assessment Model Structure

Operating models were conditioned on the 2016 assessment model which was an application of Stock Synthesis version 3.24 (SS3.24; Methot and Wetzel, 2013; NEFSC, 2017). The 2016 stock assessment for Atlantic surfclam included two SS models representing independent surfclam populations on Georges Bank and southwest of Georges Bank (termed Northern and Southern, respectively) due to limited data availability for the Northern region. Data and model structure for the Southern population, which supports the largest fraction of the surfclam fishery (NEFSC, 2017), served as the basis of this simulation analysis. To utilize upgrades to forecasting, the Southern model was translated from SS v3.24 to v3.30 (Methot et al., 2019), though this translation did not alter model convergence or results.

The Southern surfclam model incorporates the commercial fishery and three indices of abundance from the Northeast Fishery Science Center (NEFSC) dredge surveys. One index for survey trend and an associated scalar are available for the NEFSC research dredge which operated from 1982 to 2011. In 2012 the NEFSC survey transitioned to a modified commercial dredge. Two observations from 2012 and 2015 are available to the Southern model from the modified commercial dredge. Surveys occurred approximately once every three years over the 1982-2015 time period. The commercial fishery provides landings in metric tons and length-compositions collected by randomized port-sampling. Length-composition data are also available for the research dredge and modified commercial dredge surveys, in addition to conditional age-at-length compositional data. Variance adjustment factors are used to moderate sample sizes of fleet-specific length-compositions. These factors were removed during generation of simulated data, but reinstated during subsequent model runs. A variety of growth and selectivity parameters are estimated in the assessment model, though natural mortality (M = 0.15) and steepness of the Beverton-Holt broodstock-recruitment curve (h = 0.95) are fixed parameters. Operating models changed the fixed value of M and h but otherwise maintained the assessment model structure.

3.2.2 Simulation Analysis

Six model structures were used to evaluate risk from potential management strategies given uncertainty in steepness and natural mortality. Three values of h (0.40, 0.70 and 0.95) and two values of M (0.15, 0.25 yr^{-1}) were specified in alternative operating models (OM). For comparison, the stock assessment assumed $M = 0.15$ yr^{-1} and $h = 0.95$, and included a sensitivity analysis with $h = 0.33$ (NEFSC, 2017). Hennen et al. (2018) assumed $h = 0.30$ as a lower bound for sensitivity analyses. The lower bound on steepness used herein was raised to 0.40, informed by empirical estimates of steepness values ranging from about 0.40 to 0.99 for hard clam (*Mercenaria mercenaria*) populations in the Mid-Atlantic (Peterson, 2002; Kraeuter et al., 2005). Few estimates of natural mortality rate are available (Weinberg, 1999; Narváez et al., 2015), but rapid shifts in range suggest geographic variation in mortality rate (Kim and Powell, 2004; Weinberg et al., 2005; Hofmann et al., 2018). Maximum ages recorded regionally suggest local mortality rates in the core of the stock as high as 0.2 yr^{-1} and as low as 0.12 yr^{-1} (Hennen et al., 2018). As these observations emphasize local increases in mortality rate, a higher mortality rate was preferentially examined, and natural mortality was set at 0.15 yr^{-1} and 0.25 yr^{-1} (Hennen, 2018). The naming convention of operating models (and later estimation models) followed the format of H (steepness value) M (natural mortality value), such that the base operating model following the assessment model parameters of $h = 0.95$ and $M = 0.15$ yr^{-1} is named H0.95M0.15.

All model structures were used as both operating models and alternative estimation models, so efficacy of management strategies were evaluated under circumstances where M and h parameters are incorrectly specified from the “true” value in the operating model. Each operating model (OM) generated one hundred simulations of a surfclam stock using a parametric bootstrap function internal to SS (Figure 3.1). This function first uses maximum likelihood estimation to generate expected data values from input observations (Methot et al., 2019). New observations that fit within the specified error distributions were generated using the expected data values and associated standard deviations. These new data simulations of the surfclam stock span the level of uncertainty reported for observations of catch, survey, length, and age compositions.

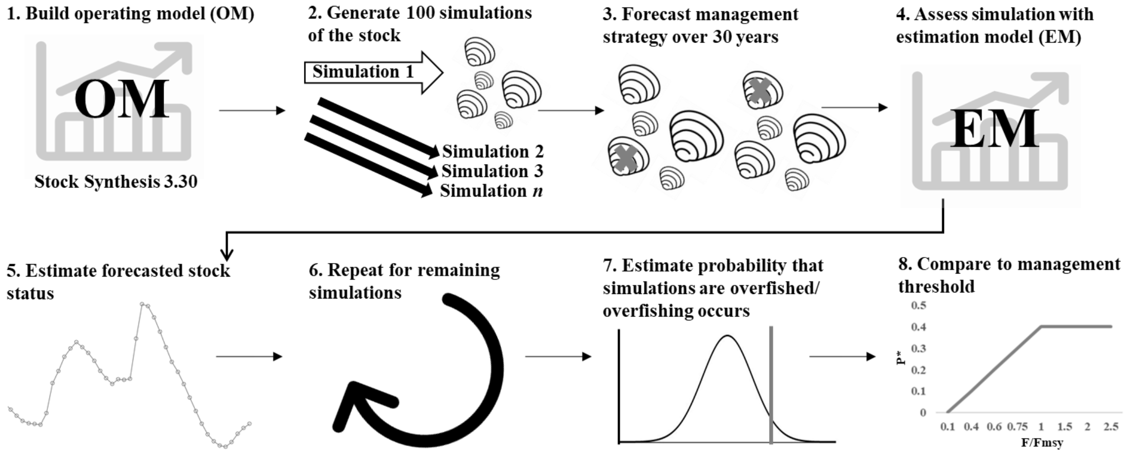

Figure 3.1 *Schematic of Simulation Analysis*

Simulations were conditioned from 1965 to 2015 and were forecasted under alternative management procedures for 30 years through 2045. To simulate stochasticity in recruitment, forecasted recruitment deviations were randomly generated from a normal distribution built with the 2016 assessment estimates of log recruitment deviations, N(0.0, 0.68). The forecasted recruitment estimates were not bias-adjusted. Simulations were forecasted with five alternative management strategies applied without error to each simulation during the forecast period (Table 3.1). The forecasted simulation was then assessed by each of the six alternative estimation models (EMs), one of which fixed *h* and *M* to the same values of the operating model from which the simulation was generated. The EM with common values to the generating OM (EM = OM) gave the “true” stock status of the simulation, whereas status estimated by all other EMs offered what managers would estimate if the assessment model incorrectly specified either or both *h* and *M*. Six hundred simulations across the six operating models were generated and each was evaluated under 30 configurations of EM structure and management control rule. A total of 18,000 simulated forecasts were generated and assessed.

Table 3.1 *Forecasted Management Strategies*

Management Rule	**Catch or *F***	**Relevance to Fishery**
Quota	Catch = 26,218 mt	Long-term fishery-implemented quota
ABC_Low	Catch = 45,524 mt	ABC assigned by MAFMC in 2016
ABC_High	Catch = 60,313 mt	ABC assigned by MAFMC prior to 2016 and again in 2018
$\mathbf{F_{0.12}}$	$F = 0.12\ yr^{-1}$	MSY Proxy determined by Hennen (2016)
$\mathbf{F_{0.4}}$	$F = 0.4\ yr^{-1}$	Hypothetical upper boundary on fishing mortality

Management strategies evaluated for Atlantic surfclam. Catch is reported as metric tons (mt), and fishing mortality is total fishing mortality rate per year.

3.2.3 Evaluation of risk

The current assessment model states that SSB_{MSY} is equal to 50% of the unexploited spawning stock biomass (SSB_0), which is calculated in each model configuration at the beginning of the timeseries in 1965. The threshold that a surfclam stock becomes overfished is ½ of SSB_{MSY}, thus a stock is overfished if SSB < ½ SSB_{MSY}. Both SSB_{MSY} and the Overfished Threshold are presented and compared to forecasted biomass estimates. The total number of simulations that became overfished during the forecasted period was reported for each combination of OM, EM, and management strategy. Estimates of F_{MSY} generated by each of the OMs (hereon, SSF_{MSY}) are reported, though the definition of overfishing used herein follows the MAFMC threshold from 2016, $F_{MSY} = 0.12\ yr^{-1}$, a proxy generated externally from the SS model by Hennen

(2016). Maximum *F* observed in forecasts for each OM, EM, and management strategy are reported and compared to the Overfishing Threshold, where overfishing is occurring if $F > F_{MSY}$. The MAFMC states that the probability of overfishing should not exceed 40% (MAFMC, 2020). This threshold was used to determine if the probability that a simulation became overfished or that overfishing occurred was within the risk-tolerance policy of the MAFMC.

3.2.4 Evaluation of Control Rule Consequences on Clam Density and Fishery Profitability

The commercial surfclam fishery relies on a catch rate of at least 1 cage hr^{-1} to maintain economic sustainability (NEFSC, 2017). The surfclam population is characteristically patchy, thus, the fishery relies on targeting dense patches of surfclam. One cage per hour equates approximately to a clam density of 0.22 clams m^{-2} under typical conditions and average gear efficiency (Powell et al., 2015). This level of clam density or greater is hereon described as “fishable”. Though total surfclam biomass may remain within management targets, thresholds for overfished and overfishing do not consider potential impacts of management strategies for maintaining a sufficient number fishable patches of clams to support the fishery. Observations of clam density m^{-2} are available from both the research dredge and modified commercial dredge surveys between 1997 and 2015. The 2016 assessment model estimated the ratio of unexploited biomass (SSB_{yr} / SSB_0) in each of these years, and these estimates were used in a simple linear regression to predict the percent of fishable survey tows (those that yielded greater than 0.22 clams m^{-2}). The estimated ratio of unexploited biomass for the final year of forecast from each simulation was then used in this regression to estimate the forecasted percent of fishable tows available to support the economic sustainability of the fishery.

3.3 Results

3.3.1 Stock Status of Operating Models

The six alternative operating models (OMs) estimated similar trends in surfclam biomass over time, though scale of biomass estimates varied with natural mortality (Figure 3.2). Initial SSB estimates for models configured with $M = 0.25\ \mathrm{yr}^{-1}$ were nearly twice as high as those for OMs configured with $M = 0.15\ \mathrm{yr}^{-1}$. Therefore, $\mathrm{SSB}_{\mathrm{MSY}}$ for OMs with $M = 0.15\ \mathrm{yr}^{-1}$ were on the scale of 22 million mt while $\mathrm{SSB}_{\mathrm{MSY}}$ estimates for OMs with $M = 0.25\ \mathrm{yr}^{-1}$ were nearly double, on the scale of 50 million mt (Table 3.2). Steepness had minimal impact on scale of biomass or estimates of recruitment deviation because biomass estimates remained high and above the point of the broodstock-recruitment curve where recruitment decreases with decreasing spawning biomass. Estimated fishing mortality across OMs was relatively similar for the duration of the timeseries, never exceeding $F = 0.03\ \mathrm{yr}^{-1}$, below the $\mathrm{F}_{\mathrm{MSY}}$ proxy of $F = 0.12\ \mathrm{yr}^{-1}$ (Figure 3.2). Some divergence between F estimates occurred after 2005, with models configured with $M = 0.25\ \mathrm{yr}^{-1}$ estimating slightly higher (~0.01) fishing mortality. Estimates of $\mathrm{SSF}_{\mathrm{MSY}}$ output from each of the operating models ranged from 0.69 to 0.71 yr^{-1}, more than 20 times the maximum estimate of fishing mortality throughout the timeseries (Figure 3.2). This high $\mathrm{SSF}_{\mathrm{MSY}}$ estimate was not approved as the overfishing definition in the 2016 stock assessment, and the Overfishing Threshold was instead calculated externally to the assessment model (NEFSC, 2017; Hennen, 2018). Similarly, OM-derived $\mathrm{SSF}_{\mathrm{MSY}}$ estimates are not examined as prospective Overfishing Thresholds for forecasted simulations, though their potential causes and implications are considered more thoroughly in the discussion.

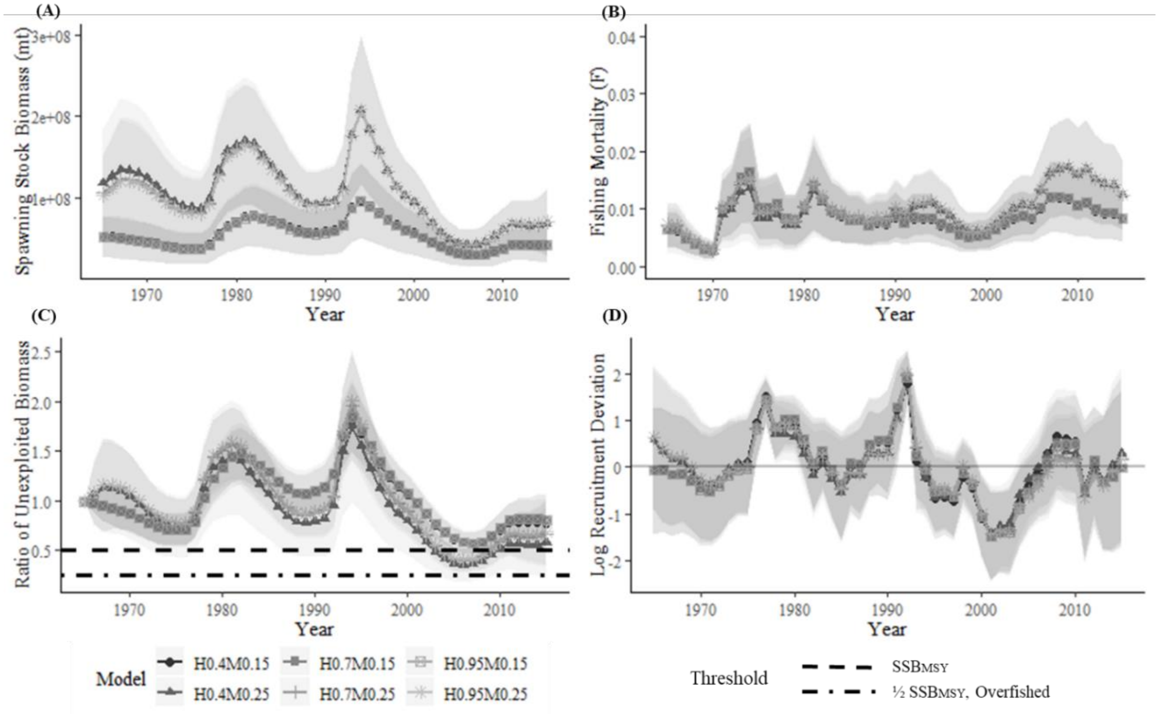

Figure 3.2 *Summary of Operating Model Timeseries*

Summary of timeseries estimates from six alternative operating models. Lines represent the estimate, and shaded greys are the confidence intervals. Dark grey shading indicates where confidence intervals overlap between models. Plots are timeseries estimates of (A) spawning stock biomass in metric tons, (B) fishing mortality rate (yr^{-1}), (C) ratio of current biomass to unexploited biomass (SSB_{yr} / SSB_0), and (D) log recruitment deviations from the specified broodstock-recruitment curve. Values in plot (C) are ratios and independent of scale, thus the common SSB_{MSY} (½ SSB_0) and Overfished Threshold (SSB < ¼ SSB_0) are marked with horizontal lines.

Table 3.2 *Operating Model Biomass Thresholds*

Model	SSB_{MSY} (million mt)	Overfished Threshold ½ SSB_{MSY} (million mt)
H0.4M0.15	23	12
H0.4M0.25	58	29
H0.7M0.15	22	11
H0.7M0.25	54	27
H0.95M0.15 (Base Model)	22	11
H0.95M0.25	57	29

Table of biomass thresholds estimated by the six alternative operating models. SSB_{MSY} is defined as 50% of the unexploited biomass and reported in metric tons. The Overfished Threshold is ½ of SSB_{MSY}.

The ratio of unexploited biomass across OMs also demonstrates considerable coherence between trends in biomass estimates. All models estimate a sharp increase in biomass in the early 1980s and mid-1990s. The decline from these peaks occurs most quickly in models with high natural mortality. The three OMs with $M = 0.25$ yr^{-1} fall below the SSB_{MSY} during the mid-2000s and finish the timeseries with the lowest estimated ratio of unexploited biomass, though all models remain above the Overfished Threshold. Finally, estimates of recruitment deviations show minor divergence at the beginning of the timeseries, though across models the timeseries of recruitment deviation estimates are largely coherent. Strong interactions between parameterizations of *h* and *M* were not apparent across the timeseries described in Figure 3.2, though H0.4M0.25 had the lowest ratio of unexploited biomass at the end of the timeseries.

3.3.2 Simulations and Forecast

Forecasts of simulations generated by the base OM, H0.95M0.15, assessed by the EM of the same parameterization, EM H0.95M0.15, and forecasted with each of the five alternative management strategies are presented in Figure 3.3 as an example of forecasted timeseries. As the OM and EM for these forecasts are the same, timeseries of biomass estimates prior to the beginning of the forecast period are identical. At the beginning of the forecast period, divergence occurs based on recruitment deviations and forecasted management. Independent of management strategy, few simulations fall below the threshold for SSB_{MSY} and no simulations fall below the Overfished Threshold in the forecasted 30 years.

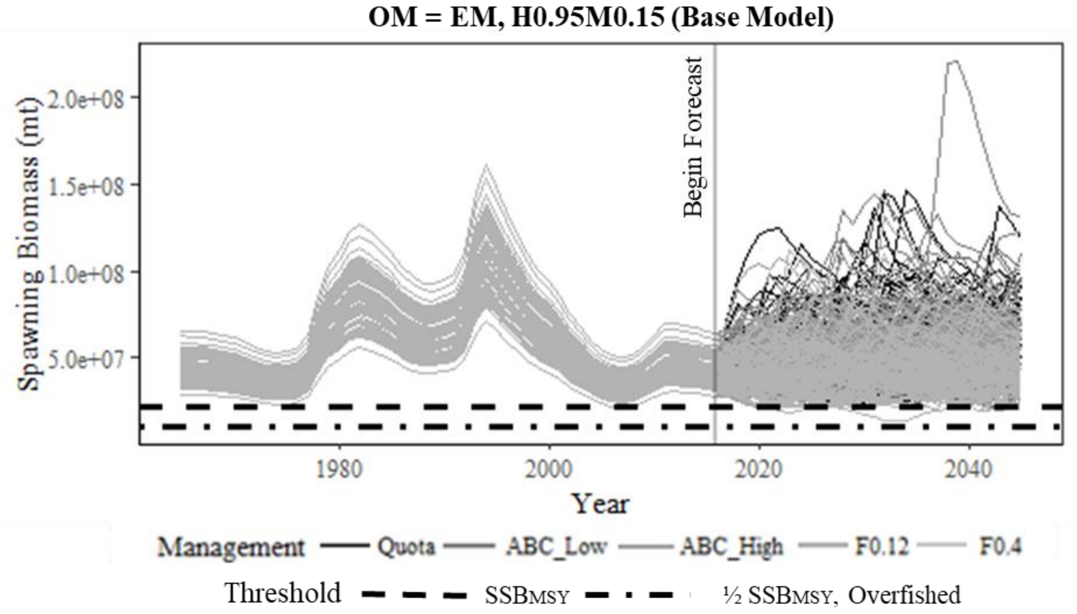

Figure 3.3 *Forecasts of Base Estimation Model*

Timeseries of spawning stock biomass estimates for each of the 100 simulations generated by the OM H0.95M0.15 and assessed using the identical EM, H0.95M0.15. Each simulation was forecasted with five alternative management strategies that remained constant throughout the forecast period.

3.3.3 Assessment of Overfished Simulations

Simulations assessed with EMs H0.4M0.15, H0.4M0.25, and H0.7M0.15 were the only forecasts that fell below the Overfished Threshold determined by the respective EM model (Table 3.3). Not surprisingly, the most extreme management strategy of $F_{0.4}$, fishing above the F_{MSY} proxy of $F = 0.12$ yr^{-1}, was responsible for the majority of simulations that became overfished across EMs. The total percent of simulations that became overfished under $F_{0.4}$ was 1.11%. Whereas EM H0.4M0.15 had the highest percentage of forecasts that became overfished at 0.67%, H0.4M0.25 was the only EM that forecasted each of the alternative management strategies to overfish in at least one simulation.

Table 3.3 *Summary of Percent Overfished Simulations*

EM	Management Strategy					% Total
	Quota	**ABC_Low**	**ABC_High**	**F0.12**	**F0.4**	
H0.4M0.15	0.00%	0.17%	0.00%	0.00%	3.83%	**0.67%**
H0.4M0.25	0.33%	0.17%	0.33%	0.83%	2.17%	**0.64%**
H0.7M0.15	0.00%	0.00%	0.00%	0.00%	0.67%	**0.11%**
H0.7M0.25	0.00%	0.00%	0.00%	0.00%	0.00%	**0.00%**
H0.95M0.15	0.00%	0.00%	0.00%	0.00%	0.00%	**0.00%**
H0.95M0.25	0.00%	0.00%	0.00%	0.00%	0.00%	**0.00%**
% Total	**0.06%**	**0.06%**	**0.06%**	**0.14%**	**1.11%**	

Percent of simulations run through each EM and harvested according to each management strategy that forecasted SSB below the overfished threshold (Table 3.2) during the forecast period. Grey scale indicates an increasing percentage of overfished simulations. Each combination of EM and management strategy forecasted 600 total simulations generated by the 6 alternative OMs.

No forecasted simulations became overfished for EMs H0.7M0.25, H0.95M0.15 and H0.95M0.25, so Table 3.4 focusses only on the EMs that forecasted an overfished stock. Notice in Table 3.4 that the row for "% Total" matches respective values for each EM and Management strategy in Table 3.3, though here the OMs that generated overfished simulations are explored. Managing with $F_{0.4}$ again results in the highest percentage of overfished simulations. Eight percent of simulations generated by OM H0.95M0.25, assessed by EM H0.4M0.15 and managed at $F_{0.4}$ became overfished. This OM was also responsible for the highest percent of overfished simulations for EM H0.4M0.25 and H0.7M0.15. In general, OMs parameterized with $M = 0.25\ \text{yr}^{-1}$ had the highest overfished percentage across management strategies and EMs. The most diverse set of overfished simulations were seen with EM H0.4M0.25, most of which were accounted for by OMs with $M = 0.25$ yr^{-1}, though H0.4M0.15 also became overfished by $F_{0.12}$ and $F_{0.4}$ when assessed by EM H0.4M0.25.

Table 3.4 *Details of Overfished Simulations*

Model		**Management Strategy**					**% Total**
EM	**OM**	**Quota**	**ABC_Low**	**ABC_High**	**F0.12**	**F0.4**	
H0.4M0.15	**H0.4M0.15**	0.00%	0.00%	0.00%	0.00%	3.00%	**0.60%**
	H0.4M0.25	0.00%	0.00%	0.00%	0.00%	6.00%	**1.20%**
	H0.7M0.15	0.00%	0.00%	0.00%	0.00%	1.00%	**0.20%**
	H0.7M0.25	0.00%	1.00%	0.00%	0.00%	3.00%	**0.80%**
	H0.95M0.15	0.00%	0.00%	0.00%	0.00%	2.00%	**0.40%**
	H0.95M0.25	0.00%	0.00%	0.00%	0.00%	8.00%	**1.60%**
	% Total	**0.00%**	**0.17%**	**0.00%**	**0.00%**	**3.83%**	
H0.4M0.25	**H0.4M0.15**	0.00%	0.00%	0.00%	1.00%	2.00%	**0.60%**
	H0.4M0.25	1.00%	0.00%	1.00%	1.00%	4.00%	**1.40%**
	H0.7M0.15	0.00%	0.00%	0.00%	0.00%	1.00%	**0.20%**
	H0.7M0.25	1.00%	0.00%	0.00%	2.00%	2.00%	**1.00%**
	H0.95M0.15	0.00%	1.00%	0.00%	0.00%	0.00%	**0.20%**
	H0.95M0.25	0.00%	0.00%	1.00%	1.00%	4.00%	**1.20%**
	% Total	**0.33%**	**0.17%**	**0.33%**	**0.83%**	**2.17%**	
H0.7M0.15	**H0.4M0.15**	0.00%	0.00%	0.00%	0.00%	0.00%	**0.00%**
	H0.4M0.25	0.00%	0.00%	0.00%	0.00%	1.00%	**0.20%**
	H0.7M0.15	0.00%	0.00%	0.00%	0.00%	0.00%	**0.00%**
	H0.7M0.25	0.00%	0.00%	0.00%	0.00%	0.00%	**0.00%**
	H0.95M0.15	0.00%	0.00%	0.00%	0.00%	0.00%	**0.00%**
	H0.95M0.25	0.00%	0.00%	0.00%	0.00%	3.00%	**0.60%**
	% Total	**0.00%**	**0.00%**	**0.00%**	**0.00%**	**0.67%**	

Details of the three EMs that forecasted overfished stocks. Increasing grey scale indicates a greater percentage of overfished simulations. The OM from which the overfished simulations were generated are presented, with the total percent overfished from Table 3.3 (% Total) available at the bottom of each EM for reference.

Estimation model H0.4M0.15 had the greatest total percentage of overfished simulations, most of which were managed with $F_{0.4}$. Timeseries of forecasted simulations managed under the highest ($F_{0.4}$) and lowest (Quota) harvest policies are displayed in Figure 3.4. Whereas many simulations fall below SSB_{MSY} when fished at Quota, no simulation generated from any OM falls below the Overfished Threshold. The median trajectory for the forecasted timeseries of each OM is increasing, though there is a clear disparity between OMs based on natural mortality. Operating models parameterized with $M = 0.15$ yr^{-1} have higher SSB estimates throughout the forecast. This persists when simulations were fished at $F_{0.4}$. When simulations are fished at $F_{0.4}$, immediate decline in median trajectory occurs at the onset of the forecast, and many more simulations fall below SSB_{MSY} than when managed at Quota. Some simulations also fall below the Overfished Threshold and a few stocks crash to zero SSB.

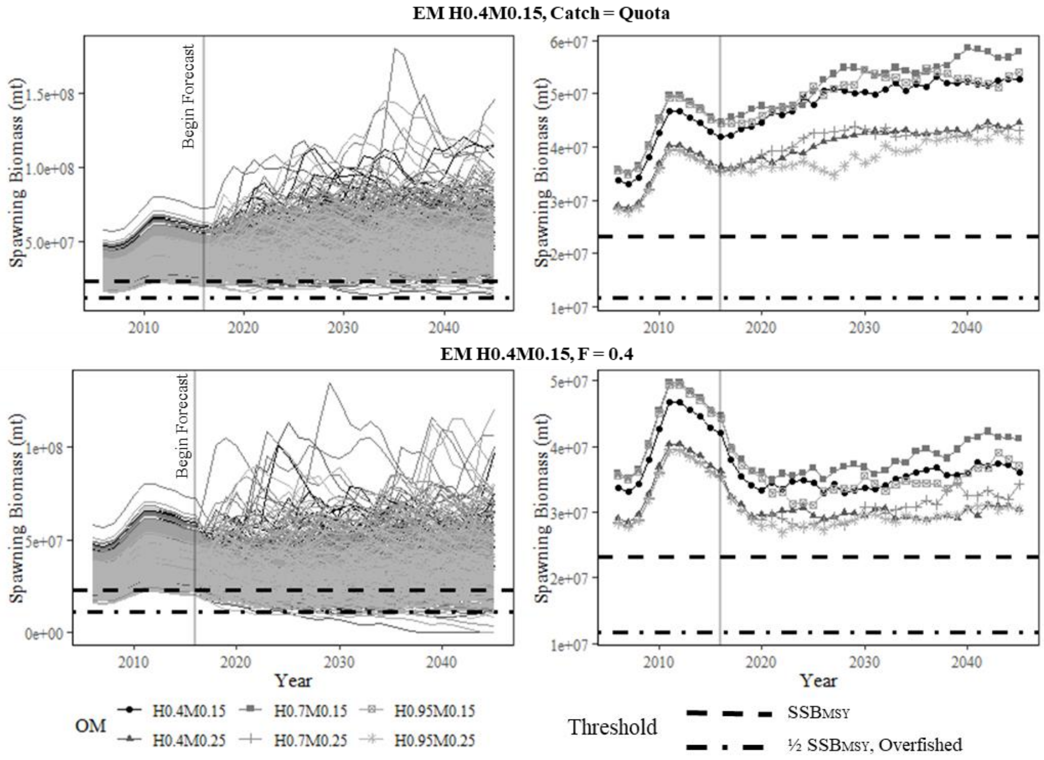

Figure 3.4 *Overfished Simulation Timeseries*

Forecasts of EM H0.4M0.15 harvested according to the Quota of 26,218 mt (top) and fishing mortality of $F = 0.4$ yr^{-1} (bottom). Forecasted timeseries for all simulations generated by each OM are on the left, and the median forecasted SSB for simulations from each OM are on the right. SSB_{MSY} and the Overfished Thresholds for EM H0.4M0.15 from Table 3.2 are displayed as horizontal lines. Note difference in y-axis scales across plots.

3.3.4 Occurrence of Overfishing

The FMSY proxy presented in the 2016 assessment of FMSY = 0.12 yr-1 was used as the Overfishing Threshold. Overfishing is first examined for forecasts of simulations where EM = OM, representing the “true” fishing mortality estimate, then compared to fishing mortality estimates from all simulations assessed with each EM. Fishing mortality unsurprisingly is driven by management strategy, and F0.4 results in overfishing in 100% of simulations (Figure 3.5). Managing with F0.12 resulted in overfishing of 69 – 84% of simulations. The percent of simulations experiencing overfishing was greatest in simulations with high natural mortality, and this carried through to simulations managed with ABC_High. Between 2 and 4% of high mortality simulations experienced overfishing from managing at ABC_High, while low mortality simulations remained below the Overfishing Threshold. Overfishing occurred in slightly differing proportions between simulations assessed by EM = OM and all simulations forecasted with each EM, though no clear pattern or direction of these differences was observed. Estimation model H0.4M0.25 estimated overfishing of <1% of simulations managed with ABC_Low, though managing at quota estimated no overfishing across EMs.

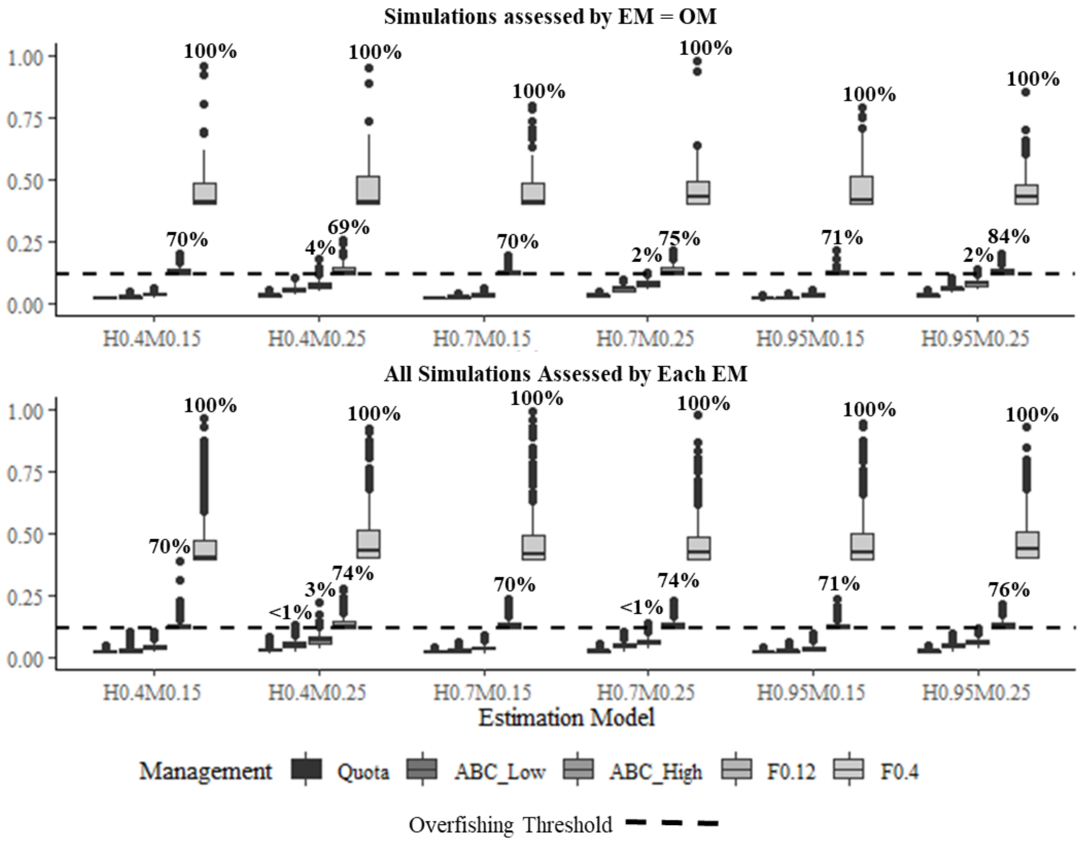

Figure 3.5 *Incidence of Overfishing in Simulations*

Maximum fishing mortality yr^{-1} observed during the forecast of a simulation. Top plot separates models by OM, representing the “true” fishing mortality. Bottom plot is maximum fishing mortality estimated by EMs. If simulations from a management strategy and EM passed the Overfishing Threshold of $F_{MSY} = 0.12\ yr^{-1}$, the percent of simulations that did so is displayed.

3.3.5 Fishery Profitability

The annual percent of fishable tows observed by the NEFSC survey ranged from 20% to 45% and was significantly related to estimated ratio of unexploited biomass (SSB_{yr} / SSB_0) from the 2016 stock assessment ($p < 0.01$, $r^2 = 0.80$; Figure 3.6). Because estimation models are an interpretation of the stock while operating models act as the true realization of the generated stock, forecasted estimates of percent fishable tows are only displayed for simulations assessed with the EM of the same configuration to the generating OM. Across models, forecasted estimates of percent fishable tows were in line with observations by the NEFSC survey, between 25 and 50% (Figure 3.7). Estimated percent of fishable tows for H0.4M0.15 declined the most with increasing fishing mortality, suggesting low steepness could compound with low natural mortality to limit proportion of fishable tows. Percent fishable tows from high mortality models responded less to increasing fishing pressure, though lowest percent across models was generally observed at $F_{0.12}$ and $F_{0.4}$.

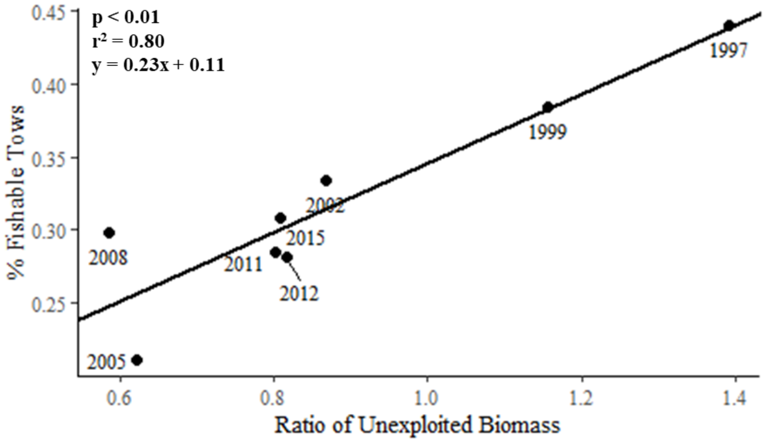

Figure 3.6 *Regression of Observed Fishable Tows*

Each point indicates the percent of NEFSC survey tows that were “fishable”, defined as capturing more than 0.22 clams m^{-2} (Powell et al., 2015) in each year the survey was performed between 1997 and 2015. The x-axis is the ratio of unexploited biomass (SSB_{yr} / SSB_0) in each corresponding year estimated by the 2016 stock assessment.

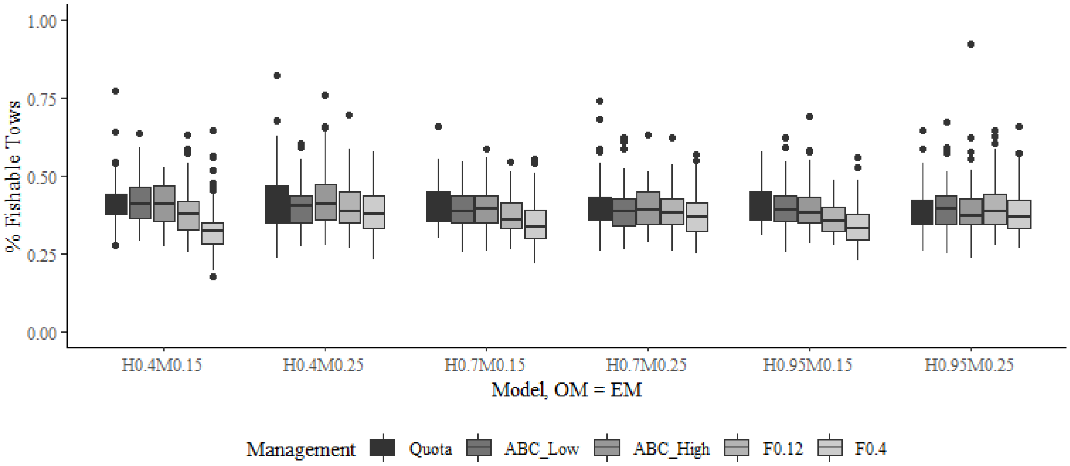

Figure 3.7 *Simulated Percent Fishable Tows*

Percent of fishable tows estimated from the ratio of unexploited biomass (SSB_{yr} / SSB_0) in the terminal year of forecast for each simulation where EM = OM.

3.4 Discussion

Despite uncertainty in natural mortality and steepness, the Atlantic surfclam Southern stock appears to be robust to overfishing across a variety of management strategies. The Atlantic surfclam quota has remained stable since the 1980s and below the ABC because of economic constraints within the fishery. In the simulations presented here, across all model specifications, fishing at Quota never permitted fishing mortality to rise above the assessment proxy for $F_{MSY} = 0.12$ yr^{-1} and fewer than 1% of simulations forecasted with ABC_Low breached this threshold. ABC_High and $F_{0.12}$ led to overfishing in many simulations, especially those with high natural mortality. Management strategies $F_{0.12}$ and $F_{0.4}$ fell outside of the risk-tolerance policy of the MAFMC, overfishing the stock in reference to $F_{MSY} = 0.12$ yr^{-1} in more than 40% of simulations across OM and EM structures.

Managing at $F_{0.4}$ was also the strategy that caused the most simulations to become overfished, especially for stocks with high natural mortality or if the assessment model overestimated steepness. For example, although 3% of simulations generated by OM H0.4M0.15, assessed by the identical EM H0.4M0.15 and forecasted with $F_{0.4}$ became overfished, no EM with steepness greater than 0.4 perceived this overfished state. To a lesser extent, this is true for H0.4M0.25 as well. These simulations suggest that while the broodstock-recruitment curve is not well understood for surfclam, if the steepness is in fact low, assessments parameterized with high steepness may not detect an overfished state. Though estimation models with steepness values of 0.4 or 0.7 predicted some overfished simulations, fewer than 40% of simulations became overfished, within the MAFMC risk-tolerance policy.

Across OM and EM structures, managing with $F_{0.4}$ was responsible for the greatest proportion of overfishing and the most overfished simulations. However, it is also important to note that $F_{0.4}$ is an extreme management strategy used herein to juxtapose the comparatively conservative quota and ABCs. The surfclam fishery is a high volume, relatively low value fishery, that depends on high CPUE to meet economic requirements. The fishery is not constrained by the current quota and unlikely to pursue fishing at such volumes that would decrease profit margins, a consequence of fewer fishable tows predicted in forecasts of this management strategy. Simulating management at $F_{0.4}$ does add credence to the external development of F_{MSY} proxies for surfclam, however. F_{MSY} based on the stock assessment has never been used for surfclam management. Rather, F_{MSY} has been based on a population simulation conducted outside of the stock assessment framework (Hennen, 2018). One of the primary reasons for this is that the surfclam stock has been near or above SSB_{MSY} throughout the observed timeseries and consequently unable to inform on the broodstock-recruitment relationship at low stock size. In addition, the 2016 surfclam stock assessment was highly uncertain in scale. An F_{MSY} value from the assessment (i.e., SSF_{MSY}) would also be highly uncertain, and potentially inappropriate for management. Managers therefore chose to set the *F* threshold based on *F* values from a selected portion of the timeseries during which fishing was thought to have little measurable effect on the indices of stock abundance (a period of relatively low intensity fishing). The current *F* threshold for management is an expansion of the average *F* over this period (Hennen, 2018).

Results presented here reinforce the reasons behind the external derivation of F_{MSY} and the potential risk of using SSF_{MSY} output from the assessment model as the management threshold. Despite differences in scale of absolute biomass across OMs, SSF_{MSY} estimates varied little between operating models independent of steepness or natural mortality, ranging between 0.69 and 0.71 yr^{-1}. These high estimates could be a result of delayed selectivity in the fishery. As mentioned previously, while Atlantic surfclam fully mature by age-2 (Chintala and Grassle, 1995), the fishery begins to select for clams around age-5. With spawning biomass outside of the fishery selectivity, SS converges on a high estimate of SSF_{MSY}, one that is much larger than any historical estimates of fishing mortality. Given the number of simulations that became overfished when fishing at $F_{0.4}$, setting a threshold for overfishing at $SSF_{MSY} = 0.70$ yr^{-1} could lead to an overfished stock before overfishing is detected by management, especially with the consideration of uncertainty around steepness.

The issue of fishery selectivity carries through to natural mortality and the uncertainty in scale of absolute biomass of the surfclam stock. Operating models with high natural mortality estimated nearly double the unexploited stock size as the low mortality counterparts. Punt et al. (2021) explained why natural mortality can contribute uncertainty to biomass estimates. As with the commercial fishery, the surfclam survey largely observes clams age-5 and older, making it difficult to estimate the unexploited equilibrium age distribution of younger clams. Higher natural mortality increases the rate of decline in numbers at age, requiring a greater equilibrium number of age-0 clams to support the observed numbers of age-5+ individuals. Given early maturity, the larger number of young clams contributes to the greater spawning stock biomass. Above age-5 when age-distribution data is more available, equilibrium age distributions between operating models with $M = 0.15\ \mathrm{yr}^{-1}$ and $0.25\ \mathrm{yr}^{-1}$ largely correlate, which may explain why estimates of F are similar across operating models, though scale of biomass varies.

The prospective influence of ocean warming on increasing natural mortality rates across some portion of the surfclam stock (Monroe et al., 2013; Narvaez et al., 2015; Monroe et al., 2016; Hofmann et al., 2018) fuels concerns for how changes in natural mortality may alter the actual or perceived scale of biomass and uncertainty in future assessments. Atlantic surfclam are sensitive to temperatures exceeding 21°C (Munroe et al., 2013), and modern warming of the northwest Atlantic is thought to be a driver of mortality events at the inshore and southern extents of the stock (Kim and Powell, 2004). Furthermore, increased observations of recruitment events further north and offshore of their typical range suggest a changing distribution (Hofmann et al., 2018). These events are coincident with declines in patchiness (Timbs et al., 2019) and maximum size over much of the geographic range (Munroe et al., 2013, 2016) with potential consequences to regional mortality and economics of the commercial fishery (Powell et al., 2015, 2016).

Profitability of the commercial surfclam fishery is dependent on the number and density of clam patches, a long-understood constraint that (at least in part) led the industry to impose a quota cap to prevent the reduction in clam density below what is economically stable (Adelaja et al., 1998; Rountree, 2015). This quota has been and continues to remain below the Council's ABC management control rule and has likely contributed to the sustainability of the Atlantic surfclam stock, a fishery that the stock assessment has never designated as overfished nor noted the occurrence of overfishing (NEFSC, 2017). These results demonstrate that the quota and ABCs are conservative to the risk-tolerance policies of the MAFMC, though in the face of global warming and potential shifts in surfclam distribution, alternate management approaches such as rotating closures may need to be explored to insulate the fishery from unexpected declines (Kuykendall et al., 2017).

While fishery economics may falter from decreases in fishable patches before an overfished status is determined, our results suggest that if population and fishery dynamics persist in a largely status-quo manner for the foreseeable future (save for moderate recruitment variation), proportion of fishable patches will remain high enough to support the current commercial fishery. However, the timeseries of NEFSC survey tows demonstrate that while the fishery has remained relatively consistent since the 1990s, clam density and biomass has fluctuated over that same period. Environmental conditions are likely to affect population dynamics of the surfclam stock inconsistently throughout their distribution, reinforcing the difficulty of forecasting the stock in a dynamic and warming ocean. This work demonstrates that even with uncertainties in steepness and natural mortality, the surfclam stock is unlikely to become overfished or experience overfishing from currently implemented management strategies. However, consequences of overestimating steepness in forecasts demonstrate that variation in steepness or mortality could result in misrepresentation of an overfished stock under high fishing pressure. Population dynamics of surfclam are stochastic and that stochasticity is, at least in part, related to environmental conditions that are rapidly changing in the northwest Atlantic. Future evaluations are needed to determine how the population varies in forecasts when population dynamics parameters are allowed to vary in a multi-year or decadal fashion. Variable growth or temporal variability in the rate of range recession inshore and expansion offshore could be the uncertainties of focus in future simulation analyses and management.

CHAPTER IV – DO MANAGEMENT STRATEGIES GUIDED BY SEX-AGGREGATED MODELS EFFECTIVE AT MANAGING A SEXUALLY-DIMORPHIC STOCK?

4.1 Introduction

Summer flounder (*Paralichthys dentatus*) supports a large commercial and recreational fishery along the US Eastern seaboard, and management of this fishery has historically been contentious (Terceiro, 2001, 2011, 2018). Some of the animus has risen from difficulty modeling complex population dynamics parameters (notably sex-specific growth, mortality and spatial distribution [Maunder & Wong, 2011; Maunder, 2012; Henderson et al. 2014]) to effectively describe the stock and estimate outcomes of management decisions. Though it is known that summer flounder exhibit sexual dimorphism (Morson et al. 2012), spatio-temporal variation of summer flounder distribution inshore, offshore, and throughout the US-Atlantic coast (Buchheister et al. 2010; Henderson et al. 2014) has made it difficult to adequately describe the sex-specific complexities in a single, coastwide stock assessment model (Terceiro, 2018). Despite the extensive distribution of summer flounder and evidence of environmental selection (Hoey & Pinsky, 2018), genetic homogeneity persists throughout their range, suggesting a single spawning stock that justifies managing with a coastwide assessment model (Irwin et al. 2022). While models incorporating some of these complexities in population dynamics have been presented and discussed at benchmark assessment meetings, the assessment model has remained sex-aggregated, due at least in part to insufficient evidence that additional sex-specific complexity has compensated with reduced uncertainty in stock assessment model estimates (NEFSC, 2019).

4.1.1 Retrospective Error

Whereas the current structure of the assessment model has been selected over alternative models and approved by the Scientific and Statistical Committee during research track assessments, retrospective errors in estimates of recruitment, *SSB* (spawning stock biomass), and *F* (fishing mortality) have underscored uncertainty in how well the model structure describes current stock status (Terceiro, 2018; NEFSC, 2019). Retrospective analyses have consistently demonstrated positive inconsistencies in terminal year estimates of *SSB* and recruitment, in which updated estimates of contemporary estimates are revised downward. Meanwhile, *F* has negative retrospective inconsistencies, in some years by as much as -0.20 yr^{-1}.

When adjusted for internal retrospective error, the estimates of *SSB* and *F* are within 90% confidence intervals of previous assessments (NEFSC, 2019), though efficacy of management decisions guided by this adjustment may have consequences on long-term yield (Deroba, 2014). Although retrospective patterns were minimized in the 2018 assessment, in part due to recalibration of recreational landings data from 1982 – 2017 (NEFSC, 2019), *SSB* and *F* are the basis from which managers determine if a stock is overfished or overfishing is occurring, and the directionality of retrospective errors in the 2018 assessment favored the estimation of a sustainable stock. Among the unresolved issues is the severe bias towards large females in the recreational fishery landings (ref). Because the assessment model is sex-aggregated and retrospective errors were resolved with the recalibration of historical recreational landings, further consideration needs to be given to how uncertainty in the female-dominated recreational fishery may contribute to retrospective errors and the degree to which sex-specificity might affect stock status inferred from the aggregated assessment model.

4.1.2 Uncertainty in Recreational Landings

Recreational landings have been monitored and estimated since 1982. The NMFS Marine Recreational Fishery Statistics Survey (MRFSS) estimated recreational landings and discards from 1982 to 2003 and was then replaced by the Marine Recreational Information Program (MRIP) which has operated since 2004. In 2018 the historical timeseries of MRFSS/MRIP estimates were recalibrated to account for new survey methods that were fully implemented in 2018. This recalibration led to substantial changes in estimates of historical recreational fishery landings and discards. On average, recreational landings estimates increased by 84% (~3,300 mt) and discards by 70% (521 mt). The recalibrated MRIP estimates now suggest that the recreational harvest limit (RHL) was exceeded in each year since 2000. Despite the apparent historical overharvest (relative to annual RHL), the new MRIP estimates increased the assessment model estimate of SSB, and subsequently the RHL was increased in 2019 from 2,300 mt to 5,200 mt (ASFMC, 2018; ASFMC, 2019; NEFSC, 2019).

Female flounder account for 90% of recreational landings (Morson et al. 2017), due in part to the sexual dimorphism of summer flounder. Females tend to be larger (Langan et al. 2019), live longer (Maunder & Wong, 2011), and are observed at higher ratios in shallow inshore waters where the recreational fishery operates (Morson et al. 2015), though Morson et al. (2017) noted that males dominated recreational discards. Minimum size limits in both the recreational and commercial fishery inherently exclude a greater portion of the males than females from fishery harvest. As the ratio of female flounder is skewed in recreational landings, and recreational landings are highly uncertain (Hicks & Shnier, 2016), it is imperative to account for how management decisions informed by a sex-aggregated assessment model may impact the future spawning potential of the summer flounder stock.

4.1.3 Objectives

Here, a simulation analysis is conducted to evaluate the potential consequences of using a sex-aggregated assessment model to describe the sexually-dimorphic summer flounder fishery. A provisional sex-specific model is developed to an alternative sex-aggregated assessment model. Retrospective patterns in *SSB*, *F*, and recruitment are presented to compare with errors observed by previous assessment models. Simulations generated by the sex-specific operating model and forecasted with sex-aggregated estimation models may inform on the risk of managing summer flounder with a sex-aggregated assessment model.

4.2 Methods

4.2.1 Assessment Model Structure

The Age Structured Assessment Program (ASAP; a forward-computing age structured model; Legault & Restrepo, 1998) is currently used to model the summer flounder stock (NEFSC, 2019). The stock is modeled from 1982 to 2019 with four fishing fleets and 26 age-specific survey indices. Age compositions for flounder are aggregated by sex and modeled from age-0 to -7+, where individuals older than seven are aggregated into this plus group. The four fishing fleets are commercial landings, commercial discards, recreational landings and recreational discards. Of the 26 survey indices, seven are coastwide federal surveys and the remainder are state or academic surveys conducted over a smaller spatial range. Three of the federal indices are trawl surveys (Fall, Winter and Spring) and two are larval SSB surveys. Matrices of natural mortality, maturity, and weight-at-age are specified for each year, consistent with observations of interannual growth variability in summer flounder (Nys et al. 2016). Finally, fleet-specific selectivity-at-age is divided over time-blocks that represent historical shifts in management.

4.2.2 Conversion to Stock Synthesis

The underlying structure of the 2019 assessment in ASAP (NEFSC, 2019) was used to develop a sex-specific operating model (OM) in stock synthesis (SS) version 3.30 (Methot et al. 2019). SS is a flexible likelihood-based statistical catch-at-age model that can emulate a statistical catch-at-age model like ASAP with sex structure and has internal bootstrapping and forecasting functions that make it ideal for running simulation analyses. Li et al. (2021) demonstrated that when configured in the same manner, both SS and ASAP model structures produced similar results from simulated data. Thus, the ASAP assessment model structure was used to configure a sex-aggregated SS model. The sex-aggregated SS model then formed the basis of comparison between both the ASAP assessment model and sex-specific SS model.

Wherever possible, the ASAP model configuration was maintained to support comparison with the currently accepted stock assessment, though some changes were necessary to account for differences in parameter requirements between model structures. The state and academic survey indices were excluded from the SS model because of their restricted spatial extent, incoherent trends between surveys, and difficulty in determining the extent that sex-specific data was subsampled for each survey. Sex-specific information was also unavailable for the federal larval surveys. Thus, for a more direct-comparison between the sex-aggregated and sex-specific SS models, only the four fishing fleets and three NEFSC trawl surveys were incorporated into SS models.

Matrices for age-specific maturity and natural mortality were reduced to the most recent ten-year averages. Average maturity-at-age from 2009-2018 was calculated from the ASAP assessment model and fixed as the vector of maturity in SS. Sex aggregated natural mortality was set to the assessment average of $M = 0.25$ yr^{-1}. A double logistic selectivity pattern was open to estimation for all fleets, and time-varying selectivity was allowed for each of the fisheries.

A sex-specific model was then constructed using the sex-aggregated model structure. Alternative male- and female-only assessment models were presented at the 2016 stock assessment model workshop (NEFSC, 2016), which provided sex-specific landings-at-age data from 1982 – 2016 for the four fishing fleets and three NEFSC trawl surveys. The average ratio of fleet- and sex-specific landings-at-age from 2006 – 2015 was used to parse fleet-specific landings-at-age from 2016 to 2019. Length data was also available for the fisheries, though these data were down-weighted to zero in the SS models. In part, this is because length-compositions cannot be included in ASAP, so by down-weighting lengths the SS models further mirrored the ASAP structure. In addition, allowing length-compositions to be modeled by SS led to issues in model convergence in both the sex-aggregated and sex-specific SS models, therefore length-compositions are included in the model framework, though are turned off to estimation for the purposes of these simulations. Natural mortality followed the parameters used in the male- and female-only ASAP models, where male and female natural mortality were set to 0.30 and 0.20 yr^{-1}, respectively, informed in part by Maunder and Wong (2011).

Estimates of unexploited recruitment (R_0), unexploited spawning stock biomass (SSB_0), and SSB at maximum sustainable yield (SSB_{MSY}) generated by each of the SS models are reported and compared to values generated by the 2019 ASAP assessment model. Retrospective analyses were also conducted for each of the SS models to examine if any of the patterns previously observed in the ASAP assessment were observed in these model configurations.

4.2.3 Simulation Analysis

An operating model (OM) was conditioned on results from the provisional sex-specific SS model with time-varying selectivity. Simulations were generated using the SS bootstrap function, which uses maximum likelihood estimation to simulate new observations of available data constructed from the error and associated distribution of each observation (Methot et al. 2017). Ten simulations of the summer flounder dataset were generated from the OM model, which were then assessed by both the sex-specific OM and alternative sex-aggregated estimation model (EM) structure. Each simulation was then forecasted with four management strategies that either represent recent management decisions for the commercial and recreational fishery or F_{MSY}-proxy reference points from recent assessments (Figure 4.1). Error in recreational harvest was also examined to consider the impacts of implementation error historically observed in the fishery. Recreational harvest in each year was randomly selected around the recreational harvest limit of 3,700 mt, with error allowance of 2,000 mt above or below the assigned harvest. Finally, a forecast of Zero Fishing was implemented to ensure forecasts and simulations were operating properly. Simulations were forecasted for 30 years, representing more than two generations of summer flounder. This offers a long-term reference to how management decisions would perform for the sex-specific stock, and how the stock would be interpreted by sex-aggregated model configurations.

Table 4.1 *Forecasted Management Control Rules*

Management Rule	Catch or F	Error	Relevance to Fishery
No Error	Commercial Quota = 5,600 mt; Recreational Harvest Limit = 3,700 mt	No	2019 Commercial Quota, Recreational Harvest Limit
Implementation Error	Commercial Quota = 5,600 mt; Recreational Harvest Limit = 3,700 mt	+/- 2,000 mt	2019 Recreational Commercial Quota, Harvest Limit plus error
F35_Low	$F = 0.309\ y^{r-1}$	No	2013 estimated F associated with 35% of Maximum Spawning Potential
F35_High	$F = 0.448\ yr^{-1}$	No	2019 estimated F associated with 35% of Maximum Spawning Potential
No Fishing	$F = 0$	No	Check of Forecast Performance

Management strategies forecasted for summer flounder. Error in the recreational fishery catch was randomly selected in each year between 0 and 2,000 mt metric tons above or below the recreational harvest limit.

Forecasted spawning stock biomass for each of the simulations was then compared to SSB_{MSY} and the overfished threshold (1/2 SSB_{MSY}) of the sex-specific operating model. However, in sex-specific SS models, only female biomass contributes to the calculation of spawning stock biomass, where SSB in a sex-aggregated model accounts for biomass of all spawning individuals, both male and female. Brooks et al. (2008) found that management targets calculated with female-only or sex-aggregated biomass similarly estimated the true reference point for a stock in a simulation study. Therefore, the sex-specific OM estimate of SSB_{MSY} was used as the threshold to determine if a forecasted simulation was overfished for simulations assessed by both the sex-specific OM and sex-aggregated EM, though note that SSB of sex-aggregated forecasts are higher than sex-specific counterparts because all aggregated spawning biomass, independent of sex, contributes to the spawning stock biomass.

4.3 Results

4.3.1 Model Comparison

The two stock synthesis model configurations are abbreviated as SS_Sex (sex-specific operating model) and SS_Agg (sex-aggregated estimation model). Though R_0 values were similar across both SS models, estimates of SSB_0 for the sex-aggregated model was nearly double the sex-specific counterpart because in sex-specific models SS only attributes female biomass to the calculation of SSB (Table 4.2). Though estimates from the Sex_Agg model were most similar to ASAP, SSB_0 was lower than ASAP for both SS configurations. Unexploited values between ASAP and SS models were dissimilar, though values were more coherent in the timeseries of SSB (Figure 4.1). From 1982 to the early 2000s the sex-aggregated timeseries tracs along the ASAP estimates of SSB. Fishing mortality estimates between the SS models were also strongly coherent, with peaks in fishing mortality in the early 1990s that tapered into the early 2000s. While recruitment estimates for the ASAP model are consistently higher than the SS models, trends in recruitment are similar until 2016.

Table 4.2 *Model Comparisons*

	Model Structure		
	ASAP	**SS_Agg**	**SS_Sex**
R_0 (millions)	50.5	23.01	22.51
SSB_0 (mt)	145,924	108,273	53,972
SSB_{MSY} (mt)	26,583	18,310	9,591
$SSB_{Threshold}$ (mt)	13,291	9,155	4,796

Comparison between the two SS models and ASAP. Unexploited recruit numbers (R0, in millions), unexploited spawning stock biomass (SSB0. in metric tons), estimates of SSB at maximum sustainable yield (SSB_{MSY}, in metric tons), and the overfished threshold are compared between the ASAP assessment and SS models. Note that sex-specific SS models calculate SSB using only spawning female biomass while biomass from all mature individuals contributes to SSB in sex-aggregated models.

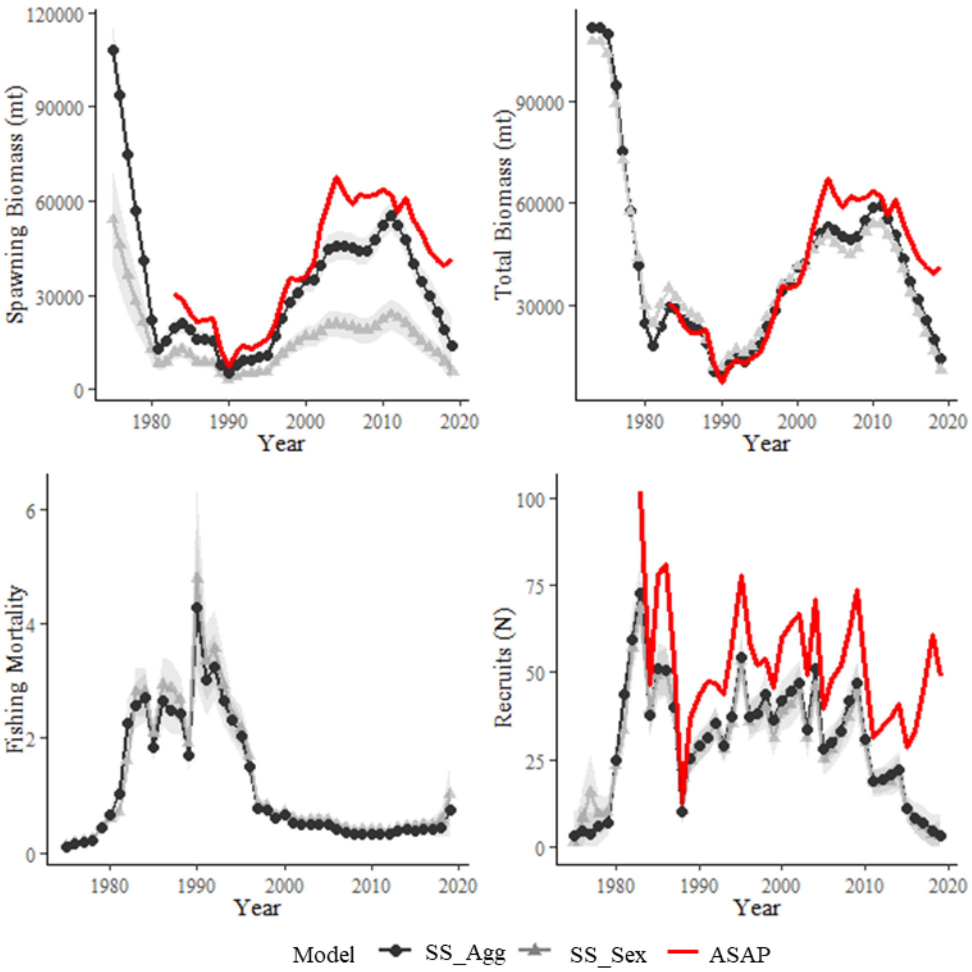

Figure 4.1 *Timeseries of the Four Base SS Models*

Plots are timeseries of (A) spawning stock biomass estimates in metric tons, (B) total biomass estimates in metric tons, (C) estimated fishing mortality per year, and (D) estimated number of recruits in millions. Annual fishing mortality estimates were not available from the 2019 assessment document, thus the ASAP model values are not shown for plot C. Shaded grey are confidence intervals around estimates. Note that sex-specific SS models calculate SSB using only spawning female biomass while biomass from all mature individuals contributes to SSB in sex-aggregated models.

4.3.2 Retrospective Analysis

Retrospective patterns in spawning stock biomass were most visible for the sex-aggregated model (Figure 4.2). Terminal year estimates of SSB had a pattern of positive retrospective inconsistencies for the sex-aggregated model, though this pattern was most overt between 2011 and 2015. The sex-specific SS model also demonstrated this pattern, though it was less consistent. Alternatively, retrospective errors in fishing mortality were greater for the sex-specific model. Fishing mortality had a pattern of negative retrospective inconsistencies in the terminal year, though it appears that estimates of fishing mortality resolve to the eventual estimate within one year. No discernible pattern in retrospective errors could be identified in estimates of recruitment across model configurations.

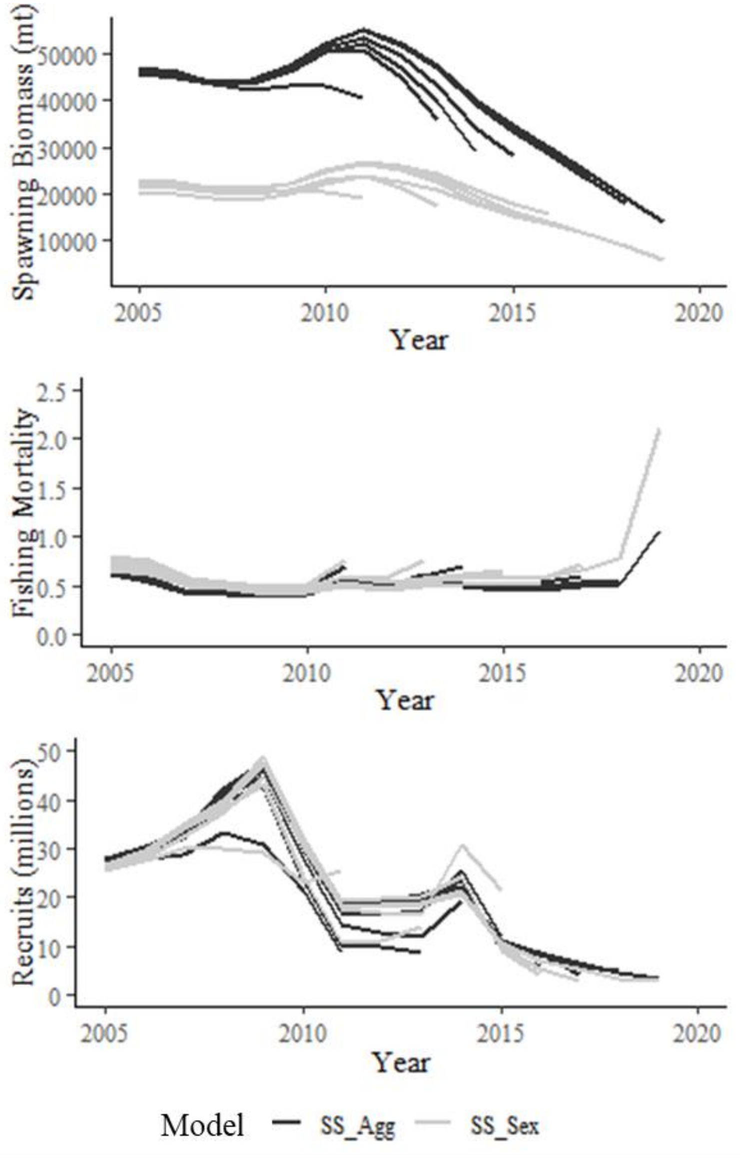

Figure 4.2 *Retrospective Analysis of SS Models*

Retrospective error in (top) Spawning stock biomass in metric tons, (B) fishing mortality yr-1, and (C) number of recruits in millions. Terminal years of retrospective models extend from 2011 to 2019. Note that sex-specific SS models calculate SSB using only spawning female biomass while biomass from all mature individuals contributes to SSB in sex-aggregated models.

4.3.3 Simulation Analysis

The operating model (OM), SS_Sex, generated 100 sets of simulated data. Model convergence was achieved with 88 of these simulated data sets, and only those converged simulations were run through the sex-aggregated estimation model, SS_Agg. The simulated biomass timeseries from the sex-aggregated EM mirrored the dynamics observed in the base model runs (Figure 4.3). The sex-aggregated model estimated higher SSB than the sex-specific OM because biomass from all mature individuals contributes to the SSB in a sex-aggregated model, while only female biomass contributes to SSB in the sex-specific model. All simulations assessed by both the sex-aggregated EM and sex-specific OM remained above both the SSB_{MSY} and ½ SSB_{MSY} overfished threshold generated by the operating model, SS_Sex. Note that because the SSB thresholds were generated by the sex-specific OM, simulations assessed by the sex-aggregated model were more likely to remain above these thresholds because biomass from all mature individuals contributed to the SSB.

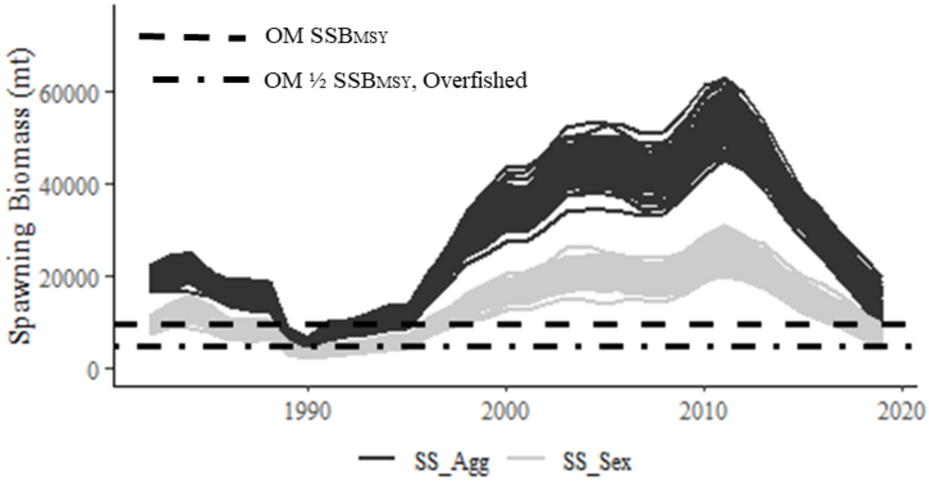

Figure 4.3 *Simulated Spawning Stock Biomass Estimates*

Each of the 88 simulated timeseries from the operating model, SS_Sex, were assessed by the alternative estimation model, SS_Agg. Note that 100 simulations were generated, though only 88 of those simulations converged. Thresholds of SSB_{MSY} and ½ SSB_{MSY}, the overfished threshold, for the operating model are shown. Note that sex-specific SS models calculate SSB using only spawning female biomass while biomass from all mature individuals contributes to SSB in sex-aggregated models.

4.3.3.2 Forecasts

Management strategies No Fishing, F35_Low and F35_High resulted in no simulations becoming overfished across EM model structures (Table 4.3; Figure 4.4). Though managing with F35_High resulted in lower biomass than either No Fishing or F35_Low, the equilibrium biomass from these forecasts was the nearest to SSB_{MSY}. When simulations were managed without error in the commercial quota and recreational harvest limit, 19% of simulations experienced population collapse, though the sex-aggregated EM only detected 3% of these collapses. When implementation error was added to harvest, 31% of simulations collapsed, and 11% of these were detected by the sex-aggregated model. Of the simulations that sustained throughout the forecasted period, more than 50% of simulations were overfished during some period of the forecast, though between four and 11% were detected by SS_Agg (Table 4.3). An overfished state was less likely to be detected by the sex-aggregated model when implementation error affected adherence to the management strategy.

Table 4.3 *Summary of Overfished Simulations*

OM = SS_Sex						
	Management Strategy					
EM	**No Fishing**	**F35_Low**	**F35_High**	**No Error**	**Implementation Error**	**% Total**
SS_Agg	0.0%	0.0%	0.0%	11.2%	4.2%	**3.0%**
SS_Sex	0.0%	0.0%	0.0%	53.6%	52.6%	**21.2%**
% Total	**0%**	**0%**	**0%**	**32.4%**	**28.9%**	

Details of the number of simulations that became overfished in forecasts relative to ½ SSBMSY of the operating model, SS_Sex. Overfished simulations are separated out by the estimation model which assessed the forecasts and management strategy that was applied in forecasts.

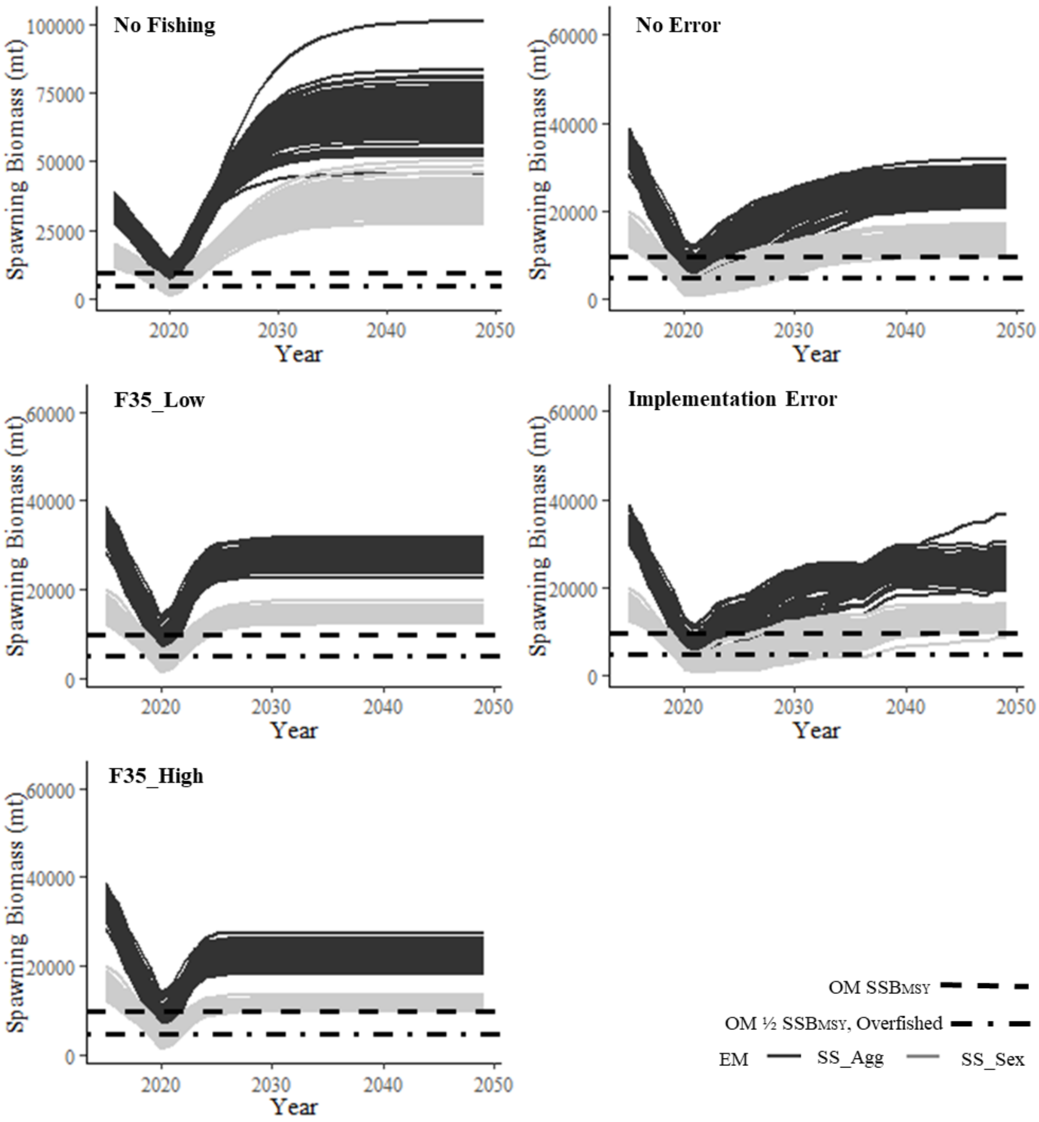

Figure 4.4 *Simulation Forecasts of Spawning Stock Biomass from EM Structures*

Forecasted spawning stock biomass estimates for simulations generated by the operating model SS_Sex, assessed by each EM model configuration in SS, and forecasted with each of the five examined management strategies. Note that sex-specific SS models calculate SSB using only spawning female biomass while biomass from all mature individuals contributes to SSB in sex-aggregated models.

4.4 Discussion

4.4.1 Implications of Biomass Estimates

Modeling summer flounder sex-specific dynamics has been an ongoing effort, and these simulations describe both why it is important and why it is difficult. The sex-specific and sex-aggregated models presented here demonstrate that in many ways a sex-aggregated model captures trends in biomass, fishing mortality, and recruitment. Estimates of spawning stock biomass for the sex-specific model were approximately half of those from the sex-aggregated counterpart, though this differential is due to how stock synthesis calculates SSB in sex-specific models. In sex-aggregated models, biomass from all spawning individuals contribute to the SSB, where in sex-specific models, only the female spawning biomass contributes to SSB. In general, SSB generated only with female biomass is effective at generating management targets so long as reduction in male biomass is not likely to reduce fertilization rate (Brooks et al. 2008). However, as female-only SSB was nearly half of the aggregated SSB, and females are overrepresented in recreational landings, generating management thresholds with sex-aggregated SSB may have implications if reduction in biomass of female flounder could subsequently reduce spawning potential. In forecasted simulations, fishing at the current quota led to more than 50% of the sex-specific simulations to become overfished. Meanwhile, the sex-aggregated model predicted less than 10% of these overfished states when implementation error was in effect. However, as the SSB from sex-aggregated simulations could not be disaggregated into male and female biomass, this may not be an adequate comparison to thresholds set by a sex-specific model. Nonetheless, these forecasts demonstrate the need to understand how adequately a sex-aggregated model that generates management targets with a sex-aggregated SSB can describe a sex-specific population with sexual-dimorphism that carries over to differential fishery selectivity between sexes.

More than 60% of summer flounder are mature at age 1, and 100% by age 3 (Morse, 1982; Maunder & Wong, 2011). In part because of size limits, the commercial and recreational fisheries generally begin targeting flounder at age-2, which means that the fishery largely lands individuals from the spawning stock. As females tend to be larger (Langan et al. 2019), minimum size limits bias landings of female flounder (ASFMC, 2021; Morson et al. 2017). Females are also found in higher ratios at shallow depths where the recreational fishery operates, perhaps responsible for the bias in landing of females in the recreational fishery (Morson et al. 2015). Considering the reliance on the spawning stock to meet minimum size limits, if the spawning stock is overestimated in the sex-aggregated model it is possible that current harvest limits could overfish the stock.

4.4.2 Options for Future Model Development

The provisional sex-aggregated, time-varying SS model was meant to capture the configuration of the ASAP assessment model. While timeseries of SSB between SS_Agg and ASAP were relatively similar, SS estimates of unexploited recruitment were nearly half those of ASAP and unexploited biomass was about two-thirds. Despite the incongruence, this model was the best of many configurations that were tested, and there are lessons to be learned from those efforts.

One of the biggest struggles in transferring the model from ASAP to SS was the different manners in which each model structure reads parameter lines. For example, the

ASAP model uses matrices with dimensions for the number of years and ages to specify weight-at-age in each year. This is one of many time-varying attributes of the ASAP model, and not all could be incorporated. Ultimately, emphasis was placed on time-varying selectivity because of clear changes in size-limits from management at various points in the time series. To provide for this emphasis, growth parameters remained constant throughout the time series. This is one avenue in the future, however, that could lead to better agreement between ASAP and SS realizations of the summer flounder stock.

Another concern that remains between the ASAP and SS models is the terminal year estimates of recruitment. Where ASAP estimates higher recruitment throughout the timeseries (relative to SS models), the patterns are similar. From 2016 to 2019, however, ASAP estimates much higher recruitment than SS. One cause could be misfitting of the stock-recruitment (S-R) curve. The S-R curve has never been well-described (though see Maunder [2012]). Fitting of the S-R curve was tested during preliminary model runs by opening steepness to estimation. The model continued to estimate a steepness between 0.95 and 1, a value that suggests recruitment is independent of spawning biomass (though recruitment may rely more on the environment [O'Leary et al. 2019]). However, this value is also used in the assessment, and would not explain the divergence in recruitment. Future edits to the SS model may consider including some or all of the larval survey indices provided by federal, state and academic surveys, which may be responsible for unrealized recruitment at the end of the SS timeseries.

Finally, while discordance between ASAP and SS models cannot be attributed to length-compositions, as ASAP does not allow for the inclusion of length-compositions and therefore the length observations were down-weighted to zero, future model development may focus on including length compositions. Management, especially of the recreational fishery, focusses heavily on size-limits with the goal to allow fish to reach a mature size and contribute to the spawning stock before being subjected to fishing pressure. This management tactic has been partially responsible for the disproportionate landing of large females in the recreational fishery, prompting some to argue for slot-limit or cumulative size-limit management instead (Powell et al. 2010; Morson et al. 2017). As SS allows for length, and summer flounder exhibit sexual-dimorphism in length, it may prove advantageous to incorporate length compositions in a sex-disaggregated model of summer flounder.

4.4.3 Concluding Remarks

Summer flounder has historically been an important recreational and commercial resource for the US North- and Mid-Atlantic, though complex population dynamics have made the species difficult to sample, model, manage and forecast. One of the persisting concerns in the management of summer flounder is the sex-specific dynamics in both the population and the fishery. The models presented herein help describe that concern, especially with relation to spawning stock biomass. In the absence of adequate data and resources to generate a sex-specific assessment model, it is important to continue evaluating the fishery biases on summer flounder, and how that may be overlooked in a sex-aggregated model.

CHAPTER V – CLOSING COMMENTS

Fisheries modeling has always faced uncertainties, and simulation analysis will not resolve those uncertainties. What simulation analysis does allow for is the accounting for uncertainty in fisheries management. With the right tools, fisheries can be sustainably managed despite uncertainty. In this dissertation three species representing important commercial fisheries on the US East and Gulf coast were examined. First, a model was constructed to generate MSY-based reference points for both the Eastern oyster reef and fishery. This model provided rebuilding goals that allow managers to account for uncertainty in natural, disease and fishing mortality. With this framework, shell planting and seed fishing can be incorporated to anticipate impacts of management decisions on the reef.

A second simulation analysis, for Atlantic surfclam, used the stock assessment model as a framework from which current management control rules could be assessed and related to risk-tolerance policies of the management council. Forecasts accounted for uncertainty in population dynamics parameters and concluded that while the fishery is unlikely to become overfished or experience overfishing, the density of clam patches may impact the fishery before the stock reaches management thresholds.

Finally, the impact of modeling summer flounder, a species which exhibits sexual dimorphism, with a sex-aggregated model was examined. Using the current commercial quota and recreational harvest control rule, forecasts applied to simulations of a sex-specific assessment model. The sex-aggregated assessment model did not detect an overfished stock, though more than 50% of the operating model simulations became overfished under current regulations. Disparity in estimates of spawning stock biomass between sex-aggregated and sex-specific models may lead to overharvest that is undetected by a sex-aggregated model.

These three examples of simulation analysis contribute to efforts to evaluate uncertainty in fisheries models and inform managers of how harvest policies and thresholds could impact fishery resources in the near-term future. These analyses provide frameworks from which risk-based assessments can be adapted to other fishery resources with similar uncertainties and support efforts to conduct risk-based assessments of management decisions.

REFERENCES

Aalto, E.A., Micheli, F., Boch, C.A., Montes, J.A.E., Woodson, C.B., and de Leo, G.A. 2019. Catastrophic mortality, Allee effects, and marine protected areas. Am. Nat. **193**: 391-408.

Abbe, G.R. 1988. Population structure of the American oyster, *Crassostrea virginica*, on an oyster bar in central Chesapeake Bay: changes associated with shell planting and increased recruitment. J. Shellfish Res. **7**: 33-40.

Able, K. W., Sullivan, M. C., Hare, J. A., Bath-Martin, G., Taylor, J. C., & Hagan, R. (2011). Larval abundance of summer flounder (*Paralichthys dentatus*) as a measure of recruitment and stock status. *Fishery Bulletin*, *109*(1).

Adelaja, A., McCay, B., & Menzo, J. (1998). Market share, capacity utilization, resource conservation, and tradable quotas. *Marine Resource Economics*, *13*(2), 115-134.

Andrews, J.D. 1988. Epizootiology of the disease caused by the oyster pathogen *Perkinsus marinus* and its effects on the oyster industry. Am. Fish. Soc. Spec. Publ. **18**: 47-63.

Ascenio, A.L.A., Enriquez, D.M., Martínez, M.I., and Aldana, A.D. 2016. Efecto de la temperature y la salinidad en el ciclo reproductor de hembras y machos de *Crassostrea virginica* (Bivalvia: Ostreidae). Rev. Biol. Trop. **64**: 449-459.

Ashton-Alcox, K.A., Bushek, D., Gius, J.E., and & Morson, J. 2018. Stock Assessment Workshop New Jersey Delaware Bay oyster beds (20th SAW) Final Report. Rutgers University Haskin Shellfish Research Laboratory, Port Norris, NJ. 107 pp.

Ashton-Alcox, K.A., Morson, J.M., Powell, E.N., Gius, J.E., Munroe, D.M., and Bushek, D. 2021. Oyster recruitment and persistence on planted versus native substrate over 13 years in the Delaware Bay oyster fishery resource. J. Shellfish Res. **40**:191-211.

Atlantic States Marine Fisheries Commission. "ASMFC & MAFMC Approve Catch and Landings Limits for Summer Flounder, Scub, Black Sea Bass and Bluefish for 2019." 2018. 20 August, 2018, FOR IMMEDIATE RELEASE (asmfc.org).

Atlantic States Marine Fisheries Commission. "ASMFC & MAFMC Set Specifications for Jointly Managed Species and Initiate a Joint Action on Summer Flounder, Scup, and Black Sea Bass Commercial/Recreational Allocations." 11 October, 2019, FOR IMMEDIATE RELEASE (asmfc.org).

Austin, H.M., Evans, D., and Haven, D.S. 1996. A retrospective time series analysis of oyster, *Crassostrea virginica*, recruitment (1946-1993). J. Shellfish Res. **15**: 565-582.

Beck, M.W., Brumbaugh, R.D., Airoldi, L., Carranza, A., Coen, L.D., Crawford, C., Defeo, Edgar, G.J., Hancock, Kay, M., Lenihan, H., Luckenbach, M.W., B., Toropova, C.L., Zhang, G. 2009. Shellfish reefs at risk a global analysis of problems and solutions. The Nature Conservancy, Arlington, VA 52 pp.

Beck, M.W., Brumbaugh, R.D., Airoldi, L., Carranza, A., Coen, L.D., Crawford, C., Defeo, O., Edgar, G.J., Hancock, B., Toropova, C.L., Zhang, G., and Guo, X. 2011. Oyster reefs at risk and recommendations for conservation, restoration, and management. Bioscience **61**: 107-116.

Beck, S., and La Peyre, M.K. 2015. Effects of oyster harvest activities on Louisiana reef habitat and resident nekton communities. Fish. Bull. **113**: 327-340.

Bergquist, D.C., Hale, J.A., Baker, P., and Baker, S.M. 2006. Development of ecosystem indicators for the Suwanee River estuary: oyster reef habitat quality along a salinity gradient. Estuaries Coasts 29, 353-360.

Boothe, D.M., and Heck Jr., K.L. 2009. Effects of the American oyster *Crassostrea virginica* on growth rates of the seagrass *Halidule wrightii*. Mar. Ecol. Prog. Ser. **309**: 117-126.

Brooks, E.N. 2013. Effects of variable reproductive potential on reference points for fisheries management. Fish. Res. **138**: 152-158.

Brooks, E.N., and Powers, J.E. 2007. Generalized compensation in stock-recruit functions: properties and implications for management. ICES J. Mar. Sci. **64**: 413-424.

Brooks, E. N., Shertzer, K. W., Gedamke, T., & Vaughan, D. S. (2008). Stock assessment of protogynous fish: evaluating measures of spawning biomass used to estimate biological reference points.

Buchheister, A., & Latour, R. J. (2010). Turnover and fractionation of carbon and nitrogen stable isotopes in tissues of a migratory coastal predator, summer flounder (Paralichthys dentatus). *Canadian Journal of Fisheries and Aquatic Sciences*, *67*(3), 445-461.

Bushek, D., Ford, S.E., Burt, I. 2012. Long-term patterns of an estuarine pathogen along a salinity gradient. J. Mar. Res. **70**: 225-251.

Camp, E.V., Pine III, W.E., Havens, K., Kano, A.S., Walters, C.J., Irani, T., Lindsey, A.B., and Morris Jr., J.G. 2015. Collapse of a historic oyster fishery: diagnosing cause and identifying paths toward increased resilience. Ecology Society **20**: #45.

Carlsson, J., Carnegie, R.B., Cordes, J.F., Hare, M.P., Leggett, A.T., and Reece, K.S.

2008. Evaluating recruitment contribution of a selectivity based aquaculture line of the oyster, *Crassostrea virginica* used for restoration efforts. J. Shellfish Res. **27**: 1117-1124.

Cheng, B.S., Chang, A.L., Deck, A., and Ferner, M.C. 2016. Atmospheric rivers and the mass mortality of wild oysters: insight into an extreme future? Proc. R. Soc. B Biol. Sci. 283: #20161462, 9 pp.

Chintala, M. M., & Grassle, J. P. (1995). Early gametogenesis and spawning in juvenile Atlantic surfclams, *Spisula solidissima*. *Journal of Shellfish Research*, *14*(2), 301-306.

Choi, K-S., Powell, E.N., Lewis, D.H., and Ray, S.M. 1994. Instantaneous reproductive effort in female American oysters, *Crassostrea virginica*, measured by a new immunoprecipitation assay. Biol. Bull. **186**: 41-61.

Chute, A. S., Mcbride, R. S., Emery, S. J., & Robillard, E. (2016). Annulus formation and growth of Atlantic surfclam (*Spisula solidissima*) along a latitudinal gradient in the western North Atlantic Ocean. *Journal of Shellfish Research*, *35*(4), 729-737.

Christmas, J.F., McGinty, M.R., Randle, D.A., Smith, G.F., and Jordan, S.J. 1997. Oyster shell disarticulation in three Chesapeake Bay tributaries. J. Shellfish Res. **16**: 115-123.

Coen, L.D., Brumbaugh, R.D., Bushek, D., Grizzle, R., Luckenbach, M.W., Posey, M.H., Powers, S.P., and Tolley, S.G. 2007. As we see it. Ecosystem services related to oyster restoration. Mar. Ecol. Prog. Ser. **341**: 303-307.

Cope, J.M. 2013. Implementing a statistical catch-at-age model (Stock Synthesis) as a tool for deriving overfishing limits in data-limited situations. Fish. Res. **142**: 3-14.

Cordue, P.L. 2012. Fishing intensity metrics for use in overfishing determination. ICES J. Mar. Sci. **69**: 615-623.

Damiano, M.D., and Wilberg, M.J. 2019. Population dynamics of eastern oysters in Choptank River Complex, Maryland during 1989-2015. Fish. Res. **212**: 196-207.

Dekshenieks, M.M., Hofmann, E.E., Klinck, J.M., and Powell, E.N. 2000. Quantifying the effects of environmental change on an oyster population: a modeling study. Estuaries **23**: 593-610.

Dietl, G. P., & Alexander, R. R. (1997). Predator-prey interactions between the naticids *Euspira heros* Say and *Neverita duplicata* Say and the Atlantic surfclam *Spisula solidissima* Dillwyn from Long Island to Delaware. *Journal of Shellfish Research*, *16*(2), 413-422.

Doering, K.L., Wilberg, M.J., Liang, D., and Tarnowski, M. 2021 Patterns of oyster natural mortality in Chesapeake Bay, Maryland using a Bayesian model. Fish. Res. 236: #105838.

Dowling, N.A., Dichmont, C.M., Haddon, M., Smith, D.C., Smith, A.D.M., and Sainsbury, K. 2015. Guidelines for developing formal harvest strategies for data-poor species and fisheries. Fish. Res. **171**: 130-140.

Fegley, S.R., Ford, S.E., Kraeuter, J.N., and Haskin, H.H. 2003. The persistence of New Jersey's oyster seedbeds in the presence of oyster disease and harvest: the role of management. J. Shellfish Res. **22**: 451-464.

Finley, C., and Oreskes, N. 2013. Food for thought maximum sustained yield: a policy disguised as science. ICES J. Mar. Sci. **70**: 245-250.

Ford, S.E. 1996. Range extension by the oyster parasite *Perkinsus marinus* into the northeastern United States: response to climate change. J. Shellfish Res. **15**: 45-56.

Ford, S.E., Cummings, M.J., and Powell, E.N. 2006. Estimating mortality in natural assemblages of oysters. Estuaries Coasts **29**: 361-374.

Francis, R. I. C. C., & Shotton, R. (1997). “Risk” in fisheries management: a review. *Canadian Journal of Fisheries and Aquatic Sciences*, *54*(8), 1699-1715.

Frérotte, B., Raguideau, A. and Cuif, J-P. 1983. Dégradation in vitro d'un test carbonate d'invertébré, *Crassostrea gigas* (Thunberg), par action de cultures bactériennes. Intèrêt pour l'analyse ultrastructurale. C.R. Acad. Sci. Paris Ser. 2 Mech.-Phys.-Chim. Sci Univ. Sci. Tierre. **297**: 383-388.

Friedland, K. D., Morse, R.E., Manning, J. P., Melrose, D. C., Miles, T., Goode, A. G., Brady, D. C., Kohut, J. T., Powell, E. N. (2020). Trends and change points in surface and bottom thermal environments of the US Northeast Continental Shelf Ecosystem. *Fisheries Oceanography*, *29*(5), 396-414.

Garton, D., and Stickle, W.B.1980. Effects of salinity and temperature on the predation rate of *Thais haemastoma* on *Crassostrea virginica* spat. Biol. Bull. **158**: 49-57.

Gedan, K.B., Kellogg, L., and Breitburg, D.L. 2014. Accounting for multiple foundation species in oyster reef restoration benefits. Restoration Ecol. **22**: 517-524.

Gledhill, J.H., Barnett, A.F., Slattery, M., Willett, K.L., Easson, G.L., Otis, S.S., and Gochfeld, D.J. 2020. Mass mortality of the eastern oyster Crassostrea virginica in the western Mississippi Sound following unprecedented Mississippi River flooding in 2019. J. Shellfish Res. **39**: 235-244.

Grabowski, J.H., Brumbaugh, R.D., Conrad, R.F., Keeler, A.G., Opuluch, J.J., Peterson, C.H., Piehler, M.F., Powers, S.P., and Smith, A.R. 2012. Economic valuation of ecosystem services provided by oyster reefs. Bioscience **62**: 900-909.

Grizzle, R., Ward, K., Goselbracht, L., and Birch, A. 2018. Distribution and condition of intertidal eastern oysters (*Crassostrea virginica*) reefs in Apalachicola Bay, Florida based on high-resolution satellite imagery. J. Shellfish Res. **37**: 1027-1038.

Haltuch, M.A., Punt, A.E., and Dorn, M.W. 2008. Evaluating alternative estimators of fishery management reference points. Fish. Res. **94**: 290-303.

Hancock, D.A. (1973). The relationship between stock and recruitment in exploited invertebrates. *Rapports et Proces-Verbaux des Réunions Conseil International pour l'Exploration de la Mer*, *164*, 113-131.

Harding, J.M., Mann, R., Southworth, M.J., and Wesson, J.A. 2010. Management of the Piankatank River, Virginia, in support of oyster (*Crassostrea virginica*, Gmelin 1791) fishery repletion. J. Shellfish Res. **29**: 867-888.

Harding, J.M., Powell, E.N., Mann, R. and Southworth, M.J. 2013. Variations in eastern oyster (*Crassostrea virginica*) sex-ratios from three Virginia estuaries: protandry, growth and demographics. J. Mar. Biol. Assoc. U. K. **93**: 519-531.

Harding, J.M., Southworth, M.J., Mann, R., and Wesson, J.A. 2012. Comparison of *Crassostrea virginica* Gmelin (Eastern oyster) recruitment on constructed reefs and adjacent natural oyster bars over decadal time scales. N. E. Nat. **19**: 627-646.

Hargis Jr., W.J., and Haven, D.S.1988. Rehabilitation of the troubled oyster industry of the lower Chesapeake Bay. J Shellfish Res **7**: 271-279.

Hartill, B.W, Cryer, M., and Morrison, M.A. 2005. Estimates of biomass, sustainable yield, and harvest: neither necessary nor sufficient for the management of non-commercial urban intertidal shellfish fisheries. Fish. Res. **71**: 209-222.

Hayes, P. and Menzel, R.W. 1981.The reproductive cycle of early setting *Crassostrea virginica* (Gmelin) in the northern Gulf of Mexico, and its implications for population recruitment. Biol. Bull. **160**: 80-88.

Hemeon, K.M., Ashton-Alcox, K.A., Powell, E.N., Pace, S.M., Poussard, L.M., Solinger, L.K., and Soniat, T.M. 2020. Novel shell stock–recruitment models for *Crassostrea virginica* as a function of regional shell effective surface area, a missing link for sustainable management. J. Shellfish Res. *39*: 633-654.

Henderson, M. J., Fabrizio, M. C., & Lucy, J. A. (2014). Movement patterns of summer flounder near an artificial reef: Effects of fish size and environmental cues. *Fisheries Research*, *153*, 1-8.

Hennen, D.R. 2015. How should we harvest an animal that can live for centuries? N. Am. J. Fish. Manage. 35: 512-527.

Hennen, D. R. (2018). An empirical method for estimating the scale of Atlantic surfclam abundance. *Northeast Fisheries Science Center*.

Hennen, D. R., Jacobson, L. D., & Tang, J. (2012). Accuracy of the Patch model used to estimate density and capture efficiency in depletion experiments for sessile invertebrates and fish. ICES journal of marine science, 69(2), 240-249.

Hennen, D.R., Mann, R., Munroe, D.M., Powell, E.N. 2018. Biological reference points for Atlantic surfclam (*Spisula solidissima*) in warming seas. Fish. Res. **207**: 126-139.

Hicks, R., & Schnier, K. (2016). Commercial and recreational allocation for summer flounder. *USA: Mid-Atlantic Fishery Management Council*.

Hilborn, R. (1987). Living with uncertainty in resource management. *North American Journal of Fisheries Management*, *7*(1), 1-5.

Hoenig, J. M. (1983). Empirical use of longevity data to estimate mortality rates. *Fishery Bulletin*, *82*(1), 898-903.

Hoey, J. A., & Pinsky, M. L. (2018). Genomic signatures of environmental selection despite near-panmixia in summer flounder. *Evolutionary Applications*, *11*(9), 1732-1747.

Hofmann, E.E., Powell, E.N., Klinck, J.M., and Wilson, E.A. 1992. Modeling oyster populations. III. Critical feeding periods, growth and reproduction. J. Shellfish Res. **11**: 399-416.

Hofmann, E. E., Powell, E. N., Klinck, J. M., Munroe, D. M., Mann, R., Haidvogel, D. B., Narváez, D. A., Zhang, X., & Kuykendall, K. M. (2018). An overview of factors affecting distribution of the Atlantic surfclam (*Spisula solidissima*), a continental shelf biomass dominant, during a period of climate change. *Journal of Shellfish Research*, *37*(4), 821-831.

Hopkins, S.H. 1954. Oyster setting on the Gulf coast. Proc. Natl. Shellfish. Assoc. **45**: 52-55.

Ingle, R.M. 1951. Spawning and setting of oysters in relation to seasonal environmental changes. Bull. Mar. Sci. Gulf Caribb. 1: 111-135.

Jackson, J.B.C., Kirby, M.X., Berger, W.H., Bjorndal, K.A., Botsford, L.W., Bourque, B.J., Bradbury, R.H., Cooke, R., Erlandson, J., Estes, J.A., Hughes, T.P., Kidwell, S., Lange, C.B., Lenihan, H.S., Pandolfi, J.M., Peterson, C.H., Steneck, R.S., Tegner, M.J., and Warner, R.R. 2001. Historical overfishing and the recent collapse of coastal ecosystems. Science **293**: 629-637.

Jacobson L, & Hennen, D. (2019). Improving the NEFSC clam survey for Atlantic surfclams and ocean quahogs. *Northeast Fisheries Science Center Reference Document*, 19-06; 89 p.

Johnson, K.D., and Smee, D.L. 2014. Predators influence the tidal distribution of oysters (*Crassostrea virginica*). Mar. Biol. **161**: 1557-1564.

Jones, D. S. (1981). Reproductive cycles of the Atlantic surfclam *Spisula solidissima*, and the ocean quahog Arctica islandica off New Jersey. *Journal of Shellfish Research*, *1*(1), 23-32.

Jones, M. L., Catalano, M. J., & Peterson, L. K. (2016). Stakeholder-centered development of a harvest control rule for Lake Erie walleye. In *Management Science in Fisheries* (pp. 183-203). Routledge.

Kennedy, V.S., Breitburg, D.L., Christman, M.C., Luckenbach, M.W., Paynter, K., Kramer, J., Sellner, K.G., Dew-Baxter, J., Keller, C., and Mann, R. 2011. Lessons learned from efforts to restore oyster populations in Maryland and Virginia, 1990 to 2007. J. Shellfish Res. **30**, 719-731.

Kim, Y., & Powell, E.N. (2004). Surfclam histopathology survey along the Delmarva mortality line. *Journal of Shellfish Research*, *23*(2), 429-442.

Kjelland, M.E., Piercy, C.D., Lackey, T., and Swannack, T.M. 2015. An integrated modeling approach for elucidating the effects of different management strategies on Chesapeake Bay oyster metapopulation dynamics. Ecol. Modelling **308**: 45-62.

Klinck, J.M., Powell, E.N., Kraeuter, J.N., Ford, S.E., and Ashton-Alcox, K.A. 2001. A fisheries model for managing the oyster fishery during times of disease. J. Shellfish Res. **20**: 977-989.

Kraeuter, J.N., Buckner, S., and Powell, E.N. 2005. A note on a spawner-recruit relationship for a heavily exploited bivalve: the case of northern quahog (hard clams), *Mercenaria mercenaria* in Great South Bay New York. J. Shellfish Res. **24**: 1043-1052.

Kraeuter, J.N., Ford, S., and Cummings, M. 2007. Oyster growth analysis: a comparison of methods. J. Shellfish Res., **26**: 479-491.

Kritzer, J.P., Delucia, M-B., Greene, E., Shumway, C., Topolski, M.F., Thomas-Blate, J., Chiarella, L.A., Davy, K.B., and Smith, K. 2016. The importance of benthic habitats for coastal fisheries. Bioscience **66**: 274-284.

Kuykendall, K.M., Moreno, P., Powell, E.N., Soniat, T.M, Colley, S., Mann, R., and Munroe, D.M. 2015. The exposed surface area to volume ratio: is shell more efficient than limestone in promoting oyster recruitment? J. Shellfish Res. **34**: 217–225.

Kuykendall, K. M., Powell, E. N., Klinck, J. M., Moreno, P. T., & Leaf, R. T. (2017). Management strategy evaluation for the Atlantic surfclam (*Spisula solidissima*) using a spatially explicit, vessel-based fisheries model. *Fishery Bulletin, 115*(3), 300-325.

Kuykendall, K. M., Powell, E. N., Klinck, J. M., Moreno, P. T., Leaf, R. T. (2019). The effect of abundance changes on a management strategy evaluation for the Atlantic surfclam (*Spisula solidissima*) using a spatially explicit, vessel-based fisheries model. *Ocean & Coastal Management, 169*, 68-85.

Langan, J. A., McManus, M. C., Schonfeld, A. J., Truesdale, C. L., & Collie, J. S. (2019). Evaluating Summer Flounder spatial sex-segregation in a southern New England estuary. *Marine and Coastal Fisheries, 11*(1), 76-85.

La Peyre, M.K., Geagham, J., Decossas, G., and La Peyre, J.F. 2016. Analysis of environmental factors influencing salinity patterns, oyster growth, and mortality in

Lower Breton Sound Estuary, Louisiana, using 20 years of data. J. Coast. Res. **32**: 619-630.

La Peyre, M.K., Gossman, B., and LaPeyre, J.F. 2009. Defining optimal freshwater flow for oyster production: effects of freshet rate and magnitude of change and duration on eastern oysters and *Perkinsus marinus* infection. Estuaries Coasts **32**: 522-534.

Legault, C. M., & Restrepo, V. R. (1998). A flexible forward age-structured assessment program. *ICCAT. Col. Vol. Sci. Pap*, *49*, 246-253.

Lenihan, H.S., and Peterson, C.H. 1998. How habitat degradation through fishery disturbance enhances impacts of hypoxia on oyster reefs. Ecol. Appl. **8**: 128-140.

Leonhardt, J.M., Casas, S., Supan, J.E., and La Peyre, J.F. 2017. Stock assessment for eastern oyster seed production and field grow-out in Louisiana. Aquaculture **466**: 9-19.

Li, B., Shertzer, K. W., Lynch, P. D., Ianelli, J. N., Legault, C. M., Williams, E. H., ... & Supernaw, M. (2021). A comparison of 4 primary age-structured stock assessment models used in the United States. *Fishery Bulletin*, *119*.

Link, J.S., Brodziak, J.K.T., Edwards, S.F., Overholtz, W.J., Mountain, D., Jossi, J.W., Smith, T.D., and Fogarty, M.J. 2002. Marine ecosystem assessment in a fisheries management context. Can. J. Fish. Aquat. Sci. **59**: 1429-1440.

MacKenzie Jr., C.L. 2007. Causes underlying the historical decline in eastern oyster (*Crassostrea virginica* Gmelin, 1791) landings. J. Shellfish Res. **26**: 927-938.

MAFMC (2017). 2017 surfclam AP fishery information document. Mid-Atlantic Fisheries Management Council, 17 p.

MAFMC (2020). Omnibus acceptable biological catch and risk tolerance framework adjustment. Mid-Atlantic Fisheries Management Council, 116 p.

Mangel, M., MacCall, A.D., Brodziak, J., Dick, E.J., Forrest, R.E., Pourzand, R., and Ralston, S. 2013. A perspective on steepness, reference points, and stock assessment. Can. J. Fish. Aquat. Sci. **70**: 930-940.

Mann, R., and Powell, E.N. 2007. Why oyster restoration goals in the Chesapeake Bay are not and probably cannot be achieved. J. Shellfish Res. **26**: 905-917.

Mann, R., Harding, J.M., and Southworth, M.J. 2009b. Reconstructing pre-colonial oyster demographics in the Chesapeake Bay, USA. Estuar. Coast. Shelf Sci. **85**: 217-222.

Mann, R., Southworth, M., Harding, J.M., and Wesson, J.A. 2009a. Population studies of the native eastern oyster, *Crassostrea virginica*, (Gmelin, 1791) in the James River, Virginia, USA. J. Shellfish Res. **28**: 193-220.

Martell, S.J.D., Pine III, W.E., and Walters, C.J. 2008. Parameterizing age-structured models from a fisheries management perspective. Can. J. Fish. Aquat. Sci. **65**: 1586-1600.

Maunder, M.N. 2003. Is it time to discard the Schaefer model from the stock assessment scientist's toolbox. Fish. Res. **61**: 145-149.

Maunder, M. N. (2012). Evaluating the stock–recruitment relationship and management reference points: application to summer flounder (Paralichthys dentatus) in the US mid-Atlantic. *Fisheries Research*, *125*, 20-26.

Maunder, M. N., & Wong, R. A. (2011). Approaches for estimating natural mortality: application to summer flounder (Paralichthys dentatus) in the US mid-Atlantic. *Fisheries Research*, *111*(1-2), 92-99.

McAfee, D., and Bishop, M.J. 2019. The mechanisms by which oysters facilitate invertebrates vary across environmental gradients. Oecologia **189**: 1095-1106.

McCay, E., Borrett, S.R., LaPeyre, M.K., and Peterson, B.J. 2017. Estimating the impact of oyster restoration scenarios on transient fish production. Restoration Ecol. **25**: 798-809.

McCay, B. J., Brandt, S., & Creed, C. F. (2011) Human dimensions of climate change and fisheries in a coupled system: the Atlantic surfclam case. *ICES Journal of Marine Science*, *68*(6), 1354-1367.

Methot, R. D., & Wetzel, C. R. (2013). Stock synthesis: A biological and statistical framework for fish stock assessment and fishery management. *Fisheries Research, 142*, 86-99.

Methot, R. D., Wetzel, C. R., & Taylor, I. G. (2019). Stock Synthesis User Manual Version 3.30. 13. *NOAA Fisheries. Seattle, Washington*.

Meyer, T. L., Cooper, R. A., & Pecci, K. J. (1981). The performance and environmental effects of a hydraulic clam dredge. *Marine Fisheries Review, 43*(9), 14-22.

Miller, T.J., Blair, J.A., Ihde, T.F., Jones, R.M., Secor, D.H., and Wilberg, M.J. 2010. Fish Smart: an innovative role for science in stakeholder-centered approaches to fisheries management. Fisheries **35**: 424-433.

Miller, T. J., Curti, K., Loewensteiner, D., Sharov, A. F., Muffley, B., Christman, M. C., Volstad, J. H., Houde, E. D. (2004). Abundance, Distribution and Diversity of Chesapeake Bay Fishes: Results from CHESFIMS (Chesapeake Bay Fishery Independent Multispecies Fisheries Survey). In *Chesapeake Bay Fisheries Research Program Symposium Report FY* (pp. 21-34).

Moore, J.L., Puckett, B.J., and Schreiber, S.J. 2018. Restoration of eastern oyster populations with positive density dependence. Ecol. Appl. **28**: 897-909.

Morse, W. W. (1981). Reproduction of the summer flounder, Paralichthys dentatus (L.). *Journal of Fish Biology*, *19*(2), 189-203.

Morson, J. M., Bochenek, E. A., Powell, E. N., Hasbrouck, E. C., Gius, J. E., Cotton, C. F., Gerbino, K. & Froehlich, T. (2015). Estimating the sex composition of the Summer Flounder catch using fishery-independent data. *Marine and coastal fisheries*, *7*(1), 393-408.

Morson, J. M., Munroe, D., Harner, R., & Marshall, R. (2017). Evaluating the potential for a sex-balanced harvest approach in the recreational Summer Flounder fishery. *North American Journal of Fisheries Management*, *37*(6), 1231-1242.

Munroe, D.M., Hofmann, E.E., Powell, E.N., and Klinck, J.M. 2013. How do shellfisheries influence genetic connectivity in metapopulations? A modeling study examining the role of lower size limits in oyster fisheries. Can. J. Fish. Aquat. Sci. **70**: 1813-1828.

Munroe, D. M., Powell, E. N., Mann, R., Klinck, J. M. & Hofmann, E. E. (2013). Underestimation of primary productivity on continental shelves: evidence from maximum size of extant surfclam (*Spisula solidissima*) populations. *Fisheries Oceanography*, *22*(3), 220-233.

Munroe, D.M., Klinck, J.M., Hofmann, E.E., and Powell, E.N. 2014. A modelling study of the role of marine protected areas in metapopulation genetic connectivity in Delaware Bay oysters. Aquat. Conserv. Mar. Freshw. Ecosystems **24**: 645-666.

Munroe, D.M., Powell, E.N., Ford, S.E., Hofmann, E.E., and Klinck, J.M. 2015.

Outcomes of asymmetric selection pressure and larval dispersal on evolution of disease resistance: a metapopulation modeling study with oysters. Mar. Ecol. Prog. Ser. **531**:221-239.

Munroe, D. M., Narváez, D. A., Hennen, D., Jacobson, L., Mann, R., Hofmann, E. E., Powell, E. N., & Klinck, J. M. (2016). Fishing and bottom water temperature as drivers of change in maximum shell length in Atlantic surfclams (*Spisula solidissima*). *Estuarine Coastal and Shelf Science*, *170*, 112-122.

Narváez, D.A., Klinck, J.M., Powell, E.N., Hofmann, E.E., Wilkin, J., and Haidvogel, D.B. 2012a. Circulation and behavior controls on dispersal of eastern oyster (*Crassostrea virginica*) larvae in Delaware Bay. J. Mar. Res. **70**: 411-440.

Narváez, D.A., Klinck, J.M., Powell, E.N., Hofmann, E.E., Wilkin, J., and Haidvogel, D.B. 2012b. Modeling the dispersal of eastern oyster (*Crassostrea virginica*) larvae in Delaware Bay. J. Mar. Res. **70**: 381-409.

Newman, D., Berkson, J., and Suatoni, L. 2015. Current methods for setting catch limits for data-limited fish stocks in the United States. Fish. Res. **164**: 86-93.

Northeast Fisheries Science Center (2008). 47th Northeast Regional Stock Assessment Workshop (47th SAW) Assessment Report. US Dept Commer, Northeast Fish Sci Cent Ref Doc. 08-12a, 335 pp. http://www.nefsc.noaa.gov/publications/crd/crd0812/.

Northeast Fisheries Science Center. (2017). In: 61st Northeast Regional Stock Assessment Workshop (61st SAW) Assessment Summary Report. US Dept Commer, Northeast Fish Sci Cent Ref Doc. 16-13; 26 p. http://www.nefsc.noaa.gov/publications/Northeast Fisheries Science Center. Report of the 61st Northeast Regional Stock Assessment Workshop (61st SAW). a. Atlantic surfclam. Technical Report NEFSC Ref. Doc. 17-05, Northeast Fisheries Science Center, 166 Water Street, Woods Hole, MA 02543-1026, 2017.

Northeast Fisheries Science Center. (2019). In: 66th Northeast Regional Stock Assessment Workshop (66th SAW) Assessment Report. US Dept Commer, Northeast Fish Sci Cent Ref Doc. 19-08; 459 p. http://www.nefsc.noaa.gov/publications/

Nys, L. N., Fabrizio, M. C., & Tuckey, T. D. (2016). Multi-decadal variation in size of juvenile Summer Flounder (Paralichthys dentatus) in Chesapeake Bay. *Journal of sea research*, *107*, 112-120.

O'Leary, B.C., Smart, J.C.R., Neale, F.C., Hawkins, J.P., Newman, S., Milman, A.C., and Roberts, C.M. 2011.Fisheries mismanagement. Mar. Pollut. Bull. **62**: 2642-2648.

Pace, S.M., Poussard, L.M., Powell, E.N., Ashton-Alcox, K.A., Kuykendall, K.M., Solinger, L.K., Hemeon, K.M., and Soniat, T.M. 2020a. Dying, decaying, and dissolving into irrelevance: first direct in-the-field estimate of *Crassostrea virginica* shell loss -- a case history from Mississippi Sound. J. Shellfish Res. **39**:245-256.

Pace, S.M., Powell, E.N., Soniat, T.M., and Kuykendall, K.M. 2020b. How oyster health indices vary between mass mortality events. J. Shellfish Res. **39**: 603-617.

Parker, P. S. (1971). History and development of surf clam harvesting gear. *National Oceanic and Atmospheric Administration Technical Report*, NMFS CIRC-364, 15 pp.

Pershing, A. J., Alexander, M. A., Hernandez, C. M., L.A. Kerr, le Bris, A., Mills, K. E., Nye, J. A., Record, N. R., Scannell, H. A., Scott, J. D., Sherwood, G. D., & Thames, A. C. (2015) Slow adaptation in the face of rapid warming leads to collapse of the Gulf of Maine cod fishery. *Science*, *350*(6262), 809-812.

Peterson, C. H. (2002). Recruitment overfishing in a bivalve mollusc fishery: hard clams

(*Mercenaria mercenaria*) in North Carolina. *Canadian Journal of Fisheries and Aquatic Sciences*, *59*(1), 96-104.

Peterson, C.H., Grabowski, J.H., and Powers, S.P. 2003. Estimated enhancement of fish production resulting from restoring oyster reef habitat: quantitative valuation. Mar. Ecol. Prog. Ser. **264**: 249-264.

Poussard, L. M., Powell, E. N. & Hennen, D. R. (2021). Efficiency estimates from depletion experiments for sedentary invertebrates: evaluation of sources of uncertainty in experimental design. *Fisheries Research*, *234*, #105006, 13 pp.

Powell, E.N., Ashton-Alcox, K.A., Banta, S.E. and Bonner, A.J. 2001. Impact of repeated dredging on a Delaware Bay oyster reef. J. Shellfish Res. **20**: 961-975.

Powell, E.N., Ashton-Alcox, K.A., Kraeuter, J.N., Ford, S.E., and Bushek, D. 2008. Long-term trends in oyster population dynamics in Delaware Bay: regime shifts and response to disease. J. Shellfish Res. **27**: 729-755.

Powell, E. N., Bochenek, E. A., & DePersenaire, J. (2010). Evaluation of bag-and-size-limit options in the management of summer flounder Paralichthys dentatus. *Fisheries research*, *105*(3), 215-227.

Powell, E.N., Gendek, J.J., and Ashton-Alcox, K.A. 2005. Fisherman choice and incidental catch: size frequency of oyster landings in the New Jersey oyster fishery. J. Shellfish Res. **24**: 469-476.

Powell, E.N., Hofmann, E.E., and Klinck, J.M. 2018. Oysters, sustainability, management models, and the world of reference points. J. Shellfish Res. **37**: 833-849.

Powell, E.N., and Klinck, J.M. 2007. Is oyster shell a sustainable estuarine resource? J. Shellfish Res. **26**: 181-194.

Powell, E.N., Klinck, J.M., Ashton-Alcox, K., Hofmann, E.E., and Morson, J.M. 2012a. The rise and fall of *Crassostrea virginica* oyster reefs: the role of disease and fishing in their demise and a vignette on their management. J. Mar. Res. **70**: 505-558.

Powell, E.N., Klinck, J.M., Ashton-Alcox, K.A., and Kraeuter, J.N. 2009a. Multiple stable reference points in oyster populations: biological relationships for the eastern oyster (*Crassostrea virginica*) in Delaware Bay. Fish. Bull. **107**: 109-132.

Powell, E.N., Klinck, J.M., Ashton-Alcox, K.A., and Kraeuter, J.N. 2009b. Multiple stable reference points in oyster populations: implications for reference point-based management. Fish. Bull. **107**: 133-147.

Powell, E.N., Klinck, J.M., Guo, X., Ford, S.E., and Bushek, D. 2011c. The potential for oysters, *Crassostrea virginica*, to develop resistance to Dermo disease in the field: evaluation using a gene-based population dynamics model. J. Shellfish Res. **30**:685-712.

Powell, E.N., Klinck, J.M., Guo, X., Hofmann, E.E., Ford, S.E., and Bushek, D. 2012b. Can oysters *Crassostrea virginica* develop resistance to dermo disease in the field: the impediment posed by climate cycles. J. Mar. Res. **70**: 309-355.

Powell, E.N., Klinck, J.M., and Hofmann, E.E, 1996. Modeling diseased oyster populations. II. Triggering mechanisms for *Perkinsus marinus* epizootics. J. Shellfish Res. **15**: 141-165.

Powell, E.N., Klinck, J.M., Hofmann, E.E., and Ford, S, 1997. Varying the timing of oyster transplant: implications for management from simulation studies. Fish. Oceanogr. **6**: 213-237.

Powell, E. N., Klinck, J. M., Hofmann, E. E., Moreno, P., Kuykendall, K. M., Munroe, D.

M., Mann, R. (2016). Captains' response to a declining stock as anticipated in the surfclam (*Spisula solidissima*) fishery on the U.S. Mid-Atlantic coast by model evaluation. *Ocean & Coastal Management, 134*, 52-68.

Powell, E. N., Klinck, J. M., Munroe, D. M., Hofmann, E. E., Moreno, P. & Mann, R. (2015). The value of captains' behavioral choices in the success of the surfclam (*Spisula solidissima*) fishery on the U.S. Mid-Atlantic coast: a model evaluation. *Journal of Northwest Atlantic Fisheries Science, 47*, 1-27.

Powell, E.N., Kraeuter, J.N., and Ashton-Alcox, K.A. 2006. How long does oyster shell last on an oyster reef? Estuar. Coast. Shelf Sci. **69**: 531-542.

Powell, E.N., Mann, R., Ashton-Alcox, K.A., Kim, Y., and Bushek, D. 2016. The allometry of oysters: spatial and temporal variation in the length-biomass relationships for *Crassostrea virginica*. J. Mar. Biol. Assoc. U. K. **96**: 1127-1144.

Powell, E.N., Morson, J.M., Ashton-Alcox, K.A., and Kim, Y. 2013. Accommodation of the sex-ratio in eastern oysters *Crassostrea virginica* to variation in growth and mortality across the estuarine salinity gradient. J. Mar. Biol. Assoc. U. K. **93**: 533-555.

Powell, E.N., Staff, G.M., Callender, W.R., Ashton-Alcox, K.A., Brett, C.E., Parsons-Hubbard, K.M., Walker, S.E., and Raymond, A. 2011a. Taphonomic degradation of molluscan remains during thirteen years on the continental shelf and slope of the northwestern Gulf of Mexico. Palaeogeogr. Palaeoclimatol. Palaeoecol. **312**: 209-232.

Powell, E.N., Staff, G.M., Callender, W.R., Ashton-Alcox, K.A., Brett, C.E., Parsons-Hubbard, K.M., Walker, S.E., and Raymond, A. 2011b The influence of molluscan taxon on taphofacies development over a broad range of environments of preservation: the SSETI experience. Palaeogeogr. Palaeoclimatol. Palaeoecol. **312**: 233-264.

Powers, S.P., Peterson, C.H., Grabowski, J.H., and Lenihan, H.S. 2009. Success of constructed oyster reefs in no-harvest sanctuaries: implications for restoration. Mar. Ecol. Prog. Ser. **389**: 159-170.

Prager, M. H., & Shertzer, K. W. (2019). Deriving acceptable biological catch from the overfishing limit: implications for assessment models. *North American Journal of Fisheries Management*, *30*(1), 289-294.

Punt, A.E., Butterworth, D.S., de Moor, C.L., De Oliveira, J.A., and Haddon, M. 2016. Management strategy evaluation: best practices. Fish and Fisheries **17**: 303-334.

Punt, A. E., Castillo-Jordán, C., Hamel, O. S., Cope, J. M., Maunder, M. N., & Ianelli, J. N. (2021). Consequences of error in natural mortality and its estimation in stock assessment models. *Fisheries Research*, *233*, 105759.

Punt, A.E., Huang, T., and Maunder, M.N. 2013. Review of integrated size-structured models for stock assessment of hard-to-age crustacean and mollusc species. ICES J. Mar. Sci. **70**: 16-33.

Punt, A.E., and Szuwalski, C. 2012. How well can Fmsy and Bmsy be estimated using empirical measures of surplus production. Fish. Res. **134-136**: 113-124.

Pusack, T.J., Kimbro, D.L., White, J.W., and Stallings, C.D. 2019. Predation on oysters is inhibited by intense or chronically mild, low salinity events. Limnol. Oceanogr. **64**: 81-92.

Quijón, P. A., Grassle, J. P., & Rosario, J. M. (2007). Naticid snail predation on early post-settlement surfclams (*Spisula solidissima*) on the inner continental shelf of New Jersey, USA. *Marine Biology*, *150*(5), 873-882.

Rheault, R.B., and Rice, M.A. 1996. Food-limited growth and condition index in the Eastern oyster, *Crassostrea virginica* (Gmelin 1791), and the bay scallop, *Argopecten irradians* irradians (Lamarck 1819). J. Shellfish Res. **15**: 271-283.

Ropes, J. W. (1968). Reproductive cycle of the surf clam, *Spisula solidissima*, in offshore New Jersey. *Biological Bulletin*, *135*(2), 349-365.

Rosenberg, A. A., & Restrepo, V. R. (1994). Uncertainty and risk evaluation in stock assessment advice for US marine fisheries. *Canadian Journal of Fisheries and Aquatic Sciences*, *51*(12), 2715-2720.

Rothschild, B.J. 2000. "Fish stocks and recruitment": the past thirty years. ICES J. Mar. Sci. **57**: 191-201.

Rothschild, B.J., Ault, J.S., Goulletquer, P., and Héral, M. 1994. Decline of the Chesapeake Bay oyster populations: a century of habitat destruction and overfishing. Mar. Ecol. Prog. Ser. **111**: 29-39.

Rothschild, B.J., and Jiao, Y. 2013. Comparison between maximum sustained yield proxies and maximum sustained yield. Open Fish. Sci. J. **6**: 1-9.

Roughgarden, J., & Smith, F. (1996). Why fisheries collapse and what to do about it. *Proceedings of the National Academy of Sciences of the United States of America*, *93*(10), 5078-5083.

Rountree, B. P. (2015). Limited access privilege programs in the Mid-Atlantic fisheries. *Marine Fisheries Review*, *77*(3), 39-48.

Saba, V. S., Griffies, S. M., Anderson, W. G., Winton, M., Alexander, M. A., Delworth,

T. L. Hare, J. A., Harrison, M. J., Rosati, A., Vecchi, G. A., & Zhang, R. (2016). Enhanced warming of the northwest Atlantic Ocean under climate change. *Journal of Geophysical Research Oceans*, *121*(1), 118-132.

Schonfeld, A. J., Langan, J. A., Truesdale, C. L., McManus, M. C., & Collie, J. S. (2016). Sex-Specific Population Dynamics and Trophic Ecology of the Summer Flounder (Paralichthys dentatus) in Narragansett Bay, Rhode Island. *SURFO Technical Report No. 16-01*, 82.

Shertzer, K. W., Prager, M. H., & Williams, E. H. (2008). A probability-based approach to setting annual catch levels. *Fishery Bulletin*, *106*(3), 225-232.

Smith, G.F., Bruce, D.G., Roach, E.B., Hansen, A., Newell, R.I.E., and McManus, A.M. 2005. Assessment of recent habitat conditions of eastern oyster *Crassostrea virginica* bars in mesohaline Chesapeake Bay. N. Am. J. Fish. Manage. **25**: 1569-1590.

Solinger et al. submitted

Soniat, T.M., Smith, L.E., and Brody, M.S. 1989. Mortality and condition of the American oyster in Galveston Bay, Texas. Contrib. Mar. Sci. **31**: 77-94.

Soniat, T.M., Cooper, N.A., and Powell, E.N. 2019. Prospects for the sustainable management of public oyster resources. J. Shellfish Res. **38**: 337-349.

Soniat, T.M., Cooper, N., Powell, E.N., Klinck, J.M., Abdelguerfi, M., Tu, S., Mann, R., and Banks, P.D. 2014. Estimating sustainable harvests of eastern oysters, *Crassostrea virginica*. J. Shellfish Res. **33**: 381-394.

Soniat, T.M., Finelli, C.M., and Ruiz, J.T. 2004. Vertical structure and predator refuge mediate oyster reef development and community dynamics. J. Exp. Mar. Biol. Ecol. **310**: 163-182.

Soniat, T.M., Klinck, J.M., Powell, E.N., Cooper, N., Abdelguerfi, M., Hofmann, E.E., Dahal, J., Tu, S., Finigan, J., Eberline, B.S., La Peyre, J.F., La Peyre, M.K., and Qaddoura, F. 2012a. A shell-neutral modeling approach yields sustainable oyster harvest estimates: a retrospective analysis of the Louisiana State primary seed grounds. J. Shellfish Res. **31**: 1103-1112.

Soniat, T.M., Klinck, J.M., Powell, E.N., and Hofmann, E.E. 2012b. Understanding the success and failure of oyster populations: periodicities of *Perkinsus marinus* and oyster recruitment, mortality, and size. J. Shellfish Res. **31**: 635-646.

Southworth, M., Harding, J.M., Wesson, J.A., and Mann, R. 2010. Oyster (*Crassostrea virginica*, Gmelin 1791) population dynamics on public reefs in the Great Wicomico River, Virginia, USA J. Shellfish Res. **29**: 271-290

Stauber, L.A. 1950. The problem of physiological species with special reference to oysters and oyster drills. Ecology **31**: 109-118

Stobart, B., Mayfield, S., and McGarvey, R. 2013. Maximum yield or minimum risk. using biological data to optimize harvest strategies in a southern Australian molluscan fishery. J. Shellfish Res. **32**: 899-909.

Summerhayes, S.A., Bishop, M.J., Leigh, A., and Kelaher, B.P. 2009. Effects of oyster death and shell disarticulation on associated communities of epibiota. J. Exp. Mar. Biol. Ecol. **379**: 60-67.

Swannack, T.M., Reif, M., and Soniat, T.M. 2014. A robust, spatially-explicit model for identifying oyster restoration sites: case studies on the Atlantic and Gulf coasts. J. Shellfish Res. **33**: 395-408.

Terceiro, M. (2001). The summer flounder chronicles: science, politics, and litigation, 1975–2000. *Reviews in Fish Biology and Fisheries, 11*(2), 125-168.

Terceiro, M. (2011). The summer flounder chronicles II: new science, new controversy, 2001–2010. *Reviews in Fish Biology and Fisheries, 21*(4),681–712.

Terceiro, M. (2018). The summer flounder chronicles III: struggling with success, 2011–2016. *Reviews in Fish Biology and Fisheries, 28*(2), 381-404.

Timbs, J. R., Powell, E. N. & Mann, R. (2018). Assessment of the relationship of stock and recruitment in the Atlantic surfclam *Spisula solidissima* in the northwestern Atlantic Ocean. *Journal of Shellfish Research, 37*(5), 965-978.

Timbs, J. R., Powell, E. N., & Mann, R. (2019). Changes in the spatial distribution and anatomy of a range shift for the Atlantic surfclam *Spisula solidissima* in the Mid-Atlantic Bight and on Georges Bank. *Marine Ecology Progress Series*, *620*, 77-97.

Tolley, S.G., Volety, A.K., Savarese, M., Walls, L.D., Linardich, C., and Everham III, E.M. 2006. Impacts of salinity and freshwater inflow on oyster-reef communities in southwest Florida. Aquat. Living Resour. **19**: 371-387.

Vølstad, J.H., Dew, J., and Tarnowski, M. 2008. Estimation of annual mortality rate for eastern oysters (*Crassostrea virginica*) in Chesapeake Bay based on box counts and application of these rates to project population growth of *C. virginica* and *C. ariakensis*. J. Shellfish Res. **27**: 525-533.

Waldbusser, G.G., Steenson, R.A., and Green, M.A. 2011. Oyster shell dissolution rates in estuarine waters: effects of pH and shell legacy. J. Shellfish Res. **30**: 659-669.

Walters, C. J. (1984). Managing fisheries under biological uncertainty. In *Exploitation of Marine Communities* (pp. 263-274). Springer, Berlin, Heidelberg.

Weinberg, J. R. (1999). Age-structure, recruitment, and adult mortality in populations of the Atlantic surfclam, *Spisula solidissima*, from 1978-1997. *Marine Biology*, *134*(1), 113-125.

Weinberg, J. R., Powell, E. N., Pickett, C., Nordahl Jr., V, A., & Jacobson, L. D. (2005). Results from the 2004 cooperative survey of Atlantic surfclams. *Northeast Fisheries Science Center Reference Document,* 05-01:1-41.

Wiedenmann, J., Wilberg, M., Sylvia, A., & Miller, T. (2017). An evaluation of acceptable biological catch (ABC) harvest control rules designed to limit overfishing. *Canadian Journal of Fisheries and Aquatic Sciences*, *74*(7), 1028-1040.

Wirgin, I., Maceda, L., Stabile, J., & Waldman, J. (2022). Genetic population structure of summer flounder Paralichthys dentatus using microsatellite DNA analysis. *Fisheries Research*, *250*, 106270.

Woods, H., Hargis Jr., W.J., Hershner, C.H., and Mason, P. 2005. Disappearance of the natural emergent 3-dimensional oyster reef system of the James River, Virginia, 1871-1948. J. Shellfish Res. 24:139-142.

Woodward, C.R., and Waller, I.N. 1932. New Jersey's Agricultural Experiment Station 1880-1930 Chapt VII. New Jersey Agricultural Experiment Station, New Brunswick, New Jersey, pp. 191-207.

Worm, B., Hilborn, R., Baum, J.K., Branch, T.A., Collie, J.S., Costello, C., Fogarty, M.J., Fulton, E.A., Hutchings, J.A., Jennngs, S., Jensen, O.P., Lotze, H.K., Mace, P.M., McClanahan, T.R., Minto, C., Palumb, S.R., Pazone, A.M., Ricard, D., Rosenberg, A.A., Watson, R., and Zeller, D. 2009. Rebuilding global fisheries. Science **325**: 578-585.

Zabel, R.W., Harvey, C.J., Katz, S.L., Good, T.P., and Levin, P.S. 2003. Ecologically sustainable yield. Am. Sci. **91**: 150-157.

Zhang, X., Haidvogel, D., Munroe, D., Powell, E. N, Klinck, J., & Mann, R., & Castruccio, F. S. (2015). Modeling larval connectivity of the Atlantic surfclams within the Middle Atlantic Bight: model development, larval dispersal and metapopulation connectivity. *Estuarine Coastal and Shelf Sciences, 153*, 38-53.

Zhang, X., Munroe, D., Haidvogel, D., & Powel, E. N. (2016). Atlantic surfclam connectivity within the Middle Atlantic Bight: mechanisms underlying variation in larval transport and settlement. *Estuaine. Coastal and Shelf Science, 173*, 65-78.

Zhou, S. 2007. Discriminating alternative stock-recruitment models and evaluating uncertainty in model structure. Fish. Res. **86**: 268-279.

Zhou, S., Yin, S., Thorson, J.T., Smith, A.D.M., and Fuller, M. 2012. Linking fishing mortality reference points to life history traits: an empirical study. Can. J. Fish. Aquat. Sci. **69**: 1292-1301.

zu Ermgassen, P.S.E., Spalding, M.D., Blake, B., Coen, L.D., Dumbauld, B., Geiger, S., Grabowski, J.H., Grizzle, R., Luckenbach, M., McGraw, K., Rodney, W., Ruesink, L., Powers, S.P., and Brumbaugh, R. 2012. Historical ecology and real numbers: past and present extent and biomass of an imperilled estuarine habitat. Proc. R. Soc. Lond. B Biol. Sci. **279**: 3393-3400.

.